METAL CHELATES AS BIOLOGICAL PROBES: PREPARATION AND PROPERTIES

By

FRANCES ELIZABETH ARMITAGE

A DISSERTATION PRESENTED TO THE GRADUATE SCHOOL
OF THE UNIVERSITY OF FLORIDA IN PARTIAL
FULFILLMENT OF THE REQUIREMENTS
FOR THE DEGREE OF DOCTOR OF PHILOSOPHY

UNIVERSITY OF FLORIDA

1990

UNIVERSITY OF FLORIDA LIBRARIES

Copyright 1990

by

Frances Elizabeth Armitage

ACKNOWLEDGMENTS

Partial support for the contrast agent project was provided by the Florida Division of the American Cancer Society (Hazel C. M. Kerr Research Grant) and the Division of Sponsored Research of the University of Florida. Imaging studies were funded by internal grants from the Department of Radiology, University of Florida College of Medicine. Grateful acknowledgment is appropriate for the collaboration of many colleagues: Dr. King Li, Dr. Ron Quisling, and Dr. Chris Mladinich, D.V.M., of the Department of Radiology (College of Medicine, University of Florida) who provided time, expertise, and thoughtful insight for the imaging studies required in the contrast agent project; the many associates in the Department of Chemistry whose feedback enhanced the direction of the projects; and past and present mentors whose expressed enthusiasm toward exploring the basics of chemistry gave me the confidence to pursue this endeavor.

TABLE OF CONTENTS

page

ACKNOWLEDGMENTS..... iii

KEY TO SYMBOLS AND ABBREVIATIONS.....vi

ABSTRACT.....vii

CHAPTERS

1 INTRODUCTION.....1

2 SYNTHESIS AND ELECTROCHEMICAL PROPERTIES OF EDTA COMPLEXES OF RUTHENIUM(III).....6

Chapter Overview.....6
Synthesis and Characterization.....10
Synthesis of $[Ru^{III}(Hedta)H_2O]$.....10
Synthesis of $[Ru^{III}(Hedta)L]$ Complexes.....13
Cyclic Voltammetry Measurements.....16
Results and Discussion.....16
Evaluation of Synthetic Methods.....16
Properties of New Ru(Hedta)L Complexes.....23
Electrochemistry Results.....28
Chapter Summary.....31

3 SYNTHESIS AND CHARACTERIZATION OF POLYSACCHARIDE ESTERS OF POLYAMINOPOLYCARBOXYLIC ACIDS AND THEIR GADOLINIUM(III) COMPLEXES.....34

Chapter Overview.....34
Materials and Methods.....39
Synthesis of DTPA-Polysaccharides.....39
Determining Reaction Success by HPLC.....44
Purification of DTPA-Polysaccharide Esters...46
Nature of Reacted Polysaccharide by HPLC.....48
Synthesis and Purification of Gd^{3+} Complexes.48
Characterization of Compounds.....50
Results and Discussion.....58
Evaluation of Synthetic Methods.....58
Compound Characterization Results.....74
Relaxivity Results.....86
Chapter Summary.....98

4 MAGNETIC RESONANCE IMAGING STUDIES USING GADOLINIUM CONJUGATES AS CONTRAST AGENTS....103

Chapter Overview....103
Materials and Methods....106
Phantom Studies....106
Animal Imaging Studies....107
Results and Discussion....109
Phantom Results....109
Animal Imaging Results....119
Chapter Summary....143

5 SUMMARY....145

APPENDIX....150

REFERENCES....152

BIOGRAPHICAL SKETCH....159

KEY TO SYMBOLS AND ABBREVIATIONS

NMR = Nuclear magnetic resonance.

MRI = Magnetic resonance imaging.

T_1 = Spin - lattice (longitudinal) nuclear relaxation time.

T_2 = Spin - spin (transverse) nuclear relaxation time.

R_1 = Spin - lattice relaxivity.

T_R = Time between pulse repetitions in MRI.

T_E = Time waited between pulse and data acquisition in MRI.

ROI = Region of interest in MRI image, used to obtain signal intensity data with 95% confidence limit.

EDTA = Ethylenediaminetetraacetic acid.

EDTA-R = EDTA with functional group modification on ethylene backbone.

$Hedta^{3-}$ = EDTA ligand with 3 deprotonated carboxylate functions.

H_2edta^{2-} = EDTA ligand with 2 deprotonated carboxylate functions.

DTPA = Diethylenetriaminepentaacetic acid.

TTHA = Triethylenetetraaminehexaacetic acid.

GdDTPA = DTPA complex of gadolinium(III).

GdTTHA = TTHA complex of gadolinium(III).

GdDTPA-polysaccharide = GdDTPA linked by ester bond to either dextran or inulin.

E_f = Formal reduction potential, mV.

ΔE_p = Difference between anodic and cathodic peak potential.

Abstract of Dissertation Presented to the Graduate School of the University of Florida in Partial Fulfillment of the Requirements for the Degree of Doctor of Philosophy

METAL CHELATES AS BIOLOGICAL PROBES:
PREPARATION AND PROPERTIES

By

FRANCES ELIZABETH ARMITAGE

August 1990

Chairman: David E. Richardson
Major Department: Chemistry

Aqua ethylenediaminetetraacetato ruthenium(III) was prepared by a variety of methods. Improvement in product yield relative to prior art methods was obtained, and the synthesis results are discussed in terms of product and method suitability for future application in protein conjugate preparations. Substitution of the aqua ligand by a variety of nitrogen containing ligands was carried out, and two new complexes are reported. Reversible cyclic voltammograms were obtained, and a range in reduction potentials (versus NHE) from 0.0 to 0.5 volts was observed.

The synthesis and characterization of polysaccharides esterified with diethylenetriaminepentaacetato gadolinium(III), GdDTPA-dextrans and GdDTPA-inulin, are described. The synthetic method resulted in products labeled with an average of 0.4 mole GdDTPA per mole of

glucopyranose unit in dextrans of up to 70800 average molecular weight and 0.5 mole of GdDTPA per mole of fructofuranose unit of inulin. Chromatographic and potentiometric evidence supporting the absence of chelate induced crosslinking of the polysaccharides is presented. The thermodynamic stability, log K ($Gd^{3+} + L^{4-} \rightarrow GdL^{-}$), of the complexes was 18.02 ± 0.13 based on an independent chelate model. The *in vitro* ester hydrolysis half-life of GdDTPA-dextran 70800 (37°C, pH=7.4) was one-fourth that of the nonmetallated compound.

The conjugates exhibited T_1 relaxivities ranging from 1.5 to 2.3 times that of GdDTPA at 100 MHz, and decreasing *in vitro* relaxivity with increasing molecular weight of dextran carriers was observed. Phantom MRI studies indicate that the T_1 and T_2 effects of the complexes differ from GdDTPA, with the dextran and inulin-bound complexes exhibiting a considerably faster drop in relative signal intensity with increased concentration in T_1 and T_2 weighted pulse sequences. Tissue enhancement in normal rabbits using GdDTPA labeled dextran of 9400 and 70800 average molecular weight persists in excess of 60 minutes for liver, kidney, and brain microvascular regions. No toxic effects for the complexes were noted. These macromolecular agents have potential application in blood-pool persistent MRI contrast enhancement of organ abnormalities and blood flow studies.

CHAPTER 1

INTRODUCTION

Polyaminopolycarboxylates, chelating molecules that contain two or more amine and carboxyl functional groups, are ligands that generally form metal complexes of high thermodynamic stability.[1-4] Provided the metal ion can accommodate all of the potential donor groups of the ligand (example ligands are shown in Figure 1.1), as the number of donor groups in the ligand increases the thermodynamic stability of the metal complex generally increases.

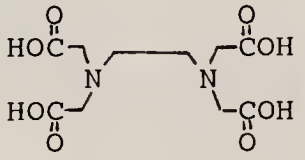

Ethylenediaminetetraacetic acid (EDTA), 6 donor groups

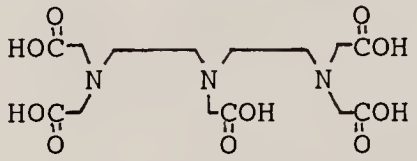

Diethylenetriaminepentaacetic acid (DTPA), 8 donor groups

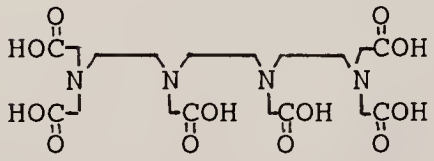

Triethylenetetraaminehexaacetic acid (TTHA), 10 donor groups

Figure 1.1. Some polyaminopolycarboxylic acids and their number of potential ligating donor groups.

The stabilization of potentially toxic metal ions by these chelates prompted their medical application in toxic metal mobilization and control of endogenous metal metabolic problems.[5] In addition to these therapeutic applications, there is considerable potential for the metal complexes of polyaminopolycarboxylates as biological probes.[6] The ligands can be modified to contain a functional group which is reactive toward functional groups of proteins or other types of biologically important molecules. In this fashion, the chelating agent becomes bifunctional in that it serves to ligate a metal ion and to covalently link the complexed metal ion to a carrier molecule in the formation of the conjugate.

Shown in Figure 1.2 are several potential biological probe applications for the metal chelates. Considerable research activity has been directed toward all of the areas represented in Figure 1.2, however, the development of radiopharmaceuticals has been the primary focus of bifunctional chelating agents in biomedical applications.[6,7] These radiopharmaceuticals may incorporate covalent linkage between the bifunctional chelate and a tumor specific antibody (or a tumor localizing carrier molecule), or the antibody may be both tumor and metal chelate specific such that no covalent linkage between the antibody and metal chelate is necessary.

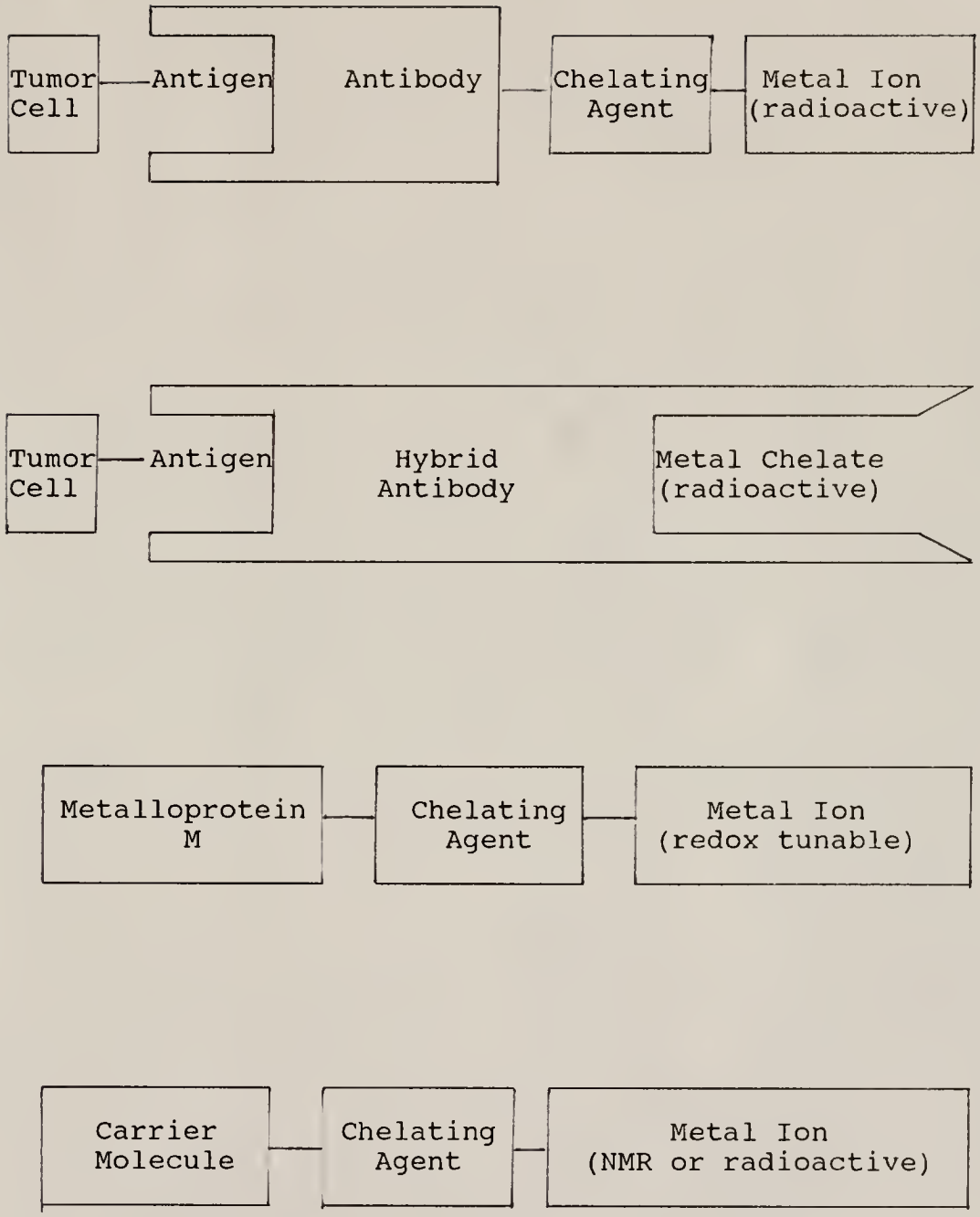

Figure 1.2. Schematic representation of biological probe applications for metal chelates.

Also shown in Figure 1.2 is the application of metal chelates in studies concerning electron transfer of metalloproteins.[8,9] In this type of application, a redox tunable metal center is linked by a bifunctional chelator to a metalloprotein. The binding of NMR active or radioactive metals to macromolecular carriers by bifunctional chelates has been developed so that abnormal tissue can be more easily distinguished from normal tissue when instruments currently available in noninvasive diagnostic medicine are used.[10,11] These applications of metal chelates are directly related to the two areas of study undertaken in the present work.

The contents of Chapter 2, "Synthesis and Electrochemical Properties of EDTA Complexes of Ruthenium (III)," are potentially useful for future investigations concerning electron transfer between redox tuned ruthenium centers and metal centers of metalloproteins. By covalently linking the Ru^{3+} metal chelate, in which there is one inner sphere coordinated water molecule, to metalloproteins and substituting other ligands for the aqua ligand, the difference between the potentials of the metal center of the metalloprotein and the ruthenium center can, in principle, be easily manipulated.

Chapter 3 describes the synthesis and characterization of gadolinium polyaminopolycarboxylate chelates which have been covalently linked by ester bond to polysaccharide

carrier molecules. These studies were undertaken so that the new gadolinium conjugates could be assessed for their potential application as contrast agents when used in magnetic resonance imaging (MRI), a noninvasive biomedical diagnostic tool. The investigation of the *in vitro* and *in vivo* behaviors of the new compounds when used as contrast agents in MRI is presented in Chapter 4.

Several techniques were used to characterize the new gadolinium conjugates in an attempt to ascertain the effect of covalent attachment of the polysaccharide on the various properties of the metal chelate unit. Additionally, some of the evaluations and suggested future evaluations represent studies that are often neglected when new compounds become candidates for potential biological applications. The final chapter (Chapter 5) includes a summary of the results of the two different areas of study and a brief discussion pertaining to the predicted directions of each project.

CHAPTER 2

SYNTHESIS AND ELECTROCHEMICAL PROPERTIES OF EDTA COMPLEXES OF RUTHENIUM(III)

Chapter Overview

The complex $[Ru^{III}(NH_3)_5H_2O]^{3+}$ undergoes substantially slower exchange of the aqua ligand with π-acid ligands than the corresponding ruthenium(II) complex.[12] The aqua complex of ruthenium(III) ethylenediaminetetraacetic acid, $[Ru^{III}(Hedta)H_2O]$, however, exhibits a lability 7 orders of magnitude greater than that of $[Ru^{III}(NH_3)_5H_2O]^{3+}$.[13] This unusual lability is such that the water in $[Ru^{III}(Hedta)H_2O]$ undergoes π-acid ligand substitution more rapidly than $[Ru^{II}(Hedta)H_2O]^-$ and represents an anomaly in the general inertness of ruthenium(III) complexes toward substitution.

Investigations which involved the chromium(III) complex of EDTA suggest that the high degree of lability of the aqua complex is attributable to the interaction between the coordinated water molecule and an uncoordinated acetate group of EDTA.[14] The structure of the ruthenium(III) complex of EDTA in solution has an uncoordinated acetate group. Through the modification of electrode surfaces with

$[Ru^{III}(Hedta)H_2O]$ by linkage of the uncoordinated acetate function, Oyama and Anson[15,16] observed that aqua substitution by pyridine and isonicotinamide occurred much faster in the Ru^{II} complex rather than the Ru^{III} complex. This reversal in order of reactivity toward substitution, however, was not observed when $[Ru^{III}(Hedta)H_2O]$ was directly attached to the electrode surface through the metal center. These results tend to support the water - acetate interaction mode of lability for the $[Ru(III)(Hedta)H_2O]$ complex.

The lability of $[Ru^{III}(Hedta)H_2O]$ is well suited for potential application in redox investigations of metalloproteins in that, following covalent attachment to the protein using a modified EDTA chelate, the inner sphere coordinated water molecule may be easily substituted by π-acid ligands. The increasing π donor ability of the substituting ligands would be expected to result in more positive reduction potentials while facile substitution would provide a means by which changes in the formal reduction potential on the ruthenium(III) center could be readily achieved.

Recent work by Matsubara and Creutz[17] involved the investigation of $[Ru^{III}(Hedta)L]$ complexes which were prepared by substitution of water in the aqua complex by thiocyanate, pyridine, imidazole, isonicotinamide, pyrazine, and acetonitrile. The complexes, including the aqua

complex, ranged in formal reduction potentials from -0.01 to +0.26 V versus NHE in pH = 5.5 acetate buffer. Their results also indicate that, in the pH range from 0.8 to 8.5, the $[Ru^{III}(edta)H_2O]^-$ species was the only reactive form of the complex involved in the ligand substitution reaction even though the pK_a of the free $-CO_2H$ function is 2.37 and the pK_a of the coordinated water is 7.63.

The mode of covalent attachment of EDTA to proteins may occur through one of the EDTA acetate groups or through a function which has been linked to the ethylene backbone of EDTA. Since the lability of the aqua complex is very likely dependent on the presence of an uncoordinated acetate function of EDTA in $[Ru^{III}(Hedta)H_2O]$, the use of one of the acetate groups in covalent linkage to the protein is not desirable. A number of modified EDTA ligands have been prepared such that covalent attachment to proteins can be achieved by a variety of methods without a reduction in the denticity of the ligand.[18] Although the reduction potentials for $[Ru^{III}(Hedta\text{-}R)L]$ in which the EDTA has been modified at the ethylene backbone may be altered relative to those of the unmodified EDTA complexes, the range of reduction potentials should be comparable.

A goal of this work was to synthesize a series of $[Ru^{III}(Hedta)L]$ complexes in which the EDTA is pentadentate and the variable ligand, L, occupies the sixth coordination site. Ideally, the series of complexes would exhibit a wide

range of reduction potentials such that they may, following covalent linkage to proteins or other macromolecules, be useful in subsequent investigations concerning antibody production or biological electron transfer. In order to accomplish this goal, an investigation of synthetic methods to produce high yields of $[Ru^{III}(Hedta)H_2O]$ was necessary.

The use of the high lability of the aqua complex to explore many of the π-acid ligands investigated by Matsubara and Creutz as well as an assessment of the redox tuning ability of other π-acid ligands needed to be conducted so that a wide range of reduction potentials could be obtained. An evaluation of the effects of pH on the reduction potentials of the complexes was also necessary, particularly in the range of physiological pH wherein relevant reduction potential data could be generated for subsequent biological studies.

Finally, the reactions required for the high yield synthesis of $[Ru^{III}(Hedta)H_2O]$ may or may not be appropriate for use with protein-modified EDTA ligands. An adjunct study required the assessment of alternative methods of $[Ru^{III}(Hedta)H_2O]$ production wherein the protein-$[Ru^{III}(Hedta\text{-}R)H_2O]$ conjugate could possibly be synthesized without protein degradation.

Synthesis and Characterization

Synthesis of $[Ru^{III}(Hedta)H_2O]$

All glassware was washed with 1 M EDTA to remove trace metals followed by thorough rinsing with deionized water. Ruthenium trichloride hydrate (Aldrich, hydrate content was not analyzed) was used in all preparations.

Reaction of ruthenium trichloride with H_2edta^{2-} without silver ion present. The procedure for the synthesis of $[Ru(Hedta)H_2O]$ was modified from that outlined by Scherzer.[19] Following dissolution in 20 mL of deionized water, 4 mmole of ruthenium trichloride was added to 20 mL of an aqueous solution which contained 4 mmole of Na_2H_2edta (Mallinckrodt). The solution was stirred while heating at 75^{o} - $80^{o}C$.

The dark brown precipitate was filtered while hot and washed with hot water followed by room temperature methanol. The product was dried under vacuum in a desiccator. Approximately 60 mL of methanol was added to the filtrate and the solution was undisturbed for 24 hours at room temperature. The green-yellow precipitate was filtered, washed with cold methanol, and air dried.

Reaction of ruthenium trichloride with H_2edta^{2-} with silver ion present. Fifteen mmole of $RuCl_3$ was added to 100 mL deionized water and heated at $60^{o}C$ while stirring for 1 hour. Thirty mmole of $AgBF_4$ (Ozark Mahoney) was added and

stirring and heating continued for 1/2 hour. The solution was filtered, allowed to stand at room temperature and filtered again. This process was repeated until no silver chloride precipitated from solution and no precipitate formed on addition of a few drops of solution to 1 M HCl.[20] A total of 15 mmole of Na_2H_2EDTA (Mallinckrodt) was added to the clear filtrate. The solution was stirred while heating at 80°C for 2 hours. After cooling to room temperature a brown precipitate was filtered, washed with methanol, and air dried. The filtrate was rotary-evaporated to approximately 40 mL and ethanol added until precipitation began. The solution was allowed to stand at room temperature for 48 hours, filtered and solid washed with methanol and dried in vacuum desiccator for 1 hour. Elemental analysis for $RuC_{10}H_{15}N_2O_9 \cdot 2H_2O$: calculated %C = 27.03, %H = 4.31, %N = 6.30; observed %C = 26.89, %H = 4.10, %N = 6.26.

Reaction of $[Ru(Hedta)Cl]^-$: process 1. The $[Ru(Hedta)Cl]^-$ was used as obtained from the direct reaction of $RuCl_3$ with H_2edta^{2-} without silver ion present (above). Conversion to the aqua complex was accomplished by method outlined by Mukaido.[21]

Reaction of $[Ru(Hedta)Cl]^-$: process 2. Solid $[Ru(Hedta)Cl]^-$, prepared as above with no silver ion present, was placed in deionized water and stirred at room temperature. Zinc amalgam was prepared from mossy zinc

which had been washed in 1 M perchloric acid, amalgamated with 0.5 M $Hg(ClO_4)_2$ in 0.5 M $HClO_4$, and rinsed with water. The amalgam was placed in the dark brown heterogeneous $[Ru(Hedta)Cl]^-$ solution and stirred at room temperature for 12 hours. The olive-green mixture was filtered and the filtrate was purged with oxygen for 1/2 hour. This resulted in an intensely yellow solution. The solution was rotary-evaporated to approximately 25 mL and pH adjusted to 2 with perchloric acid. Ethanol was added until precipitation began and solution was allowed to sit at room temperature for 12 hours. The product was filtered and washed with ethanol.

Reaction of ruthenium oxide. Ruthenium oxide was prepared by modification of methods of Cady[22] and Kallen.[23] A flask containing 75 mL concentrated sulfuric acid and 3.15 g $RuCl_3$ hydrate was heated at 80°C while stirring until the solution tested negative for chloride ion with silver nitrate solution. A solid mixture containing 16.0 g $K_2S_2O_8$ (Mallinckrodt) and 1.0 g $AgCO_3$ (Mallinckrodt) was added to the solution and the solution was heated at 80°C for 1 hour. The solution was cooled to 50°C and oxalic acid (Aldrich) was slowly added to the brown solution until the solution color turned yellow. The flask was equipped with a side arm and a collection trap immersed in an ethanol/dry ice bath. All glassware between the reaction flask and the cold trap was heated to approximately 50°C. Deionized water was added

over a 4-hour period by dropping funnel while the solution was heated at 75°C, and a flow of nitrogen gas from the solution surface to the collection trap was used to transfer the RuO_4 vapor to the trap.

The RuO_4 was dissolved in 50 mL of 2.0 M HBF_4 (Fisher) and 5 grams of 30 mesh tin was added. The mixture was stirred at room temperature for 5 hours. The pink solution, after being purged with oxygen for 1 hour, turned yellow. To this solution, 2 grams of H_4edta (Mallinckrodt) was added and dissolved by the addition of $NaHCO_3$ (Fisher). The solution was stirred at room temperature for 10 hours, then heated for 4 hours at 80°C. The solution was cooled to 40°C and methanol added to precipitate the solid. The mixture was left undisturbed at room temperature for 12 hours then filtered and washed with methanol.

Synthesis of $[Ru^{III}(Hedta)L]$ Complexes

Solutions which were 4 mM in $[Ru^{III}(Hedta)H_2O]$ were prepared in pH = 5.56 acetate, 7.09 phosphate, and 9.12 borate buffers. To separate containers of 2 mL of the solution, an 8-fold molar excess of ligand was added. The ligand reagents used were pyridine, pyrazine, 2-methylpyrazine, 2-nitrobenzonitrile, 4-nitrobenzonitrile, isonicotinamide (all obtained from Aldrich), sodium thiocyanate (Fisher), and acetonitrile (Kodak). The

complexes were not isolated. The solutions were immediately evaluated by cyclic voltammetry.

Synthesis of Ru(Hedta)1,10-phenanthroline. To 5 mL of deionized water, 0.13 gram of 1,10-phenanthroline (Aldrich gold label) was added with sufficient methanol to dissolve the solid. To the stirring solution, 32 mg of the prepared $Ru^{III}(Hedta)H_2O \cdot 2H_2O$ was added and resulted in a blood-red solution within 5 minutes. The solution was stirred at room temperature for 48 hours and rotary-evaporated to dryness. The purple solid was found to be only sparingly soluble in acetone while the 1,10-phenanthroline was very soluble. The excess ligand was removed from the solid by repeated washing and decantation with acetone and the solid was dried in a desiccator under vacuum. The calculated and observed elemental analysis of the complex $RuC_{22}H_{21}N_4O_8 \cdot 5.5H_2O$ are as follows: calculated %C = 39.46, %H = 4.82, %N = 8.37; observed %C = 38.58, %H = 4.42, %N = 8.46.

Synthesis of $[Ru^{III}(Hedta)(pyridine)_{1,2}]$. In a minimum amount of deionized water, 51 mg of the prepared $Ru^{III}(Hedta)H_2O \cdot 2H_2O$ was dissolved. To the solution, 12 mL of pyridine (Aldrich gold label) was added and solution stirred for 1 hour. The solution was then heated at 55°C for 2 1/2 hours, cooled to room temperature, and allowed to stir at room temperature for 72 hours. The light-orange solution was rotary-evaporated to dryness and washed by filtering with anhydrous ethyl ether. The dark yellow

powder was dried in a desiccator under vacuum. Based on the relative areas for each reversible voltammogram, it was calculated that the solid contained a mixture of 34.8% Ru(Hedta)(pyridine)$_2$ and 65.2% Ru(Hedta)pyridine. The calculated and observed elemental analysis for the mixture, with 5 moles of water associated per mole of ruthenium were calculated %C = 34.28, %H = 5.10, %N = 7.99; observed %C = 34.34, %H = 3.88, %N = 7.66.

Synthesis of [Ru^{III}(Hedta)(2,2'-dipyridine)]. To 10 mL deionized water, 0.16 gram of the prepared Ru^{III}(Hedta)$H_2O \cdot 2H_2O$ and 1.2 gram of 2,2'-dipyridyl (Fisher) were added. Methanol was added drop-wise to the mixture until all dipyridyl dissolved and the solution was stirred at room temperature for 12 hours. The solution was rotary-evaporated to dryness to produce dark purple crystals which were not soluble in ethyl ether. The excess dipyridyl (soluble in ethyl ether) was removed by stirring of the solid with ethyl ether and decantation of the ether solution. The washing process was repeated until three successive decantations resulted in no visible white powder upon evaporation of ethyl ether. The solid purple powder was dried in a desiccator under vacuum. Calculated elemental analysis results for $RuC_{20}H_{21}N_4O_8 \cdot 12H_2O$ were as follows: calculated %C = 31.50, %H = 5.95, %N = 7.35; observed %C = 31.78, %H = 3.52, %N = 7.21.

Cyclic Voltammetry Measurements

Buffer solutions of 0.3 M ionic strength (potassium salt of trifluoromethanesulfonic acid) of pH = 5.56 (acetate), 7.09 (phosphate), and 9.12 (borate) were used. All measurements were conducted using a silver / silver chloride reference microelectrode (Bioanalytical Systems model MF-2020), and 1/4" diameter platinum disks which had been spot welded to platinum wire for working and auxiliary electrodes. Cyclic voltammetric measurements were obtained using a Princeton Applied Research model 173 potentiostat / galvanostat and an EG&G Parc model 175 universal programmer. Voltammograms were recorded using a Houston Instrument Omnigraphic 2000 x-y recorder. A scan rate of 20 mV/sec was used for all solutions. All solutions were purged with argon prior to voltammetry. Formal reduction potentials were calculated using the midpoint of the anodic and cathodic peaks of the reversible voltammograms. Cyclic voltammetry of each complex was repeated two or more times and the deviation in formal reduction potential was less than 10 mV.

Results and Discussion

Evaluation of $Ru^{III}(Hedta)H_2O \cdot 2H_2O$ Synthetic Methods

The reaction of $RuCl_3$ with H_2edta^{2-} in aqueous solution results in the formation of the monochloro complex and aqua

complexes of the ruthenium chelate[19] and is indicated in equation 2.1.

$$2RuCl_3 + 2H_2edta^{2-}(aq) + 2H_2O \longrightarrow H^+(aq) + 5Cl^-(aq) + Ru(H_2edta)Cl\ (s) + Ru(Hedta)H_2O\ (s) \qquad (2.1)$$

The aqueous rate of precipitation of the chloro complex is substantially faster than that of the aqua complex and this difference was exploited in the synthetic method. The yield was 24% [$Ru(H_2edta)Cl$] and 1% [$Ru(Hedta)H_2O$].

The presence of silver ion in solution did not alter the yield of the chloro complex significantly (26%) but markedly effected the yield of aqua complex (25%). Equation 2.2 represents the reaction of $RuCl_3$ with silver ion present and equation 2.3 shows the subsequent reaction of the pentaqua monochloro complex with H_2edta^{2-}.

$$2H_2O + RuCl_3\ (aq) + 2\ Ag^+\ (aq) \longrightarrow 2AgCl\ (s) + RuCl(H_2O)_5^{2+}\ (aq) \qquad (2.2)$$

$$2RuCl(H_2O)_5^{2+}\ (aq) + 2H_2edta^{2-}\ (aq) \longrightarrow Ru(H_2edta)Cl\ (s) + Ru(Hedta)H_2O\ (s) \qquad (2.3)$$

Improvement in yield may be possible using a 3 to 1, rather than 2 to 1, mole ratio of Ag^+ to $RuCl_3$. The observed slow

formation of the silver chloride precipitate, however, suggests that the use of greater than a 2 to 1 mole ratio of reactants may require more time for the removal of Ag^+ remaining in solution. The slow rate of precipitation from solutions of chloro complexes of ruthenium(III) in the presence of Ag^+ was also observed by Connick and Fine[24] and the precipitate was reported as an aggregate containing Ag^+, Cl^-, and Ru^{3+} of unknown composition.

In dilute solutions of $[Ru(H_2edta)Cl]$, ligand exchange will slowly occur between the chloride ion and water, represented in equation 2.4.

$$Ru(H_2edta)Cl\ (aq) + H_2O \rightleftharpoons Ru(Hedta)H_2O + H^+ + Cl^- \qquad (2.4)$$

The most widely applied method for the conversion of the monochloro complex to the aqua complex, that of Mukaido,[21] involves the removal of H^+ and Cl^- from solution, shown in equation 2.5. The method resulted in 48% yield of the aqua complex from the monochloro complex starting material.

$$Ru(H_2edta)Cl\ (aq) + H_2O \longrightarrow Ru(Hedta)H_2O + HCl\ (g) \qquad (2.5)$$

Ruthenium(III) complexes normally undergo substitution reactions slowly.[25] By reducing the complexes to

ruthenium(II) and thereby producing a more labile species, the rate of substitution of chloride ion by water in $[Ru^{II}(H_2edta)Cl]^-$ may be substantially greater than that of the ruthenium(III) complex. The method for achieving this is represented in equations 2.6a-b. The method resulted in 78% yield of the aqua complex and this result tends to support the assumption that the lability of $[Ru^{II}(H_2edta)Cl]^-$ complex is significantly greater than that of $[Ru^{III}(H_2edta)Cl]$. This method of synthesis represents considerable improvement when compared with the yield obtained with Mukaido's method (78% versus 48%).

$$Zn\ (s) + 2Ru^{III}(H_2edta)Cl\ (aq) \longrightarrow 2Ru^{II}(H_2edta)H_2O\ (aq) + 2Cl^-\ (aq) + Zn^{2+}\ (aq) \qquad (2.6a)$$

$$4Ru^{II}(H_2edta)H_2O\ (aq) + O_2\ (g) \longrightarrow 4Ru^{III}(Hedta)H_2O\ (aq) + 2H_2O \qquad (2.6b)$$

The preparation of $[Ru(Hedta)H_2O]$ from ruthenium oxide eliminated the problem encountered in reactions of $RuCl_3$ wherein the competitive reaction to produce the monochloro complex took place. The reaction scheme involving RuO_4, represented by equation 2.7a-c, resulted in 16% yield.

$$RuO_4\ (s) + 8H_3O^+\ (aq) + 3Sn\ (s) \longrightarrow Ru(H_2O)_6{}^{2+}\ (aq) + 6H_2O + 3Sn^{2+}\ (aq) \qquad (2.7a)$$

$$4Ru(H_2O)_6^{2+}\ (aq) + O_2 + 4H_3O^+\ (aq) \longrightarrow 4Ru(H_2O)_6^{3+}\ (aq) + 6H_2O \qquad (2.7b)$$

$$Ru(H_2O)_6^{3+}\ (aq) + H_2edta^{2-}\ (aq) \longrightarrow Ru(Hedta)H_2O\ (s) + 4H_2O + H_3O^+\ (aq) \qquad (2.7c)$$

Although the synthesis of [Ru(Hedta)H_2O] from ruthenium oxide resulted in relatively low yield, the method is potentially important in the development of processes wherein the chelate is covalently attached to proteins or other macromolecular carriers. For these processes, two possible modes of synthesis, utilizing EDTA in which the ethylene backbone has been modified (EDTA-R), are represented in Schemes 2.1 and 2.2.

$$\text{Protein} + \text{EDTA-R} \longrightarrow (\text{Protein-R-Hedta})^{3-} + 3H^+ \quad \text{a.}$$

$$(\text{Protein-R-Hedta})^{3-} + Ru(H_2O)_6^{3+} \longrightarrow Ru(\text{Protein-R-Hedta})H_2O + 5H_2O \quad \text{b.}$$

Scheme 2.1

$$\text{Protein} + Ru(\text{Hedta-R})H_2O \longrightarrow Ru(\text{Hedta-R-Protein})H_2O$$

Scheme 2.2

Based on the results from the various methods of synthesis of [Ru^{III}(Hedta)H_2O] in this work, a suitable method for the production of the protein modified complex

outlined in Scheme 2.1 would involve the synthesis of the EDTA modified protein followed by metallation using $[Ru(H_2O)_6]^{3+}$ which had been produced by reduction of ruthenium oxide. For application to Scheme 2.2, the most suitable method would involve the synthesis of $Ru(H_2edta\text{-}R)Cl$ followed by its reduction then oxidation in aqueous media to produce $Ru(Hedta\text{-}R)H_2O$. The complex could then be allowed to react with the protein to produce the protein modified complex.

An important potential problem associated with Scheme 2.2, however, involves the known[26] dimerization of $[Ru^{III}(Hedta)H_2O]$ in aqueous solutions above pH = 8.5. Although no data is available at physiological pH (the likely pH for reaction with proteins) there exists a possibility that the complex will dimerize prior to reaction. Evidence supporting this was found in the UV-Visible spectra for pH = 7.34 solutions of $[Ru^{II}(Hedta)H_2O]^-$ which were obtained immediately following solution preparation and oxidation to Ru^{III} with O_2 and 24 hours after solution preparation (Figure 2.1). The appearance of the absorption band with λ_{max} =390 nm in the solution which was allowed to stand 24 hours is consistent with the reported formation of the dimer. The production of a strong absorption band with λ_{max} = 568 nm at pH = 11.3 which shifts to lower wavelengths with decreasing pH was reported by Ni, et al. in the same paper[26] and the species undergoes

reduction at a potential very close to that of the monomer. The observed formation of the dimer species in solution at physiological pH suggests that Scheme 2.2 may only be appropriate for use if the reaction is carried out very quickly, however, product purity may be questionable. It is concluded that the more suitable method for conjugate synthesis would follow that of Scheme 2.1.

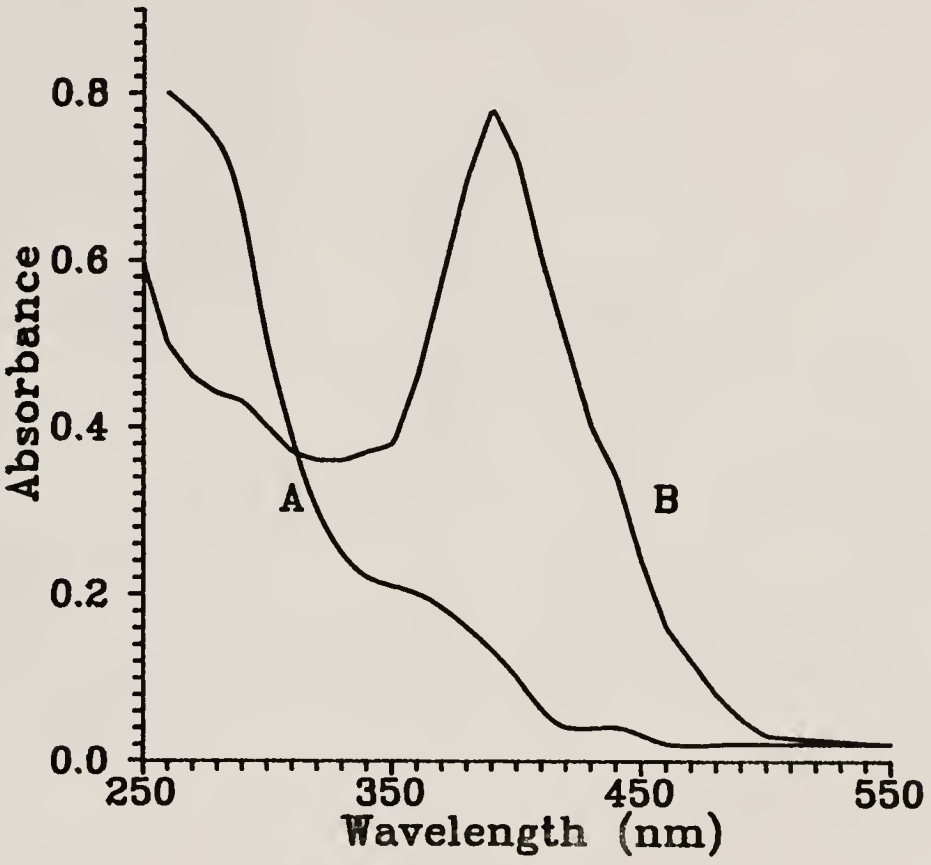

Figure 2.1. UV-Visible spectra of (a) freshly prepared $[Ru^{III}(Hedta)H_2O]$ in pH = 7.34 phosphate buffer and (b) the same solution after 24 hours.

Properties of New [Ru(Hedta)L] Complexes

[Ru^{III}(Hedta)1,10-phenanthroline]. The cyclic voltammogram of the complex dissolved in pH = 5.56 acetate buffer is reversible and is shown in Figure 2.2. The formal reduction potential was + 443 mV versus NHE, and the difference between anodic and cathodic peaks was 75 mV.

[Ru^{III}(Hedta)(pyridine)$_{1,2}\cdot 5H_2O$]. The cyclic voltammogram of the product dissolved in pH = 5.56 acetate buffer of 0.3M ionic strength is shown in Figure 2.3. Two formal reduction potentials were obtained from the reversible voltammograms. The first, representing the reduction of [Ru(Hedta)pyridine], was + 93 mV versus NHE with a difference in peak potentials of 88 mV. The second represents the reduction of [Ru(Hedta)$(pyridine)_2$] and occurred at + 400 mV versus NHE with a difference between anodic and cathodic peaks of 100 mV. Based on the relative areas for each reversible scan, it was calculated that the solid contained a mixture of 34.8% Ru(Hedta)$(pyridine)_2$ and 65.2% Ru(Hedta)pyridine.

[Ru^{III}(Hedta)(2,2'-dipyridine)$\cdot 12H_2O$]. The reversible cyclic voltammogram of the product dissolved in pH = 5.56 acetate buffer of 0.3M ionic strength is shown in Figure 2.4. The formal reduction potential was + 512 mV versus NHE and the difference between anodic and cathodic peaks was 75 mV. Shown in Figure 2.5, the UV-visible spectrum of Ru^{II}(Hedta)2,2'-dipyridine in phosphate buffer differs from

that of the oxidized form primarily in the region of 2,2'-dipyridyl absorption.

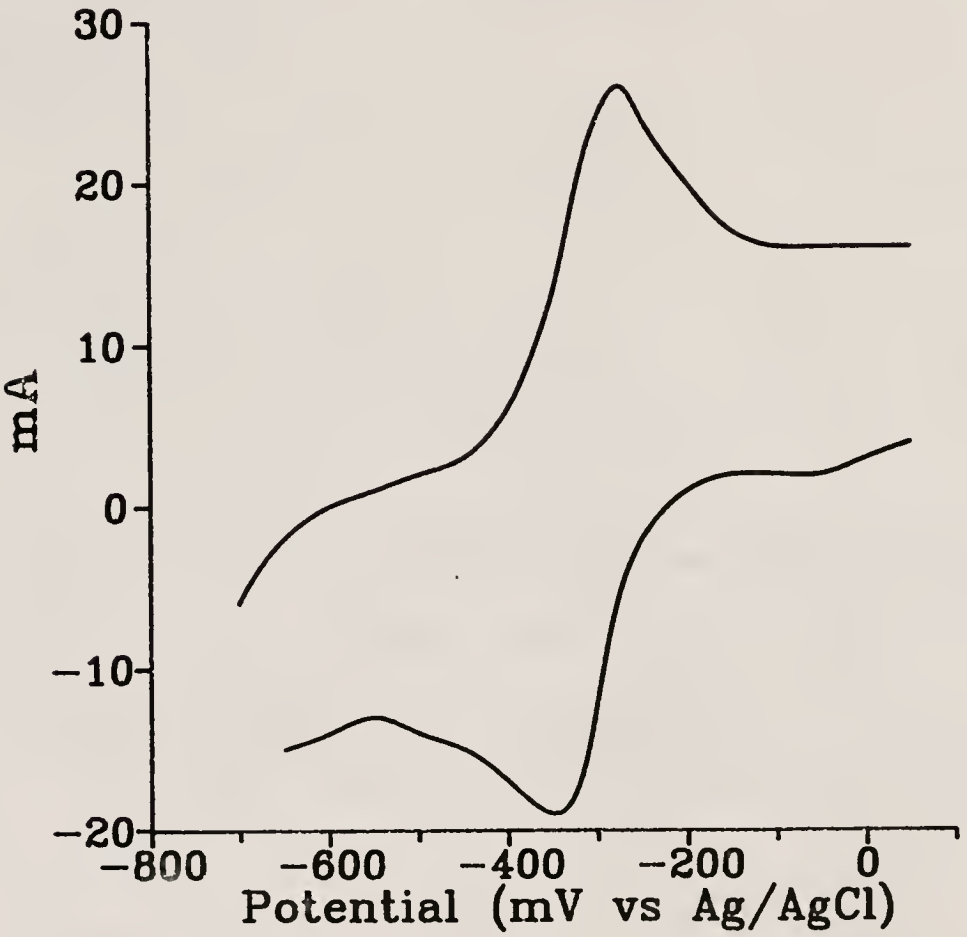

Figure 2.2. Cyclic voltammogram for Ru(Hedta)1,10-phenanthroline in pH = 5.56 acetate buffer, 0.3M ionic strength versus Ag/AgCl reference electrode. 20 mV/sec scan rate.

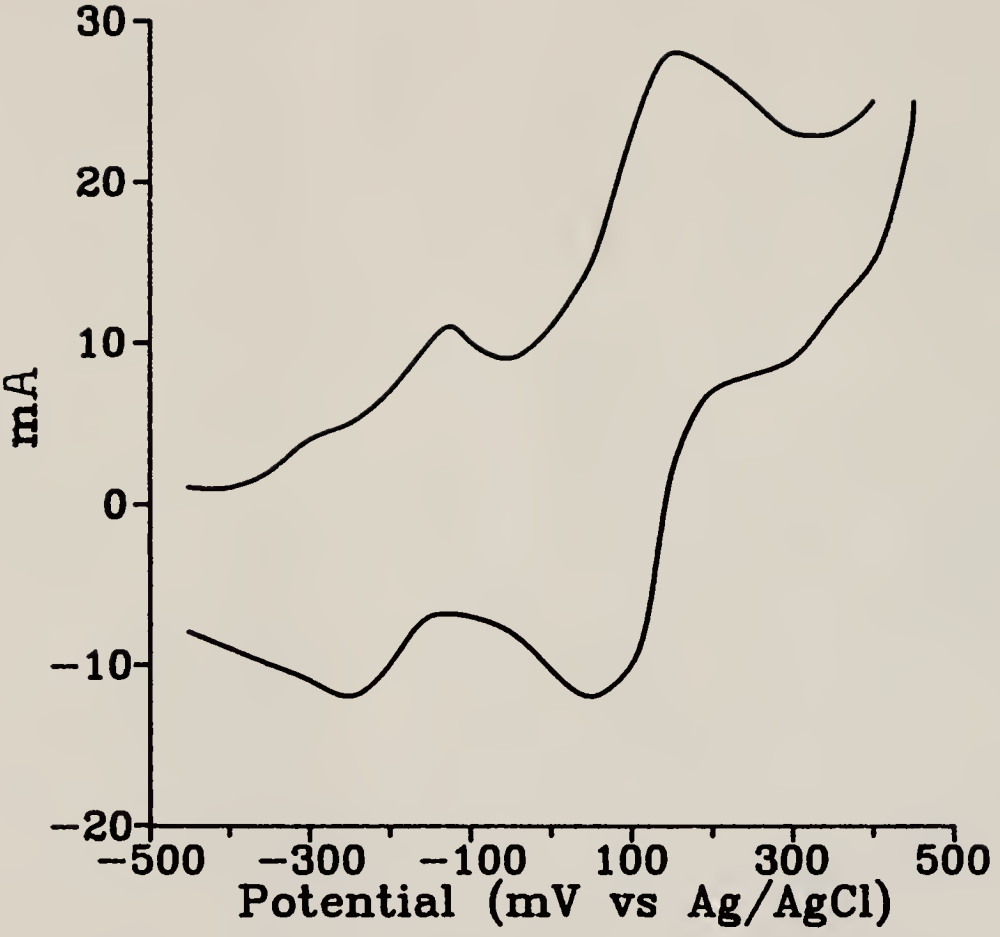

Figure 2.3. Cyclic voltammogram versus Ag/AgCl reference electrode of Ru(Hedta)(pyridine)$_{1,2}$·5H$_2$O in pH = 5.56 acetate buffer of 0.3 M ionic strength. 20 mV/sec scan rate.

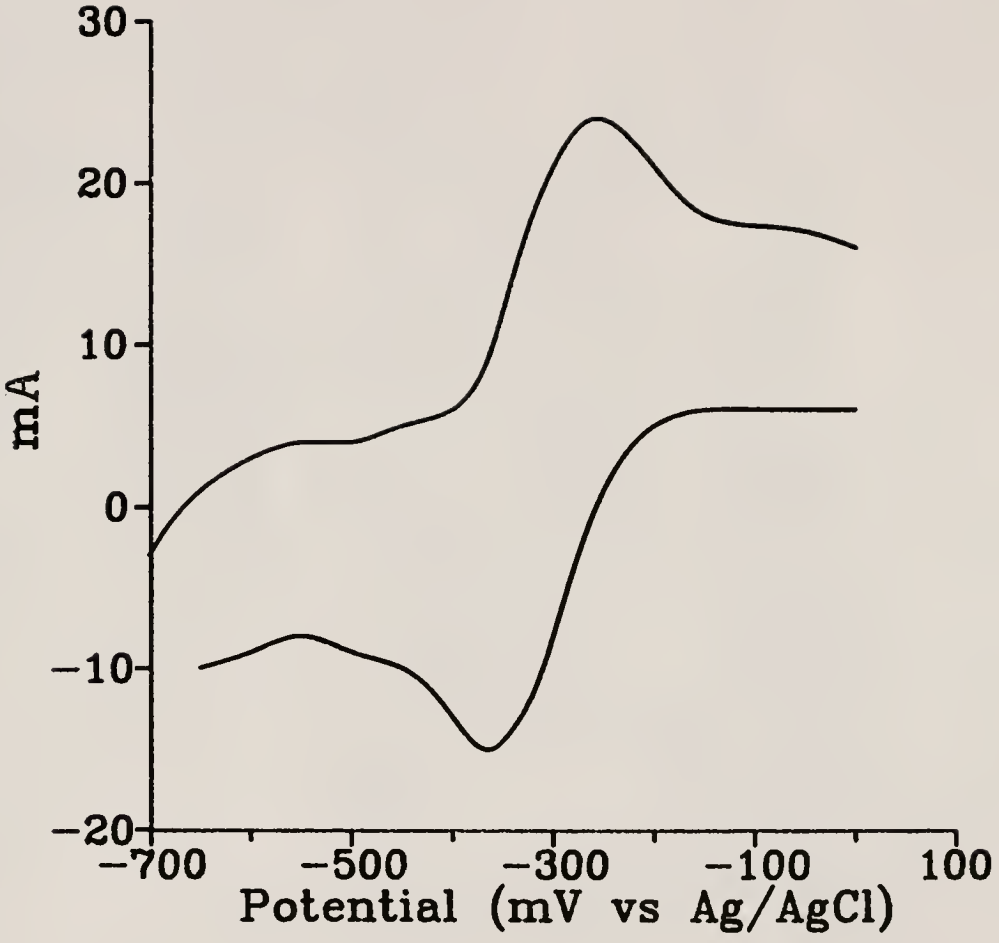

Figure 2.4. Cyclic voltammogram versus Ag/AgCl reference electrode for Ru(Hedta)2,2'- dipyridyl·12H_2O in pH = 5.56 acetate buffer of 0.3 M ionic strength. Scan rate = 20 mV/sec.

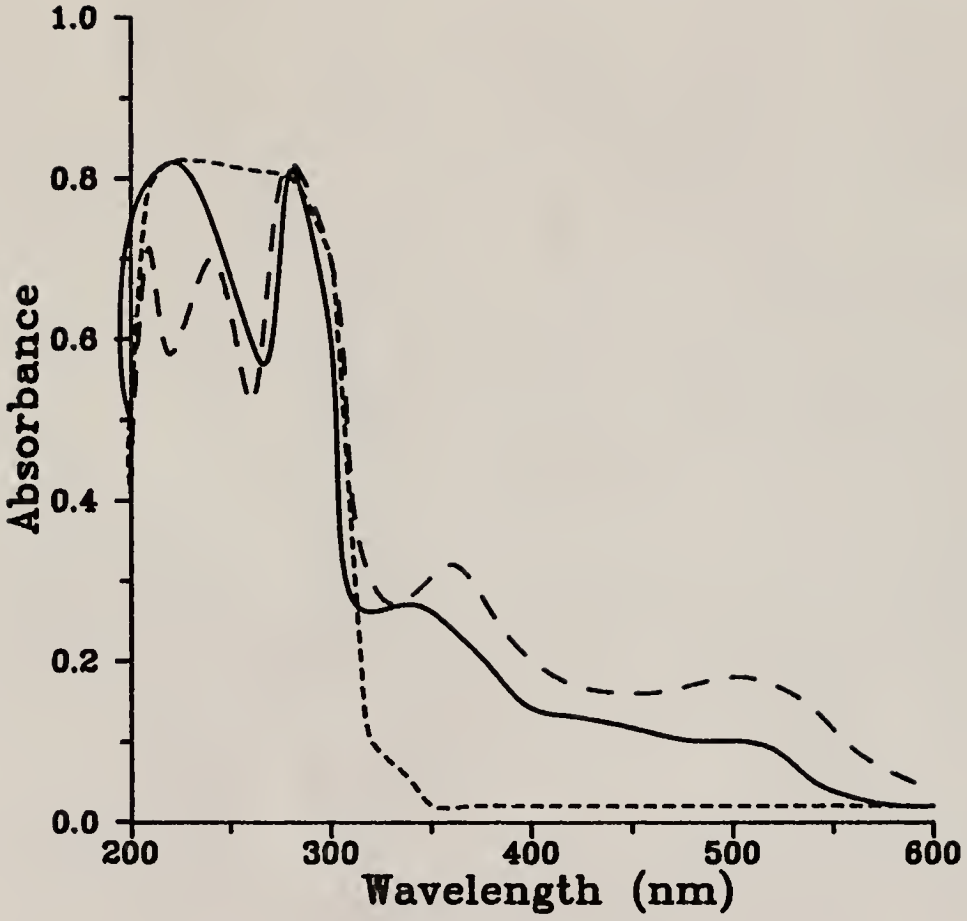

Figure 2.5. UV-Visible spectra for $[Ru^{III}(Hedta)2,2'\text{-dipyridyl}]$ (solid line) and $[Ru^{II}(Hedta)2,2'\text{-dipyridyl}]^{1-}$ (dashed line) and 2.2'- dipyridyl (dotted line) in pH = 7.36 phosphate buffer, 0.15 M ionic strength.

Electrochemistry Results

Reversible voltammograms were obtained for all complexes studied. Shown in Table 2.1, the formal reduction potentials for [Ru^{III}(Hedta)L] (for L = water, thiocyanate, acetonitrile, isonicotinamide, pyrazine and pyridine) obtained in this work at pH = 5.56 are, with the exception of thiocyanate, all within 20 mV of the pH = 5.5 values reported by Matsubara and Creutz.[17] The observed formal reduction potential for [Ru^{III}(Hedta)thiocyanate]$^-$ (+ 112 mV) was approximately 40 mV greater than that reported and may be accounted for by the presence of more than one inner sphere coordinated thiocyanate ion. In the same report, Matsubara and Creutz reported resolvable spectral changes as a result of the binding of one and two thiocyanate ions. Since the conditions for the preparation of [Ru^{III}(Hedta)L] in the present work were such that thiocyanate was in excess, it is probable that the species undergoing reduction may have been bis-isothiocyanato.

The large deviation in differences between anodic and cathodic peak potentials (ΔE_p) from the Nernstian 59 mV may be due in part to adsorption of the complexes on the working electrode while reduction was occurring. Thorough washing of the electrode prior to sample reduction did not alter this difference in peak potentials. The use of a hanging mercury drop electrode may provide for smaller peak potential differences.

Table 2.1. Formal reduction potentials, in mV versus NHE, for [Ru^{III}(Hedta)L] complexes.

Ligand	pH=5.56 E_f	pH=5.56 ΔE_p	pH=7.30 E_f	pH=7.30 ΔE_p	pH=8.95 E_f	pH=8.95 ΔE_p
water	-8	100	+18	113	-70	150
2-nitrobenzonitrile	+12	100	+8	106	-53	140
4-nitrobenzonitrile	+52	100	+15	118	-67	131
thiocyanate	+112	75	+102	95	+78	94
isonicotinamide	+190	81	+168	100	+133	130
acetonitrile	+249	75	+237	125	+225	140
pyrazine	+212	75	+256	90	+225	135
2-methylpyrazine	+249	75	+231	90	+213	160
pyridine (mono)	+112	81	+95	80	+72	160
(bis)	+402	81	+376	80	+363	85
1,10-phenanthroline	+443	75	NA		NA	
2,2'-dipyridyl	+512	75	NA		NA	

NHE = Normal Hydrogen Electrode.
ΔE_p = Difference between anodic and cathodic peak potentials (mV).
NA = Not assessed.

The most notable effect of pH on formal reduction potentials was observed for the aqua complex. At pH = 5.56, 7.30, and 8.95, the complex exhibited reduction potentials of -8, +18, and -70 mV, respectively. At the lower two pH values, the difference in reduction potentials are close to experimental error, however, at high pH a significant shift toward more negative reduction potential was observed and supports that the hydroxo complex was undergoing reduction. For the other complexes, with the exception of pyrazine, a general trend of more negative reduction potentials with increased pH is observed.

As shown in Table 2.1, at pH = 5.56 a potential range from -8 to +512 mV versus NHE was obtained when the new compounds [Ru(Hedta)1,10-phenanthroline] and [Ru(Hedta)(2,2'-dipyridine)] are included in the series of complexes. This represents a range which is 400 mV wider than the series investigated by Matsubara and Creutz. The inclusion of Ru(Hedta)$(pyridine)_2$, possibly a seven coordinate[27] complex, in the series at pH = 7.30 and 8.95 results in potential ranges from +18 to +376 and -70 to +363 mV versus NHE, respectively. It is expected that the inclusion of the 1,10-phenanthroline and 2,2'-dipyridyl complexes in these series of higher pH would increase the observed range in potentials by 200 mV.

Chapter Summary

The results of this work show that a number of different methods can be used to synthesize $[Ru^{III}(Hedta)H_2O]$. Of these methods, greatest yields are obtained from the conversion of $[Ru^{III}(H_2edta)Cl]$ to the aqua complex by either the presence of silver ion or the reduction of $[Ru^{III}(H_2edta)Cl]$ to form $[Ru^{II}(H_2edta)H_2O]$. A method of preparation involving the reaction of ruthenium oxide provides an alternative wherein the chelate is allowed to react directly with $[Ru(H_2O)_6]^{3+}$. This method resulted in low yields but may be the most viable for future application in modifying proteins with ruthenium chelates.

The nature of the bond between the protein and EDTA and potential implications concerning the lability of the inner-sphere coordinated water molecule when $[Ru^{III}(Hedta)H_2O]$ has been covalently linked to the protein needs to be addressed in future work. The electron withdrawing ability of the linking function on EDTA, carrier hydrogen bonding with the uncoordinated acetate function or steric crowding by the carrier could adversely effect the rate of aqua ligand substitution and may present potential problems for synthesis and use of these new conjugates. It is important that the lability of $[Ru^{III}(Hedta)H_2O$ be maintained following conjugation so that the substitution reaction with π-acids can be utilized to easily prepare a series of

protein-[edtaRu^{III}L] complexes from the protein-[edtaRu$^{III}H_2O$] conjugate. Prior to evaluating these protein conjugates, cyclic voltammetry should be conducted using complexes which contain the modified EDTA and results compared with the reduction potentials obtained in this work.

The complexes [Ru^{III}(Hedta)1,10-phenanthroline] and [Ru^{III}(Hedta)2,2'-dipyridine] represent new compounds, and their formal reduction potentials are so positive that their inclusion in the series of complexes provides a range in reduction potentials 400 mV wider than that obtained in previous work involving [Ru^{III}(Hedta)L] complexes. The reduction potentials for both complexes suggest that both nitrogen donor atoms in the ligands are coordinated to the metal center. Whether a coordinating acetate function of EDTA is displaced as a result of the substituting ligand's apparent bidenticity or the metal center becomes seven coordinate as a result of the substitution reaction has not been evaluated. Further investigations of these complexes should include nuclear magnetic resonance (proton and carbon) and X-ray crystallography to provide information concerning their structure.

Examination of frequency shifts of the acetate carbonyl stretch for the series of [Ru^{III}(Hedta)L] complexes does not provide information concerning the relative electron density on the metal as a function of the π-acidity of the ligand,

L, but frequency intensity data does provide information concerning the absence or presence of a protonated free arm of the EDTA ligand.[28] An investigation of the intensities of infrared carbonyl stretches for the 1,10-phenanthroline and 2,2'-dipyridyl complexes may provide information concerning the denticity of the EDTA ligand when these other ligands are coordinated to Ru^{3+}. These new complexes of [Ru^{III})(Hedta)1,10-phenanthroline] and [Ru^{III}(Hedta)2,2'-dipyridine] should provide protein conjugate analogs in which the redox tuning ligand is less likely to be displaced by π-acid ligands available in biological media than many of the other ligands studied.

CHAPTER 3

SYNTHESIS AND CHARACTERIZATION OF POLYSACCHARIDE ESTERS OF POLYAMINOPOLYCARBOXYLIC ACIDS AND THEIR GADOLINIUM(III) COMPLEXES

Chapter Overview

Magnetic resonance imaging (MRI) is a noninvasive diagnostic aid that has rapidly become the method of choice for the initial screening of patients suspected of a variety of physiological disorders including certain types of cancer.[29-31] The method often benefits from the intravenous injection of paramagnetic compounds called contrast agents into patients immediately prior to data acquisition in MRI. These agents serve to provide contrast between different tissue types by enhancing the relaxation differences of the associated water protons.

Gadolinium$^{(III)}$ diethylenetriaminepentaacetic acid (GdDTPA)[32-36] and other paramagnetic compounds[37-39] have been used successfully as contrast agents to enhance the imaging of several types of carcinomas in non-clinical evaluations. GdDTPA, the only agent currently approved for human use, undergoes rapid renal excretion following

extracellular biodistribution with a blood concentration half-life of only 20 minutes.[40] The short persistence and extravascular distributive properties of GdDTPA make the contrast agent ineffective for situations where a lengthy blood-pool persistence of the agent may be required for specific organ and/or lesion uptake to occur and unsuitable for use in blood flow evaluations.

Several alternatives to GdDTPA have been proposed, including agents that contain different paramagnetic metal ions and chelating ligands[41,42] and magnetic cluster or spherical compounds.[43,44] GdDTPA, however, exhibits a large spin-lattice relaxation (T_1) effect,[45,46] the DTPA chelate affords the complex great (10^{22}) thermodynamic stability[3] and, relative to most of the proposed alternatives, these aspects of GdDTPA make the compound superior. In the development of new contrast agents it is advantageous to retain these more desirable qualities of GdDTPA.

One approach toward overcoming the specific limitations of GdDTPA involves the covalent attachment of the well characterized and clinically evaluated GdDTPA on to macromolecular carriers.[47] The use of macromolecular carriers may result in compounds that exert greater effect on T_1 relaxation of surrounding water molecules[48] as well as enhanced blood-pool persistence and possible tissue specificity relative to GdDTPA. Although several of the variables that must be considered in the design of new

contrast agents are addressed by using macromolecular carriers, the biological effect and fate of the carrier and carrier-complex must also be considered.

Carrier molecules have been used extensively in pharmaceutical applications and the same requirements for application to macromolecule carried drugs are applicable to macromolecular based contrast agents. These requirements are:[49] (1) the agent must retain activity following conjugation, (2) the carrier must be nontoxic, nonimmunogenic, and nonantigenic, (3) the carrier must be biodegradable, and (4) the desirable properties of the carrier must be retained following conjugation.

At the inception of this study, prior art consisted of the use of proteins or lipids as macromolecular carriers. Proteins such as bovine serum albumin or immunoglobulin G, which have been used as carrier molecules[50,51] in GdDTPA conjugates, would elicit an immune response when used *in vivo* and the level of loading of the paramagnetic agent on the protein is low. These properties, in addition to compromised thermodynamic and/or kinetic stabilities of the metal-chelate moiety, are also potential problems for the recently reported GdDTPA-crosslinked polysaccharide compounds[52] (compounds in which the polysaccharide chains were covalently linked together by the chelating agent). The use of polysaccharides as carrier molecules, however, specifically dextrans with average molecular weights less

than 90,000 or inulin (in which the products are not crosslinked by the chelate), may result in products which do not possess these undesirable properties.[53]

Dextran contains a large number of secondary and very few primary alcohol functions and has 1⟶6 linked α-D-glucopyranose units with some 1⟶4 side branching present. Inulin is a linear chain containing α-D-fructofuranose units with a large number of both primary and secondary alcohol functions. For both of these polysaccharides, the large number of alcohol functions available for chemical modification is an attractive feature in terms of the potential application of these compounds as macromolecular carriers.

In addition to the possibility of high GdDTPA loading relative to that attainable with proteins, dextran and inulin polysaccharides are nontoxic and undergo normal metabolism. Other desirable qualities of the polysaccharides include low expense, hydrophilicity, pH stability, precedence in drug delivery, and increased plasma persistence of the conjugated moiety.[49,54] Additionally, the potential for lanthanide - promoted decomposition of the chelate to carrier ester linkage[55] in these polysaccharide based complexes may provide a mechanism for the timely release of the metal chelate from the carrier. These properties suggest that the compounds may be useful contrast agents.

The goals of the present study included the synthesis of dextrans ranging in average molecular weight from 9,400 to 487,000 and inulin (5,000 average molecular weight) that have been extensively labeled with GdDTPA by one ester bond per GdDTPA moiety. The purpose of the work was to develop a means by which new compounds, which may exhibit properties superior to the commercially available contrast agent (GdDTPA), could be easily produced. The repetitive structure of the dextrans and inulin allows for the treatment of the DTPA-polysaccharides and GdDTPA-polysaccharides as monomer units in some of the evaluations required for product characterization. Characterization of the esters was intended to evaluate the degree of GdDTPA loading on to the polysaccharide (i.e. the number of GdDTPA molecules covalently attached to the polysaccharide molecule per repeating saccharide unit), provide viable evidence for products that are not crosslinked by the chelate, determine the thermodynamic stability of the new compounds, evaluate the relative rates of metal promoted ester hydrolysis in the gadolinium complexes and the apo-conjugates, and to investigate the *in vitro* solvent T_1 relaxation effects by the gadolinium complexes using nuclear magnetic resonance (NMR). In order to accomplish these goals, it was necessary to devise a method of synthesis that would: (1) provide reproducibly high levels of loading of the chelate on to the polysaccharide carrier, (2) result in products that are not

crosslinked by the chelate (in which only one carboxyl function of the chelate is required in ester bond formation), and (3) result in no degradation of the polysaccharide carrier.

Materials and Methods

Synthesis of DTPA-Polysaccharides

Synthesis of anhydrides of DTPA. The isobutyl and ethyl mixed anhydrides of DTPA were prepared by method of Krejcarek and Tucker[56]. A 1:5 mole ratio of DTPA (Aldrich) to triethylamine (Kodak) in anhydrous acetonitrile (Aldrich) were used. Isobutylchloroformate (Aldrich) or ethylchloroformate (Kodak) was reacted with the triethylamine salt. Following precipitation of solid triethylamine-hydrochloride, the cold mixture was filtered and solid washed by cold filtering with acetonitrile. The washings were added to the filtrate and the solution was rotary-evaporated to form a white paste. Repeated washing and decantation with anhydrous ethyl ether resulted in a white powder following vacuum drying in a desiccator.

The dicyclic anhydride of DTPA was prepared, isolated, and washed by method of Eckelman[57]. Acetic anhydride (Fisher) was reacted in a 4 to 1 mole ratio with DTPA in ACS grade pyridine (Aldrich). It was found that heating at 65^{o}C for 24 hours resulted in significant product discoloration.

Heating at 45°C did not result in the formation of the dark brown solid/solution and this temperature was used in all subsequent Eckelman based cyclic anhydride preparations.

Modifications in Eckelman's method[57] were used to produce the monocyclic and mixtures of mono- and dicyclic anhydrides of DTPA. Reaction mixtures containing mole ratios of DTPA to acetic anhydride of 1.0:1.0, 1.0:1.0 with a trace amount of trifluoroacetic anhydride (Fisher) present, 1.0:2.0, and 1.0:3.2 were used.

Halpern's method[58] of synthesis and isolation was also used to produce the reported monocyclic anhydride. Thionyl chloride (Fisher) was reacted with DTPA in the presence of excess trifluoroacetic anhydride (Fisher).

Synthesis of acid esters of polysaccharides. All glassware was oven dried prior to use. All reactions were conducted in flasks equipped with a condensing or vigreaux column topped with a calcium chloride drying tube. All preparations which required the use of trifluoroacetic anhydride or acetic anhydride were, following the reaction heating time, heated sufficiently to distill off their respective acids. Damp litmus held above the heated flask contents was used to ascertain the completeness of removal of these acids. All polysaccharides were lyophilized for 3 hours prior to use. Acetone was used to precipitate products and hydrated cyclic anhydrides (DTPA) in all preparations involving the reaction of mono- or di- cyclic

anhydrides of DTPA. Methanol or ethanol was used to precipitate products and DTPA in all preparations in which the mixed anhydrides were used. In all reaction conditions tried, a ratio of one mole of mixed or cyclic anhydride to one mole of alcohol function per mole repeating glucopyranose or fructofuranose unit of the polysaccharide was used.

The reactions of the mixed anhydrides with polysaccharides were carried out using the following three general reaction conditions:

1.) Refluxing in pyridine (or pyridine and dimethyl-sulfoxide sufficient to solubilize the dextrans) for from one to two hours.

2.) Stirring at room temperature from 15 minutes to 12 hours in dimethylsulfoxide or benzene following activation of the polysaccharide alcohol functions. This activation was accomplished by the addition of one mole of n-butyl lithium (in hexane, Aldrich) with one mole of alcohol function per mole of repeating unit on the polysaccharide.

3.) Heating at 60^{o}C in a one to one volume ratio of pyridine (Aldrich) to formamide (Kodak) solvent system for four hours with and without the presence of anhydrous zinc chloride.

The reactions which involved the dicyclic anhydride reacting with the polysaccharides were conducted using the following two general reaction conditions:

1.) Refluxing in toluene (Fisher) in the presence of a trace quantity of trifluoroacetic anhydride (Fisher) for one to four hours.

2.) Heating at 60°C in 1 to 1 volume ratio of pyridine and formamide with and without the presence of anhydrous zinc chloride.

The reactions involving the prepared monocyclic anhydride or mixture of mono- and dicyclic anhydrides reacting with the polysaccharides were conducted under the following two general reaction conditions:

1.) The monocyclic anhydride prepared by Halpern's[58] method was refluxed with the polysaccharide in 1 to 1 pyridine and formamide for four hours in the presence of zinc chloride.

2.) The monocyclic anhydrides or mixture of mono- and dicyclic anhydrides prepared by stoichiometric control of the ratio of DTPA to acetic anhydride from 1:1 to 1:3.2 were conducted with and without a trace quantity of trifluoroacetic anhydride present in 1 to 1 pyridine and formamide. The reactions were carried out at either 60°C or 45°C for 4 to 5 hours in the presence of zinc chloride (when no trifluoroacetic anhydride was used).

Optimized carrier-ligand synthesis. The optimized method of synthesis for the DTPA esters of the polysaccharides involved the synthesis of a mixture of the mono- and di-cyclic anhydrides of the acid and the sub-

sequent reaction of this mixture with the polysaccharide. A detailed method for synthesis is provided as follows.

Diethylenetriaminepentaacetic acid (0.1 mole) was placed in 200 milliliters of anhydrous pyridine and heated at 45°C while stirring for 24 hours with 3.2 mole acetic anhydride. During the process, all of the solid dissolved and near the end of the reaction time a solid precipitated. The solid was filtered, washed with acetic anhydride followed by anhydrous ethyl ether, and dried under vacuum in a desiccator.

The polysaccharide (either inulin or dextrans with average molecular weights of 9400, 40200, 78000, or 487000, all obtained from Sigma) was placed in a flask containing a 1 to 1 volume mixture of pyridine and formamide[59] which had been previously dried over molecular sieves. The weight ratio of mixed solvent to polysaccharide was approximately 250 to 1. The flask contents were stirred while heating at 40°C for 1/2 hour to dissolve the polysaccharide. For each gram of polysaccharide used, either 1/2 milliliter of anhydrous pyridine made turbid with zinc chloride or 0.1 milligram of anhydrous zinc chloride was added to the reaction flask and heating continued for 1/2 hour. One mole of the prepared cyclic anhydride per mole of repeating glucopyranose or fructofuranose unit of the polysaccharide was placed in the flask and the contents were stirred while heating at 50°C for four hours under a small reflux

condenser equipped with a calcium chloride drying tube. Glucopyranose repeating unit concentrations in all preparations were 0.1 M. In a typical procedure, 4.7 g (0.50 mmol polysaccharide, 26 mmol glucopyranose) dextran 9400 was placed in a flask with 250 mL of 1:1 volume mixture of formamide and pyridine. The flask contents were stirred while heating at 40°C for 1/2 h to dissolve the polysaccharide. Following the addition of 0.5 mg of anhydrous zinc chloride (Aldrich), the heating was continued for 1/2 h. To the solution, 10.2 g (26 mmol) of the prepared cyclic anhydride was added. The flask contents were stirred while heating at 50°C for 4 h under anhydrous conditions. After cooling to room temperature, the solution was rotary-evaporated to approximately 1/2 the original volume. The solution was cooled in an ice bath and acetone was added to precipitate the solid. The solid was filtered, washed with cold acetone followed by anhydrous ethyl ether, and dried under vacuum in a desiccator.

Determining Reaction Success by HPLC

All HPLC experimental work was conducted in pH = 7.0 phosphate buffer solution of 0.10 M ionic strength. A Waters Model 6000A solvent delivery system was used with a standard silica pre-column and Waters Protein-Pak 125 column. Detection was at 230 nm using an Instrumentation

Specialties Company model 1840 absorbance monitor. A flow rate of 0.5 mL/minute was used for all evaluations.

Following the isolation of solid esterified polysaccharides and the unreacted aminopolycarboxylates, approximately 0.5 mg of the solid was dissolved in 1.0 mL of the eluting buffer. Between 10 and 30 microliters of the solution was injected into the HPLC port. The resulting elution profiles were obtained using a detector sensitivity of 0.2 and a Scientific Products Quantigraph recorder. Traces of the elution peaks were obtained and the mass of each peak was used to calculate the approximate mass percent of DTPA reacted. It was assumed that the extinction coefficient of the product(s) was the same as that of DTPA at 230 nm.

Fractions of the eluting solution were collected over one minute intervals using an LKB Bromma Redirac model 2112 fraction collector. These fractions were subjected to sugar assay.[60] A mixture of 300 microliters of each fraction with 20 microliters of 80% phenol (in water) was vortexed for 10 seconds followed by the addition of 1.0 milliliter of concentrated sulfuric acid to the center of the vortexing solution. Following 5 additional seconds of vortexing, the solutions were cooled to room temperature and absorbances at 490 nm (IBM Model 9430 UV-Visible spectrophotometer) were recorded within one hour of solution preparation.

The sugar assay absorbances were superimposed on the HPLC elution profiles for each sample. The results were compared with : the standard elution profiles obtained by sugar assays for the unmodified polysaccharides; the elution profiles for the unmodified polysaccharides after undergoing the identical esterification reaction but without the reactant anhydride present; the elution profile for the unmodified polyaminopolycarboxylic acid.

Purification of DTPA-Polysaccharide Esters

Spectrapor molecular porous membrane tubing (Spectrum Medical Industries) with a globular protein molecular weight cut-off range from 6,000 to 8,000 average molecular weight was used. The dialysis tubing was soaked in an 80^{o}C solution of 1.0 M EDTA for 1 hour and rinsed six times with deionized water prior to use. Sugar assay (method given in HPLC section above) of the wash solutions was used to ascertain the suitability of the protein cut - off range of the tubing for the polysaccharides. The isolated solid products were dissolved in deionized water (approximately 1 g /3 mL), placed in the dialysis tubing, and dialyzed against deionized water at room temperature for 72 hours. Wash solutions were changed every 12 hours. Dialysis was terminated when the pH of the wash solutions became constant. The solid polysaccharide esters were isolated by

rotary-evaporation of the dialysis bag contents followed by lyophilization for 24 hours.

Elemental analyses of typical products obtained from the general method of synthesis were calculated based on the general formula (attached DTPA unit)$_y$(average esterified polysaccharide unit)$_1$. In all cases, the unmodified polysaccharide was analyzed independently so the effect of polysaccharide branching on the average repeating glucopyranose or fructofuranose could be accounted for. DTPA-Inulin, calculated for $(C_{14}H_{22}N_3O_9)_{0.53}(C_{5.5}H_{9.06}O_{5.11})$: C, 43.54; H, 5.86; N, 6.25. Found: C, 43.82; H, 6.05; N, 6.07. DTPA-Dextran 9400, calculated for $(C_{14}H_{22}N_3O_9)_{0.42}$ $(C_6H_{10.95}O_{6.04})$: C, 42.24; H, 6.02; N, 5.22. Found: C, 42.93; H, 6.22; N, 5.28. DTPA-Dextran 40200, calculated for $(C_{14}H_{22}N_3O_9)_{0.38}(C_6H_{11.04}O_{5.85})$: C, 41.01; H, 6.27; N, 5.12. Found: C, 41.92; H, 6.04; N, 4.92. DTPA-Dextran 70800, calculated for $(C_{14}H_{22}N_3O_9)_{0.36}(C_6H_{10.83}O_{5.75})$: C, 42.71; H, 6.09; N, 4.87. Found: C, 42.64; H, 6.20; N, 4.86. DTPA-Dextran 487000, calculated for $(C_{14}H_{22}N_3O_9)_{0.06}$ $(C_6H_{11.23}O_{6.05})$ C, 40.52; H, 6.24; N, 1.24. Found: C, 41.12; H, 6.57; N, 1.25. For dextran 487000, the product was also prepared by the general method but the reaction solution was allowed to stir at room temperature for 30 h prior to precipitation and isolation of product. The calculated mass percents for a product prepared in this

manner was $(C_{14}H_{22}N_3O_9)_{0.82}$ $(C_6H_{10.47}O_{6.05})$: C, 43.02; H, 5.89; N, 7.06. Found: C, 42.94; H, 6.05; N,7.08.

Nature of Reacted Polysaccharide by HPLC

The isolated solids (approximately 0.5 mg) were each dissolved in pH = 7.0 phosphate buffer. Approximately 20 microliters of each solution was injected into the HPLC port and an elution profile was obtained. Eluent fractions were collected at one minute intervals and subjected to sugar assay. The resulting elution profiles and superimposed sugar assays were compared with the elution profiles of the unmodified aminopolycarboxylic acids.

The HPLC results following purification (above) were compared with the sugar assays of the unmodified polysaccharides. The elution profiles were also compared with those of the polysaccharides following their subjection to conditions identical to those of the reaction but without the prepared cyclic anhydride present.

Synthesis and Purification of Gadolinium Complexes

The gadolinium complexes of EDTA, DTPA, and TTHA were prepared by a method outlined for $H_2GdDTPA$ by Wenzel.[61] Ethylenediaminetetraacetic acid (Mallinckrodt), diethylenetriaminepentaacetic acid (Sigma), and triethylenetetraaminehexaacetic acid (Sigma) were used as supplied. The hexahydrate of $GdCl_3$ (Aldrich) was used instead of Gd_2O_3

in the preparations and acetone was used to precipitate the solids.

Metallation of the esterified polysaccharides was achieved by dissolving the solids in deionized water followed by the addition of a 0.2 molar stoichiometric excess of the hexahydrate of $GdCl_3$ (Aldrich). The solutions were stirred at room temperature for 1 hour, placed in dialysis tubing, and exhaustively dialyzed against water at room temperature until the wash solutions tested negative for gadolinium ion with xylenol orange indicator (Aldrich). The dialysis bag contents were rotary-evaporated to dryness and the solids were lyophilized for 24 hours. A portion of each of the solids was retained for elemental analysis and the remainder was dissolved in deionized water and dialyzed for 48 hours against a 0.1 M solution of EDTA at room temperature followed by dialysis against water for 48 hours. The dialysis bag contents were then rotary-evaporated to dryness and lyophilized for 24 hours.

Elemental analysis and ICP analysis were conducted on the products. Some calculated and observed compositional results are as follows for products prepared as outlined in the general method of synthesis and the calculated results are based on the general formula Gd_x(attached DTPA unit)$_y$(average esterified polysaccharide unit)$_1$. GdDTPA-Inulin, calculated for $Gd_{0.52}(C_{14}H_{17}N_3O_9)_{0.57}(C_{5.5}H_{9.02}O_{5.11})\cdot 2.0H_2O$: Gd, 17.24; C,

31.60; H, 4.82; N, 5.05. Found: Gd, 17.16 +/- 1.43; C, 31.77; H, 4.77; N, 4.90. GdDTPA-Dextran 9400, calculated for $Gd_{0.36}(C_{14}H_{17}N_3O_9)_{0.36}$ $(C_6H_{11.21}O_{6.04})\cdot 0.3H_2O$: Gd, 15.06; C, 35.28; H, 4.81; N, 4.02. Found: Gd, 15.4 +/- 0.4; C, 35.16; H, 5.18; N, 3.92. GdDTPA-Dextran 40200, calculated for $Gd_{0.31}(C_{14}H_{17}N_3O_9)_{0.36}$ $(C_6H_{11.06}O_{5.85})\cdot 0.4H_2O$: Gd, 13.30; C, 36.19; H, 4.95; N, 4.13. Found: Gd, 13.7 +/- 0.6; C, 36.52; H, 5.44; N, 4.03. GdDTPA-Dextran 70800, calculated for $Gd_{0.36}(C_{14}H_{17}N_3O_9)_{0.36}$ $(C_6H_{10.83}O_{5.75})\cdot 0.8H_2O$: Gd, 14.91; C, 34.92; H, 4.92; N, 3.98. Found: Gd, 14.6 +/- 0.5; C, 35.11; H, 5.43; N, 4.00. GdDTPA-Dextran 487000, calculated for $Gd_{0.04}(C_{14}H_{17}N_3O_9)_{0.06}$ $(C_6H_{11.23}O_{6.05})\cdot 0.1H_2O$: Gd, 2.99; C, 39.02; H, 5.96; N, 1.20. Found: Gd, 2.6 +/- 0.3; C, 39.02; H, 6.17; N, 1.02. For the product in which the highly loaded DTPA-Dextran 487000 was used, the calculated for $Gd_{0.78}(C_{14}H_{17}N_3O_9)_{0.79}$ $(C_6H_{10.50}O_{6.05})\cdot 1.5H_2O$: C, 32.92; H, 4.36; N, 5.33. Found: C, 32.40; H, 4.59; N, 5.34. The product could not be evaluated by ICP analysis as it was too insoluble in deionized water for solution preparation.

Characterization of Compounds

Elemental analysis. All elemental analysis were conducted by the Department of Chemistry's Spectroscopic Services. Samples of each of the compounds were submitted

for evaluation immediately following lyophilization of the products.

Infrared analysis. The carbonyl stretching frequencies of the aminopolycarboxlyate esters of the polysaccharides, the unmodified acids, and their gadolinium complexes were evaluated by Fourier Transform Infrared spectroscopy (Nicolet 5DXB FTIR). Several of the prepared cyclic anhydrides of DTPA were also evaluated by infrared analysis of the carbonyl stretching region. All spectra were obtained as Nujol mulls of the samples using sodium chloride plates. The scans ranged from 2500 to 1000 wavenumbers. No solvent subtraction technique was employed as characteristic Nujol stretching frequencies did not interfere with those of the compounds or complexes in the spectral region evaluated.

Inductively coupled plasma analysis. Weighed samples of each of the complexes (Mettler AE163 balance) were dissolved in deionized water and evaluated for mass percent gadolinium by ICP (Perkin Elmer Plasma II Emission Spectrometer). A calibration curve of emission counts versus gadolinium concentration was obtained at the start of each session following ICP initialization. Dilutions of a standard solution of $GdCl_3$ in 1% HNO_3 (Aldrich Chemical Co.) were used to obtain the calibration curves.

Each sample solution was evaluated five times with 30 seconds read delay between successive evaluations. The

average of the trials and their standard deviations (in parts per million) was taken as the accepted solution concentration after conversion to units of molarity. Three solutions of each complex were subjected to ICP analysis, the results averaged, and mass percent gadolinium calculated. In addition to verification of mass percent gadolinium, the ICP was used in identical fashion to evaluate gadolinium concentrations for all solutions for subsequent use in *in vitro* relaxivity studies and *in vivo* imaging studies (Chapter 4).

Nuclear magnetic resonance analysis. Spectra of some of the DTPA esterified polysaccharides were obtained in deuterium oxide. A Varian XL-VXR 300 nuclear magnetic resonance instrument was used.

Potentiometric titrations. All potentiometric titrations were conducted at 25.0°C (0.05°C precision, I_2R Thermowatch Model L6 1000 SS) using a standard pH meter (Orion Research Digital pH/Millivolt Meter 611) and a semimicro combined pH electrode (Orion Research Gel Filled). All solutions were purged with argon for 1/2 hour prior to use. Solutions containing from 0.12 to 0.14 mmole DTPA or esterified DTPA were prepared in 100 mL of argon purged 0.1 M KNO_3 solutions. Metallation was accomplished by titration of the esters with a solution of 18.8 mM Gd^{3+} in 0.0100M HNO_3. The mole ratio of Gd^{3+} added per DTPA moiety was one to one. Following metallation, the added HNO_3 was

neutralized with KOH prior to potentiometric titration. Titrations were conducted using 0.100 M KOH and constant ionic strength was maintained with KNO_3. Approximate log K_a values for the ligands were obtained using the computer program PKAS,[62] and refinement of these values and the approximated thermodynamic stability constants for the metal complexes was achieved with the computer program BEST.[62]

Ester hydrolysis studies. Solutions containing 15 mM DTPA moiety of the esterified polysaccharides or 15 mM gadolinium in the esterified metal chelates were prepared in pH = 7.4 phosphate buffer of 0.15 M ionic strength. The solutions were placed in a water bath maintained at 37.0°C for 4 days. Portions of each solution were removed at regular intervals and subjected to HPLC analysis using the same phosphate buffer of 0.15 M ionic strength to elute the samples. Detection was at 235 nm and a Waters Protein Pac 125 column was used. The relative areas under the curves in each elution profile for the intact (elution peak for DTPA esterified polysaccharide) and hydrolysed ester (elution peak for DTPA) were used to calculate the percent decomposition (hydrolysed ester peak area / intact ester peak area) for the esterified polysaccharides. The relative areas under the curves in each elution profile for the intact (elution peak for GdDTPA-polysaccharide) and hydrolysed esters (elution peak for GdDTPA) were used to calculate the percent decomposition (GdDTPA peak area /

GdDTPA-polysaccharide peak area) for the gadolinium complexes of the esterified polysaccharides.

T_1 relaxivity studies. Standard solutions of each of the GdDTPA-polysaccharide complexes and Magnevist were prepared in pH = 7.4 phosphate buffer. The ionic strength of the buffer was 0.15 M (isotonic with blood) and was deoxygenated by one hour of argon bubbling. Gadolinium concentrations of each of the solutions was evaluated by inductively coupled plasma emission spectroscopy. Dilutions of each of the standard solutions with the buffer were then made such that one mL total volumes of solutions containing 1, 2, 4, and 5 mM Gd^{3+} were obtained. The solutions were sonicated to thoroughly mix for 15 minutes.

Approximately 0.5 mL of each of the solutions was placed in 5 mm NMR tubes which had been previously cleaned with 0.1 M EDTA solution to remove trace metal ions, rinsed, and oven dried. A sealed internal coaxial reference tube (prepared from 1.5 - 1.8 mm Kimax capillary tubing) containing deuterium oxide and methanol was used to provide the NMR lock signal and spectrum reference. The NMR tubes were sealed with rubber septa and stored at $4^{o}C$.

The NMR measurements were obtained using a JOEL FX100 Fourier Transform NMR spectrometer operating at 99.55 MHz resonance frequency with a probe temperature of $25^{o}C$. The method for solution T_1 evaluation was similar to that outlined by Brown and Johnson[63]. An inversion recovery pulse

sequence was used and consisted of a 180^{o} pulse followed by time Tau and a 90^{o} pulse. A total of 4096 data points were collected per scan over a spectral width of 500 Hz. Each scan required 4.09 seconds acquisition time and four free induction decay curves were obtained per τ value. The average of the 4 scans was recorded for each of the τ values. A pulse delay of 2.5 seconds was used for all gadolinium containing solutions. A pulse delay of 10 seconds was used for T_1 evaluation of the buffer solution.

Using the display monitor only, the approximate T_1 of each solution was obtained by varying values of τ manually such that the water proton signal intensity approached zero. These approximate values ranged from 5 to 150 msec and were dependent on gadolinium concentration. The $\tau_{infinity}$ data for all gadolinium containing samples was collected at τ = one second to assure accuracy in the measurement. A total of 9 to 14 τ values, excluding $\tau_{infinity}$, were used for each of the solutions and ranged within 50 msec of the manually approximated T_1 of the solution.

A stacking program (software supplied with NMR) was used to obtain spectral plots of signal intensity versus frequency as a function of τ. A printout of signal intensity and τ values was obtained after phasing and establishment of a baseline for the $\tau_{infinity}$ spectrum for each solution. All intensity data for other τ values were

derived relative to the established $\tau_{infinity}$ spectral baseline.

All plots were obtained using Grapher version 1.75 (Golden Software, Inc.). Plots of signal intensity versus τ were obtained as a preliminary determination for acceptability of the data. The signal intensity values at each τ and at $\tau_{infinity}$ were then used in the following function:

$$\ln (I_{infinity} - I_{\tau} / 2I_{infinity}) = -(\tau/T_1) + K$$

$I_{infinity}$ = Signal intensity at $\tau_{infinity}$

I_{τ} = Signal intensity at τ

T_1 = Solution spin-lattice relaxation rate

K = Solvent contribution to total $1/T_1$

Plots of $-\ln (I_{infinity} - I_{\tau}/2I_{infinity})$ versus τ were obtained for each sample and a linear least squares fit was used to obtain $1/T_1$ (the slope of the line) for the sample. The process was repeated for the solvent and each concentration of each of the compounds. Relaxivity plots ($1/T_1$ versus gadolinium concentration) were obtained.

Viscosity and Carrier-Complex Interaction Evaluation. All studies under this heading involved the collection of T_1 data under identical conditions to those given for the T_1 relaxivity studies. Values for $\tau_{infinity}$ of 2.5 seconds for gadolinium containing solutions and 10 seconds for all other solutions were used. All solutions were prepared in pH = 7.4 phosphate buffer of 0.15 M ionic strength.

To ascertain possible T_1 effects due to solution viscosity, buffer solutions containing 5, 22, 43, 104, 380, 572, 936, 1300, 1716, and 2652 mM glucopyranose (in the form of dextran 9400) were prepared. T_1 evaluation was conducted at 25°C. A plot of relaxivity versus glucopyranose concentration was obtained.

To evaluate possible T_1 effects due to interaction between the metal chelate and the free (unmodified) portions of polysaccharide, several solutions were prepared. Buffer solutions containing 1, 2, 4, and 5 mM gadolinium in GdEDTA, GdDTPA, and GdDTPA-dextran 40200 were prepared and T_1 evaluated. Identical solutions were then prepared and to the 1, 2, 4, and 5 mM gadolinium solutions 2.63, 5.26, 10.52, and 13.15 mM glucopyranose in the form of dextran 40200 was added, respectively, and evaluated by T_1 measurement.

To evaluate possible suppression of T_1 due to polysaccharide - metal chelate hydrogen bonding and / or steric restriction of exchanging water molecules, the results of the previous study were used along with T_1 results for a set of solutions prepared with isopropanol present. Buffer solutions containing 1, 2, 4, and 5 mM gadolinium in GdEDTA and GdDTPA-dextran 40200 and 2.63, 5.26, 10.52, and 13.15 mM glucopyranose, respectively, were prepared with 800 mM isopropanol (Fisher Scientific Co.) in each solution and T_1

evaluated. Plots of relaxivity versus gadolinium concentration were obtained.

Results and Discussion

Evaluation of Synthetic Methods

The method of synthesis that was developed in this work for highly loaded GdDTPA-polysaccharides required three steps: preparation of a suitably reactive anhydride of DTPA; reaction of the anhydride with the polysaccharide in a suitable anhydrous mixed solvent system under conditions that did not result in polysaccharide degradation; and reaction of the DTPA esterified polysaccharide with gadolinium ion. There was no disclosed precedence for the polyaminopolycarboxylic acid esterification of polysaccharides at the inception of the project.

The first esterified product, a model compound, was obtained for the reaction of dextran 9400 with methyl-red (p-dimethylamine azo benzene-o-carboxylic acid, Fisher). The heterogeneous reaction took place in toluene with a stoichiometric excess, relative to the number of moles of carboxylic acid function present from methyl-red, of trifluoroacetic anhydride.

HPLC was used following all esterification reactions to evaluate the reaction success, evaluate the product purity following dialysis, and evaluate the integrity of the

polysaccharide following reaction. The reaction success was determined from the relative areas of the HPLC elution profiles for the esterified product relative to the unreacted acid (methyl-red in the model case and DTPA or TTHA in subsequent esterifications). The elution profile for the methyl-red esterification of dextran, shown in Figure 3.1, indicated that approximately 16% of the methyl-red initially present in the heterogeneous mixture had reacted.

Following extraction into aqueous solution and the removal of the unreacted methyl-red by dialysis, the UV-visible spectrum of the compound was obtained in pH = 7.0 phosphate buffer and compared with the spectra of unmodified methyl-red obtained in buffers of differing pH (Figure 3.2). The normal indicator behavior[64] of methyl-red was absent in the esterified product and suggests that the carboxyl group protonation, required for indicator function, was blocked by ester bond participation. Shown in equation 3.1, the reaction of methyl-red with the polysaccharide required the formation of an intermediate species, a trifluoroacetate anhydride of methyl-red, which activates the methyl-red carbonyl function to esterification.

$$\text{R-C(O)OH} + [\text{CF}_3\text{C(O)}]_2\text{O} \longrightarrow \text{R-C(O)-O-C(O)CF}_3$$

$$\text{R-C(O)-O-C(O)CF}_3 + \text{HO-R'} \longrightarrow \text{R-C(O)-O-R'} + \text{HO-C(O)CF}_3$$

R = Remaining functionality of methyl red.
R' = Remaining functionality of polysaccharide. (3.1)

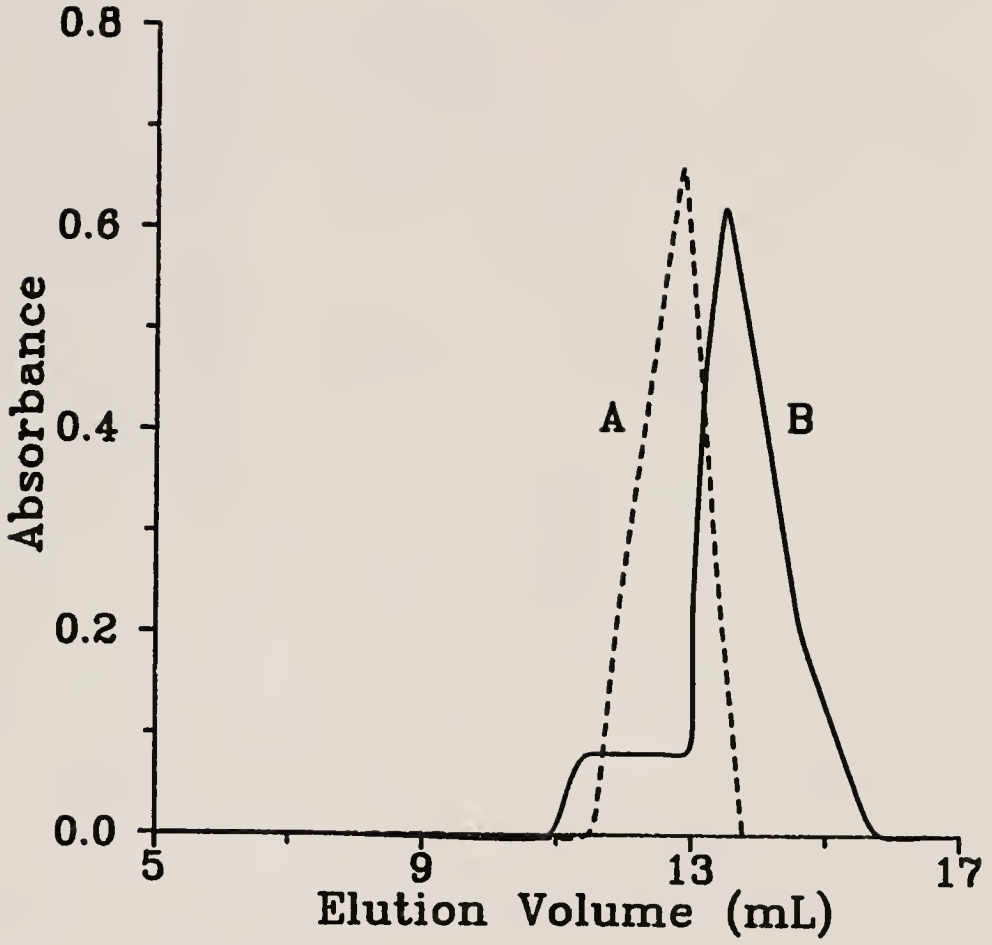

Figure 3.1. HPLC elution profile for product mixture obtained from reaction of methyl-red with dextran 9400 (solid line, B) and HPLC elution profile for unmodified dextran 9400 as obtained from sugar assay of HPLC fractions (dashed line, A).

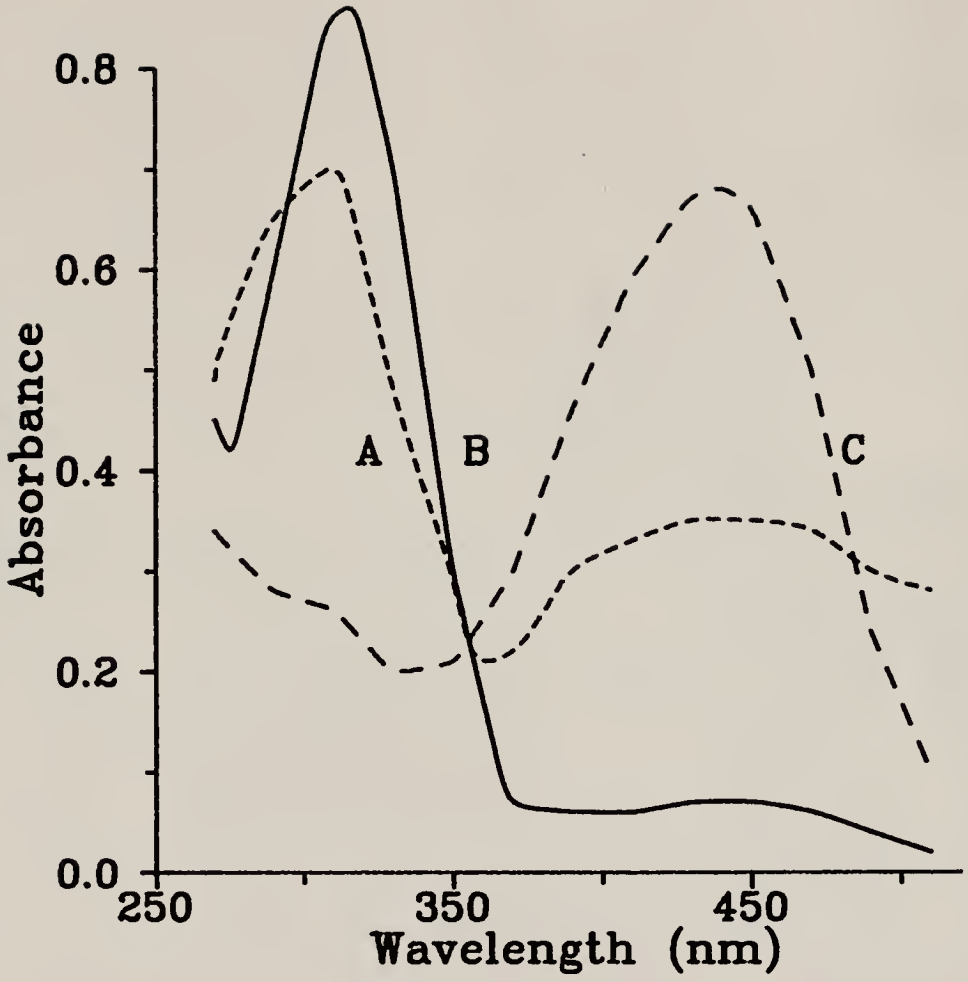

Figure 3.2. UV-Visible spectra of methyl-red esterified dextran in pH = 7.0 phosphate buffer (solid line, A), unmodified methyl-red in pH = 7.0 phosphate buffer (dashed line, B), and unmodified methyl-red in pH = 5.6 acetate buffer (dashed line, C).

The same esterification reaction conditions which were successful when methyl-red was used resulted in only 1% reaction when GdTTHA was used. Solid GdTTHA has a free (noncoordinated) carboxyl group[65] and, based on the observed low reactivity toward esterification, the result suggests that either the free carboxyl group in the solid phase is coordinated or fluxional when GdTTHA is in solution, or, the extreme low solubility of the complex in toluene is not conducive for the esterification under these conditions.

The reaction success of ethyl- and isobutyl-mixed anhydrides of DTPA with polysaccharides under various reaction conditions is shown in Table 3.1. The results strongly suggest that homogeneous reaction conditions are required for high reactivity of the anhydrides with the polysaccharides. The following additional observations were made: 1) solvents that provided homogeneous reaction conditions for reactions involving inulin did not necessarily provide the same for dextran preparations; 2) the activation of the polysaccharides with n-butyl lithium did not provide reproducible results; 3) inulin, with a much greater number of primary alcohol functions available for esterification relative to glucopyranose based polysaccharides, reacted to a significantly greater extent than dextran 9400 under the same reaction conditions.

Table 3.1 Mixed anhydride reactions with polysaccharides, the reaction conditions, and percent anhydride reacted for a series of attempted preparations.

Reactant Anhydride	Polysac.[a]	Solvent[b]	Temp./ Time	Catalyst Added	%Reacted[c]
i-butyl	D	pyr/DMSO	Reflux/2h	none	0
i-butyl	I	pyr/DMSO	"/"	"	7
ethyl	I	pyr	Reflux/1h	"	7
i-butyl	D^+	DMSO	5°C/15min	"	5-25
ethyl	D^+*	benzene	RT/12h	"	0
ethyl	I^+*	"	"/"	"	1-5
ethyl	D	1:1pyr/form	RT/60h	"	<1
ethyl	D	" "/"	60°C/3h	Zn^{2+}	24
i-butyl	D	" "/"	60°C/17h	Zn^{2+}	22

[a]D = dextran 9400, I = inulin, $^+$polysaccharide activated by n-butyl lithium, * = heterogeneous reaction conditions, all other reactions were homogeneous.

[b]pyr = pyridine; DMSO = dimethylsulfoxide; form = formamide, unless a ratio is given, all solvent mixtures were prepared such that the more polar solvent was added to the mixture of polysaccharide in the less polar solvent until the polysaccharide dissolved.

[c]Obtained from HPLC elution profiles, all values ± 2.

Equation 3.2 represents the reaction to prepare the mixed anhydride and the subsequent reaction of the anhydride with the alcohol function of polysaccharides to produce the DTPA esters.

$$R\text{-}C(O)OH + Cl\text{-}C(O)O\text{-}X \longrightarrow R\text{-}C(O)OC(O)O\text{-}X$$

$$R\text{-}C(O)OC(O)O\text{-}X + HO\text{-}R' \longrightarrow R\text{-}C(O)O\text{-}R' + CO_2 + XOH$$

R = Remaining functionality of DTPA.
X = Remaining functionality of alkyl formate.
R' = Remaining functionality of polysaccharide. (3.2)

As shown in equation 3.2, the use of mixed anhydrides in esterification processes results in the simultaneous formation of primary alcohols upon reaction of the mixed anhydride with the polysaccharide. Since the nucleophilicity of primary alcohols may be comparable with saccharide secondary alcohol functions, it is likely that the observed low reactivity of the mixed anhydrides towards dextran was due to the competing reaction of the primary alcohol with the mixed anhydride to form the alkyl ester of the polyaminopolycarboxylic acid. Although it is highly probable that this competitive reaction was occurring, the moderate heating of either the iso-butyl or ethyl mixed anhydride with dextran in 1:1 volume ratio of pyridine and formamide in the presence of Zn^{2+} resulted in significant reaction success, shown in Table 3.1. This reaction success provided a calculated degree of loading which approximated 0.2 mole DTPA per mole repeating unit of the polysaccharide.

The use of a cyclic anhydride of the reactant acid, as shown in equation 3.3, does not involve the simultaneous production of competitive primary alcohols upon esterification of the desired polysaccharide alcohol function. This reactivity of the cyclic anhydrides makes their application to esterification reactions with secondary or kinetically inhibited primary alcohol functions considerably more suitable in terms of expected yield than when mixed anhydrides are used.

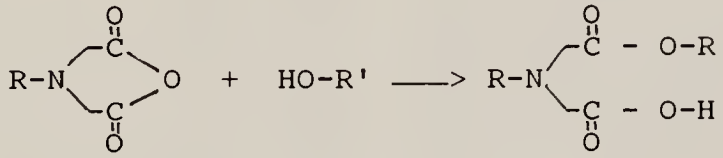

(3.3)

R = remaining functionality of aminopolycarboxylic acid
R' = remaining functionality of polysaccharide

The use of a mixture of anhydrous pyridine and formamide results in homogeneous reaction conditions for the esterification of dextrans[59] and inulin and reduces the extent of competitive hydrolysis of the cyclic anhydrides expected in aqueous media. The degree of DTPA conjugation was significantly effected by the presence of Zn^{2+} in the reaction mixture. The presence of trace quantities of zinc ion, added to the solvated polysaccharide before the addition of the reactant anhydride, resulted in a 30 fold increase in the level of DTPA loading relative to when no zinc ion was present. This result suggests that Zn^{2+} is

catalytic in the esterification reaction involving polysaccharides and is supported by the reported catalytic activity of $ZnCl_2$ in the acetate esterification of monosaccharides.[66] Additionally, the zinc ion may function to remove some of the random coiling commonly exhibited by some polysaccharides when in solution,[67] and, in so doing, may have served to reduce steric crowding near the reactive alcohol functions.

As shown in Table 3.2, a high percentage of the anhydride reacted when the commercially available dicyclic anhydride was used to esterify dextran and inulin in 1:1 volume ratio of pyridine and formamide in the presence of Zn^{2+}, however, HPLC elution band broadness of the product was observed. In the work of Gibby et al.[52], the use of the dicyclic anhydride to prepare highly crosslinked products resulted in considerable elution band broadness when a Sephacryl 400 column was used. When the dicyclic anhydride was used in our work, strong chromatographic evidence for substantial product crosslinking was observed when elution profiles were obtained from the Protein Pac HPLC column, shown in Figure 3.3. Product elution occurred near the void volume of the column (4.6 mL as assessed by Blue Dextran) and was very broad as was the eluting band at higher elution volumes. Also shown in Figure 3.3, a broad band near 9 mL, similar to that observed when the dicyclic anhydride was used, was observed when a cyclic anhydride, prepared using a

1:3.2 mole ratio of DTPA to acetic anhydride, was reacted in the presence of trace quantities of trifluoroacetic anhydride (TFAA is generally viewed as an esterification catalyst for reactions with cellulose[68]).

Table 3.2 Cyclic anhydride reactions with polysaccharides, the reaction conditions, and percent anhydride reacted for a series of attempted preparations.

Reactant[a] Anhydride	Polysac.[b]	Solvent	Temp./ Time	Catalyst[c] Added	%Reacted[d]
d-dicy	D*	toluene	reflux/3h	TFAA	0
d-dicy	D	1:1 pyr/form	60°C/24h	none	0
d-dicy	D	" "/"	60°C/3.5h RT/2h	Zn^{2+}	[88]
d-dicy	I	" "/"	" " "	Zn^{2+}	[67]
d-1:3.2	D	" "/"	65°C/24h	TFAA	16,[8]
d-mocy	D	" "/"	65°C/4h & RT/24h	Zn^{2+}	42,[7]
d-1:1.0	D	" "/"	60°C/3h & RT/12h	"	23
d-1:2.0	D	" "/"	60°C/3.5h & RT/12h	none	0
d-1:2.0	D	" "/"	60°C/1h & RT/12h	Zn^{2+}	34

continued next page

Table 3.2--continued.

Reactant[a] Anhydride	Polysac.[b]	Solvent	Temp./ Time	Catalyst[c] Added	%Reacted[d]
d-1:3.2	D	1:1 pyr/form	50°C/4h RT/2h	Zn^{2+}	59
"	D(402)	" "/"	" " "	"	60
"	I	" "/"	" " "	"	72
t-1:1.0	I	1:1pyr/form	60°C/3.5h & RT/12h	Zn^{2+}	78
t-1:2.0	D	" "/"	60°C/3h	"	15
t-1:3.0	D	" "/"	"/"	"	36
t-1:3.2	D	" "/"	"/"	"	53
t-1:3.8	Not Attempted				

[a]d- = DTPA; t- = TTHA; d-dicy = DTPA dicyclic anhydride (Aldrich); D-mocy = DTPA monocyclic anhydride prepared as outlined by Halpern, et al.[58]; ratios indicate moles DTPA or TTHA to moles of acetic anhydride used to prepare the cyclic anhydride. For example, t-1:3.0 is a cyclic anhydride of TTHA which was prepared by the reaction of a ratio of 1 mole of TTHA with 3.0 moles of acetic anhydride.

[b]D = dextran 9400; D(402) = dextran 40200; I = inulin; * = heterogeneous reaction conditions, all other reactions homogeneous.

[c]TFAA = trifluoroacetic anhydride; Zn^{2+} added as either solid $ZnCl_2$ or a mixture with anhydrous pyridine.

[d]Obtained from HPLC elution profiles, bracketed numbers represent percent reacted anhydride which formed cross-linked product (if 2 percentages are reported) or the percent reacted anhydride which formed products with very broad elution profiles. All values are ± 2.

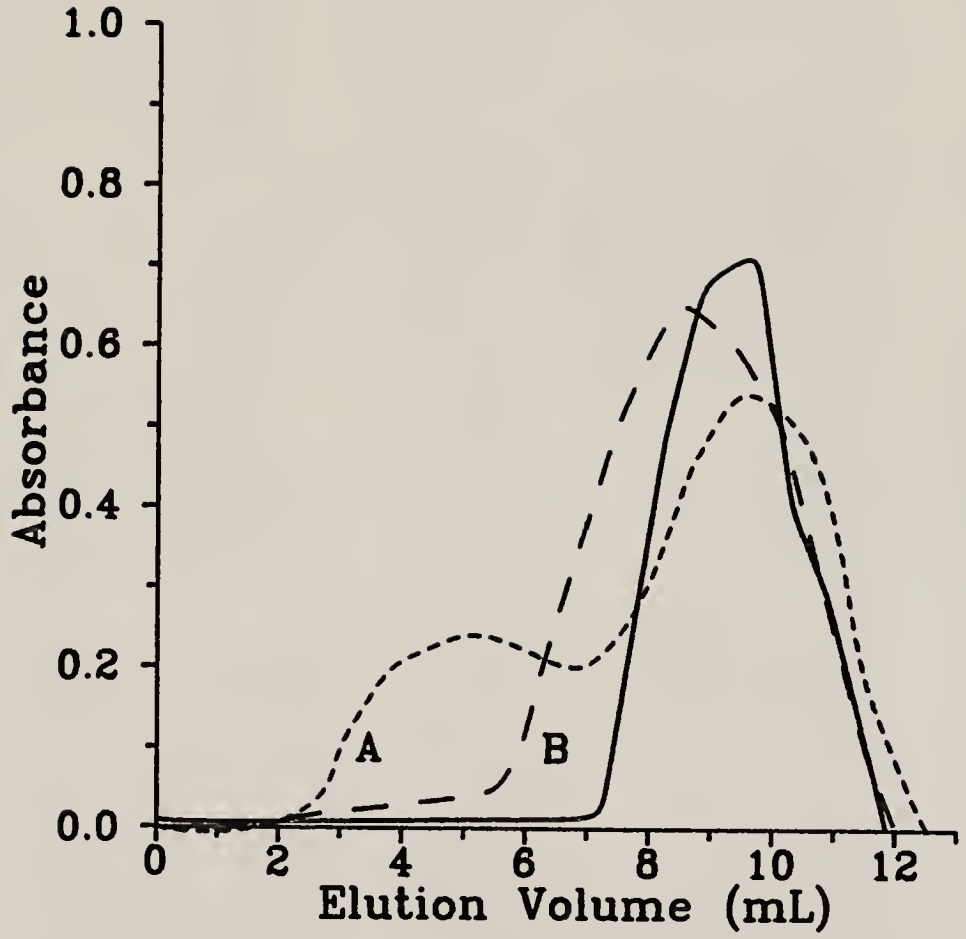

Figure 3.3. Elution profile for unmodified polysaccharide (solid line), esterification product obtained from reaction of dicyclic anhydride (dashed line, A), and from reaction of mono- and dicyclic anhydride mixture in presence of trifluoroacetic anhydride with the polysaccharide (dashed line,B).

Indicated in Table 3.2, the greatest anhydride reactivity towards the polysaccharides, without chromatographic evidence for crosslinked products, was observed for products obtained from the reaction of an anhydride prepared using a 1:3.2 mole ratio of DTPA or TTHA to acetic anhydride in 1:1 volume ratio of pyridine and formamide with Zn^{2+} present. These reaction conditions were used subsequently for all large scale preparations of DTPA esterified polysaccharides. The DTPA cyclic anhydride prepared in this fashion was a mixture containing both dicyclic and monocyclic anhydride as supported by infrared carbonyl stretching frequencies of 1820.7, 1772.1, 1757.7, and 1639.6 cm^{-1}. The two higher wavenumbers are attributed to characteristic anhydride carbonyl stretching frequencies (-C(O)-O-C(O)-) and the lowest wavenumber represents the central carboxyl group carbonyl stretch (-C(O)OH).[69] The absorbance band at 1757.7 cm^{-1} represents a terminal carboxyl group stretch[69] (-C(O)OH) that has been shifted in energy, relative to that of DTPA at 1737.9 cm^{-1}, possibly as a result of the inductive effect of the neighboring anhydride function.

Although the TTHA cyclic anhydride prepared by the reaction of a mole ratio of 1 mole TTHA to 3.2 moles acetic anhydride was not assessed by infrared spectroscopy, it is probable that a higher percentage of monocyclic anhydride was present in the TTHA mixture than in the DTPA mixture

prepared similarly due to the greater number of carboxyl functions in TTHA. The use of a 1:3.8 mole ratio of TTHA to acetic anhydride would likely result in a mixture of monocyclic and dicyclic anhydrides of which the percentage of each species closely approximated those in the DTPA cyclic anhydride mixture which was prepared by 1:3.2 DTPA to acetic anhydride. Improved yield in the polysaccharide esterification with cyclic anhydrides of TTHA may be obtained when a mole ratio of 1 mole TTHA to 3.8 moles acetic anhydride is used to prepare the anhydride mixture.

There are no reports concerning the formation of ketones on cyclization of aminopolycarboxylic acids upon heating with acetic anhydride and no evidence was obtained in this work which supported the formation of ketones. However, the Blanc rule[70] for dicarboxylic acids indicates that the formation of the anhydride or the ketone will occur depending on the relative positions of the carboxyl groups: with 1,4- and 1,5-diacids forming the anhydride and 1,6-diacids or further removed positions producing the ketone. If the Blanc rule is applicable to polyaminopolycarboxylic acids then 80% of DTPA and 87% of TTHA would form ketones upon reaction with acetic anhydride (based on the carboxyl positions and possible combinations to form either ketones or cyclic anhydrides). Based on the observed reactivity of the compounds formed by reaction of the acids with acetic anhydride, it is improbable that the Blanc rule applies.

No DTPA chelate crosslinking of the esterified polysaccharides prepared by this method was detected by HPLC (Figure 3.4) as evidenced by the lack of eluting band broadness or distinctly separate peaks at lower elution volumes relative to the unmodified polysaccharides (refer to Figure 3.3). The mobilities or elution properties of the esterified polysaccharides on the Protein-Pak column material are expected to differ from the unmodified polysaccharides as a result of the charged DTPA moiety interacting with the polysaccharide in the esterified product. The elution bands (esterified and unmodified polysaccharide) differ significantly in terms of band width, and this observation suggests that the dispersity of the molecular weights in the polysaccharide starting material may have been altered (significantly reduced) in the esterification process. Additionally, the elution bands for the unmodified polysaccharides of differing average molecular weight overlapped with one another when the Protein-Pak column was used. Therefore, the evaluation of crosslinking by HPLC elution band broadness of the unmodified polysaccharide and the esterified product could not be used. Elution band comparison of the purposely crosslinked esters with the prepared esterified polysaccharides does, however, allow the conclusion that significant crosslinking in the prepared compounds was not detected by the HPLC method.

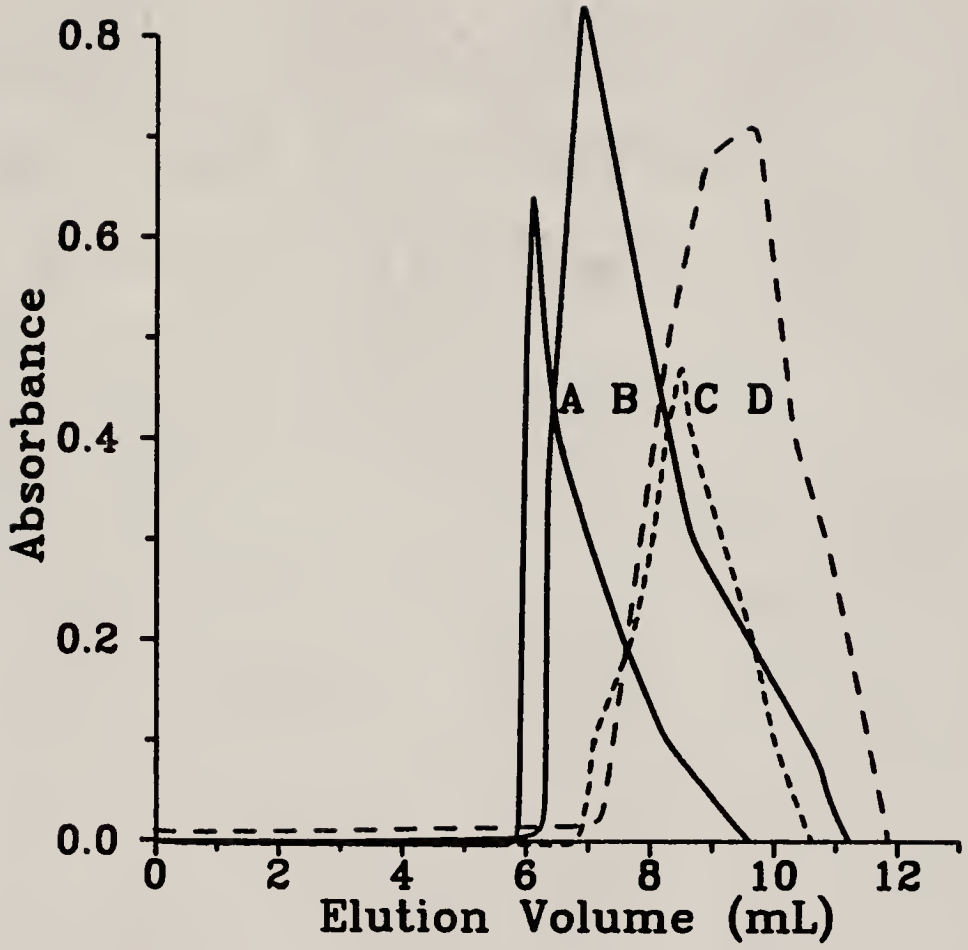

Figure 3.4. HPLC elution profile for unmodified dextran 40200 (B, solid), DTPA esterified dextran 40200 following dialysis (A, solid), DTPA esterified dextran 9400 after dialysis of product obtained (C, dashed) using the developed general reaction conditions, and unmodified dextran 9400 (D, dashed).

Compound Characterization Results

The DTPA - esterified inulin and dextrans of 9400, 40200, and 70800 average molecular weight were found to be very water soluble. Repetition of the esterification process resulted in levels of loading averaging 0.38 ± 0.05 mole DTPA per mole of repeating glucopyranose unit of the dextran compounds and 0.52 ± 0.08 mole DTPA per mole fructofuranose repeating unit in the inulin compound. The general esterification method produced a DTPA - esterified dextran 487000 with an average of 0.10 ± 0.02 mole DTPA per mole of repeating glucopyranose unit, and the products were readily water solubilized.

A modification in the general method was applied to subsequent preparations involving dextran 487000, wherein the heated reactants were cooled to room temperature and allowed to stir for 30 h prior to product isolation. This modification resulted in the reproducible production of substantially higher levels of loading (0.80 ± 0.06 mole DTPA per mole glucopyranose repeating unit) than the product produced by the general method. The product (by the modified general method) was, however, considerably less water soluble than the product prepared by the general method.

Based on elemental analysis combined with ICP analysis, the metallated products contained an average of 0.38 ± 0.06 moles of GdDTPA attached per mole of glucopyranose unit in

dextrans of 9400, 402000, and 708000 average molecular weight and 0.50 ± 0.03 moles GdDTPA per mole fructofuranose unit in inulin. As supported by elemental and ICP analysis results, all the complexes contained an average of 1.00 ± 0.04 mole Gd^{3+} per mole of DTPA moiety.

The level of loading of GdDTPA on to the polysaccharides of up to 70800 average molecular weight is roughly ten times that obtained by Ranney et al.[53] in reacting the bisanhydride of DTPA with Dextran 70,000 in aqueous media and approximately twice that reported in the work of Gibby et al.[52] which involved the synthesis of a mixture of crosslinked products from the bisanhydride (dicyclic anhydride) reaction with dextran 150,000 in anhydrous media. A recent report by Nycomed researchers[71] indicates that their GdDTPA-dextran 75,000 (conjugation bond type was not disclosed) contained an average of 15 GdDTPA moieties per polysaccharide carrier. These previous efforts to conjugate GdDTPA to dextrans resulted in either low loading of DTPA on the dextran or a continuum of molecular weight crosslinked products. High loading is a desirable aspect in macromolecule-bound contrast agents as plasma expansion is minimized. The dextran conjugates prepared by the method of synthesis developed in this work resulted in average molecular weights per gadolinium of only 13% more than GdDTPA and 11% more than GdDTPA for the inulin conjugates.

The infrared carbonyl stretching frequencies of the complexes and the nonmetallated DTPA-polysaccharide esters in the present work were compared with that of GdDTPA and DTPA. As shown in Table 3.3, the stretching frequencies of the DTPA-polysaccharide esters are nearly identical to DTPA. Similarities of carbonyl stretching frequencies for GdDTPA and the GdDTPA-polysaccharides support that gadolinium is chelated by the DTPA esterified polysaccharides.

Table 3.3. Infrared carbonyl stretching frequencies of DTPA, DTPA-dextran conjugates, and the gadolinium complexes.

Compound	Wavelength (cm^{-1})[a]		
DTPA	1630	1696	1737
DTPA-Inulin	1626		1734
DTPA-Dextran 9400	1639		1737
DTPA-Dextran 40200	1631		1737
DTPA-Dextran 70800	1628		1736
DTPA-Dextran 487000	1628		1738
H_2GdDTPA	1581	1704	
GdDTPA-Inulin	1596	1700	1738
GdDTPA-Dextran 9400	1606	1696	sh
GdDTPA-Dextran 40200	1598	sh	1737
GdDTPA-Dextran 70800	1594	1702	1723
GdDTPA-Dextran 487000	1602	sh	sh

[a] sh = shoulder of lower wavenumber absorption band.

Further evidence to support the lack of significant crosslinking in the DTPA esterified dextrans as synthesized by this new method was obtained from the potentiometric titration studies. As indicated in Figure 3.5, DTPA exhibits a sharp inflection at 3 moles OH^- added per mole acid function with a less definite inflection between 3 and 5 moles OH^- per mole acid function.[72] DTPA in solution with a 1:1 mole ratio of Gd^{3+} to DTPA exhibits a sharp inflection at 5 moles OH^- per mole acid function[3]. The potentiometric behavior of the free acid has been explained based on the assumed trizwitterionic nature of the ligand in solution as shown in Formula I.

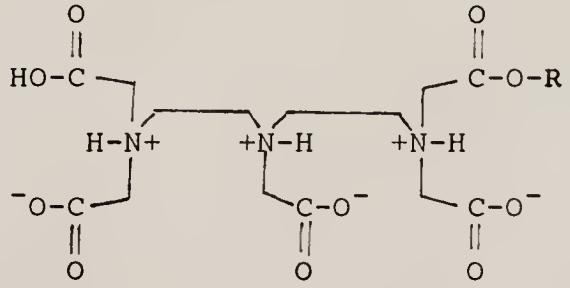

R = H in DTPA or esterified alcohol function in DTPA-Dextran.

Formula I.

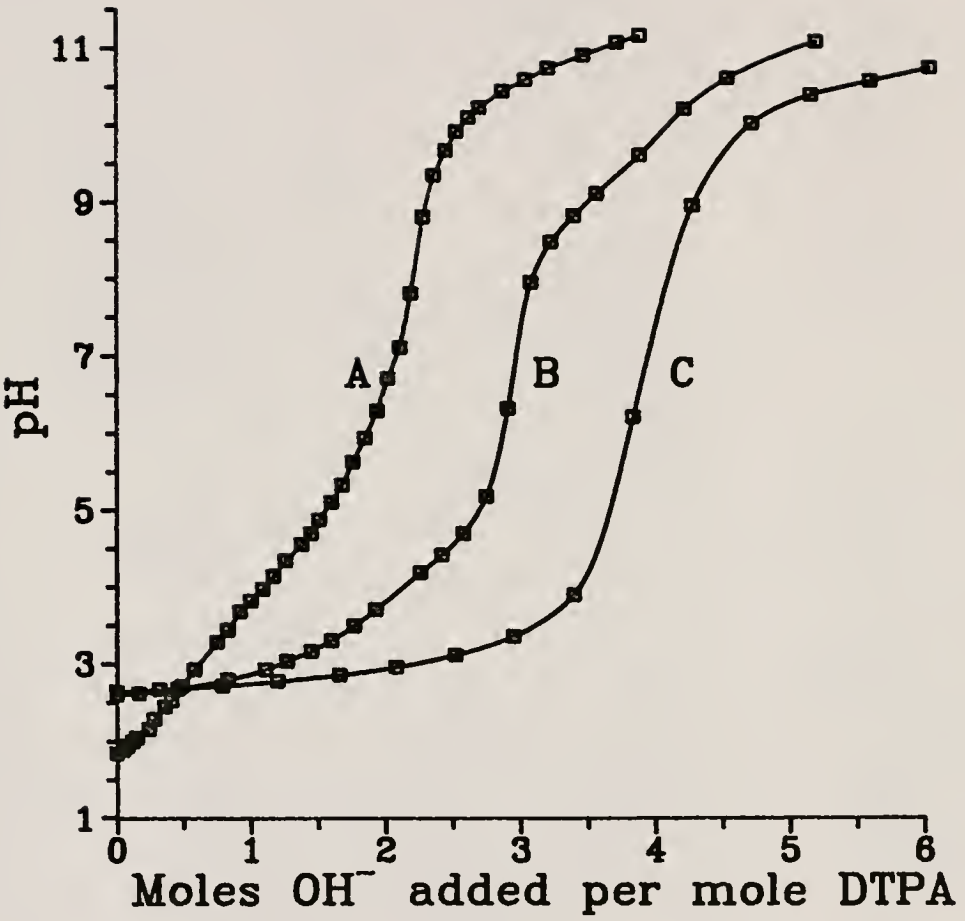

Figure 3.5. Potentiometric titration at 25.0°C with 0.1 M KOH of DTPA esterified dextran (A), DTPA (B), 1:1 Gd:DTPA-dextran (C).

Over the mole ratio (mole OH^- per mole acid function) interval from 0 to 3, two carboxyl protons and one ammonium proton are removed and the remaining ammonium protons are removed in the interval between 3 and 5.[72] In the presence of a 1:1 mole ratio of Gd^{3+} to DTPA, the single sharp inflection at 5 moles OH^- per mole acid function represents the neutralization of 5 moles of hydronium ion displaced by ligand chelation with one mole of Gd^{3+}.[3]

Indicated in Figure 3.5, all of the polysaccharide modified ligands in this work exhibited sharp inflections at 2 moles OH^- per mole acid function with ill defined inflection in the 2 to 4 equivalent range. With Gd^{3+} present in a 1:1 mole ratio of Gd^{3+} to conjugated DTPA, the single step neutralization at 4 equivalents of base added was observed. Based upon the zwitterion structure in Formula I and the known potentiometric behaviors of DTPA and DTPA in the presence of 1:1 molar addition of Gd^{3+}, these observations for the dextran esters of DTPA are consistent with products in which only one of the carboxyl functions of DTPA has been modified. For these new ligands, the remaining carboxyl proton and one ammonium proton are apparently removed in the 0 to 2 mole OH^- per mole acid function range of the titration with the remaining two ammonium protons removed in the 2 to 4 equivalents range. In the presence of 1:1 mole Gd^{3+} to conjugated DTPA, also shown in Figure 3.5, 4 moles of hydronium ions are

neutralized in the titration and represent the displacement of 4 moles of hydronium ions per mole of Gd^{3+} chelated. These results strongly support the contention that the DTPA esterified dextrans produced in this work are not significantly chelate crosslinked as sharp potentiometric inflections at 1 and 3 equivalents of base would be expected for DTPA-Dextran and 1:1 Gd^{3+} with DTPA-Dextran, respectively, in the crosslinked products.

Following dialysis against 0.1 M EDTA, the mass percent gadolinium in the GdDTPA-Dextran 9400 and 40200 complexes was not altered more than 0.4%. The observed absence of significant metal transfer to EDTA in dialysis with the prepared polymeric complexes suggests that the level of loading by DTPA on to the polysaccharides is preventing significant nonspecific metal binding (characteristic particularly to dextrans) to the investigated polysaccharides.[73,74] This observation additionally supports that the thermodynamic stability of the new complexes exceeds that of GdEDTA (log K = 10^{17}).

The thermodynamic stability constant for GdDTPA-dextran 40200, as obtained from the potentiometric titrations and assuming independent metal binding by the chelating groups, was 18.02 ± 0.13 (log K for $Gd^{3+} + L^{4-} \rightarrow GdL^{1-}$). Neither Gibby nor Ranney reported stability constants, however, recent work by Sherry et al.[75] involving the assessment of thermodynamic stabilities for mono- and di-propyl esters of

DTPA resulted in log K values of 18.91 and 16.30, respectively. The DTPA esters of dextran in the present work exhibited acid dissociation constants, shown in Table 3.4, comparable with those obtained Sherry et al.[75] for the mono-propyl ester of DTPA. The stability of the prepared gadolinium complexes when compared with the evaluated model compounds in the work of Sherry et al.[75] provides further evidence in support of non chelate-crosslinked products.

Table 3.4. Acid Dissociation Constants of DTPA-Dextrans and Propyl Esters of DTPA.

	DTPA-dextran[a]	DTPA-PE_1[b]	DTPA-PE_2[b]
pK_1	10.0	9.8	9.6
pK_2	6.7	6.6	4.8
pK_3	4.8	3.8	3.6
pK_4	1.7	1.8	low
pK_5	-	low	low

[a]Obtained by potentiometric titration (0.1 M KNO_3, 25.0°C) in this work. All values are ± 0.2.

[b]Obtained by A. D. Sherry et al.[75] Values are ± 0.1, determined potentiometrically (0.1 M NaCl, 25°C). Mono-propyl and di-propyl esters of DTPA are DTPA-PE_1 and DTPA-PE_2 respectively.

Hydrolysis Kinetics. An important issue in the development of macromolecule-bound contrast agents is the nature of the bond between the metal chelate and carrier. The covalent attachment of GdDTPA to proteins such as bovine serum albumin (BSA) has been via the formation of stable peptide bonds between the carrier and metal chelate.[76] The polysaccharides of the conjugates reported here are covalently linked with ester bonds to the metal chelate. Ester hydrolysis has been extensively studied[77] and the effect of different lanthanide ions, including Gd^{3+}, has been evaluated for amino acid esters of diacetic acids.[55] The assumed mechanism for these metal promoted hydrolysis reactions involves OH^- attack at the ester carbonyl group, and carbonyl activation occurs by metal binding to the ester carbonyl oxygen.

The ester bonded GdDTPA-polysaccharide conjugates may exhibit different *in vivo* excretory pathways than the peptide bonded conjugates as a result of the Gd^{3+} promoted ester hydrolysis. The half-lives for the ester bonds in the conjugates were obtained from slopes of logarithmic decomposition plots (first order in conjugate concentration). The half-life of GdDTPA-dextran 70800 (21 hours) was significantly shorter than the nonmetallated DTPA-dextran 70800 ester (85 hours) while for the GdDTPA-dextran 9400 complex and the nonmetallated compound the half-lives were within experimental error of each other (68

and 71 hours, respectively). The experimental error was ± 4 hours based on the repetitive determination of the HPLC elution peak areas. The presence of free GdDTPA in solutions containing the GdDTPA-dextran complexes did not decrease the half-lives of the complexes but was observed to increase the half-lives of both GdDTPA-dextran 9400 and 70800 (170 and 89 hours, respectively) to greater than that observed for their respective nonmetallated conjugate. The result suggests that gadolinium chelated by the ester bonded DTPA moiety is necessary for metal assisted ester hydrolysis to occur and that free GdDTPA (or a contaminant present in the mixture) adversely affects the rate of hydrolysis.

In working with propyl ester models of DTPA, Geraldes et al.[78] presented nuclear magnetic resonance dispersion (NMRD) evidence that supports the coordination of the ester carbonyl oxygen in gadolinium complexes. The results also tend to reinforce the suggested mechanism for metal promoted ester hydrolysis. No evidence for ester carbonyl coordination in the present work was obtained as an expected stretching mode shift to lower frequencies of the complexed ester carbonyl relative to the free ester carbonyl[69] could not be ascertained from the broad infrared peaks.

One possible explanation for the observed lack of consistent rates of ester hydrolysis among the gadolinium conjugates involves the lack of homogeneity in the

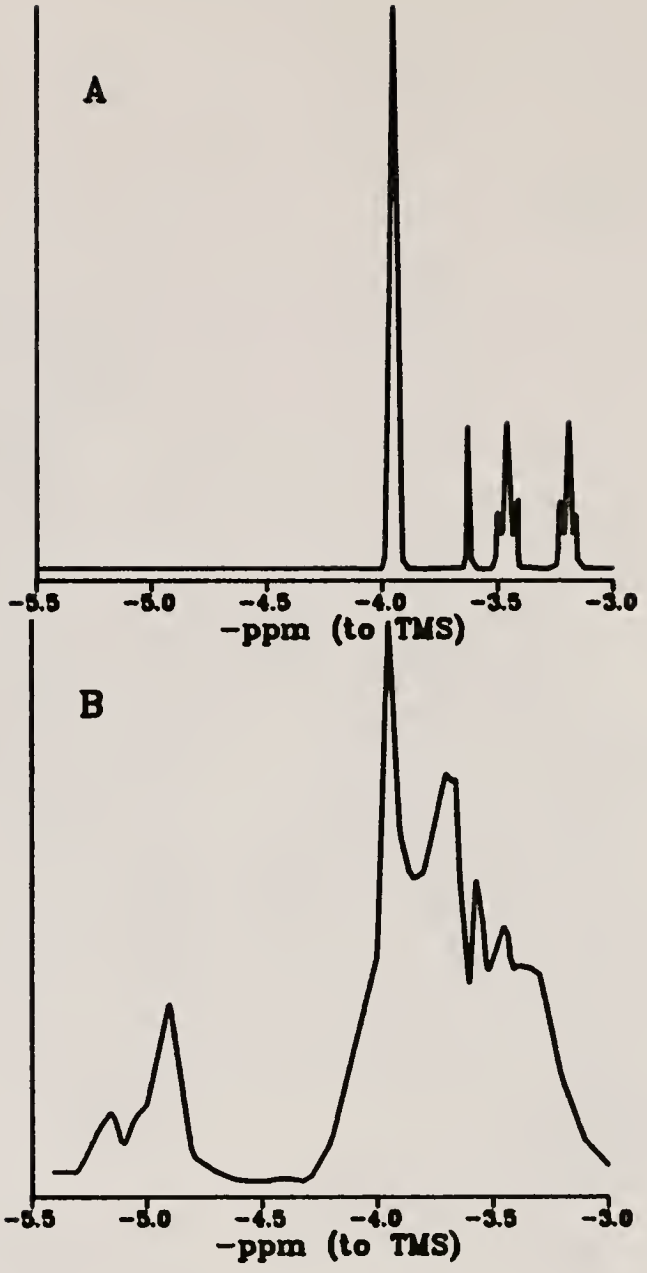

Figure 3.6. Proton NMR spectra in D_2O of (A) DTPA and (B) DTPA esterified dextran 9400.

polysaccharide bound DTPA. In Figure 3.6(a), the proton NMR spectrum of nonesterified DTPA is shown. The esterification would result in an additional peak in the spectrum corresponding to the DTPA methylene protons adjacent to the ester linkage while the other proton shifts would remain relatively unchanged. Unmodified dextran has no proton shifts in the region from 3.0 to 3.6 ppm. As shown in Figure 3.6(b), the 3.0 to 3.6 ppm region of the spectrum for the DTPA-dextran 9400 ester contained a large number of chemical shifts for the DTPA moiety. This result was also observed for the DTPA-dextran 40200 compound and the DTPA-inulin compound (unmodified inulin also has no proton shifts in the 3.0 to 3.6 ppm region). The result suggests that several different environments exist for the resonating protons of the DTPA moiety in the ester. Additionally, the sharp alcohol proton shift(s) of dextrans and inulin (at approximately 5 to 5.5 ppm) was significantly broadened by the esterification and suggests that significant intramolecular hydrogen bonding was taking place in the ester product. Future studies to investigate ester heterogeneity should include NMR of the esters in the presence of a lanthanide shift reagent, such as europium ion, in an effort to resolve the 3.0 to 3.8 ppm spectral region.

Relaxivity Results

The manual approximation of T_1 for each of the solutions evaluated by the inversion recovery technique resulted in raw data plots of signal intensity versus proton shift as a function of τ. The raw data was used to obtain plots of signal intensity versus τ, an example of which is shown in Figure 3.7. When converted to logarithmic functions of intensity versus τ plots, linearity was observed, as shown in Figure 3.8. It was observed that significant deviation from linearity only occurred at τ values greater than 40 msec from the actual solution T_1 and, for this reason, the manual approximation of T_1 and small increments between τ values are required in order to obtain reliable data. The slope of each of these logarithmic plots was equal to the T_1 of the solution and this information was used along with the gadolinium concentration in each of the solutions to construct a relaxivity plot of $1/T_1$ versus gadolinium concentration, as illustrated in Figure 3.9.

As shown in Table 3.5, the T_1 relaxivities of the GdDTPA-polysaccharides ranged from 1.5 to 2.3 times that of GdDTPA at 100 MHz ($25^{o}C$). The increase in T_1 relaxivities for the prepared conjugates relative to that of GdDTPA are consistent with relaxivities reported for other covalently attached GdDTPA-macromolecules[47,79-81] relative to GdDTPA.

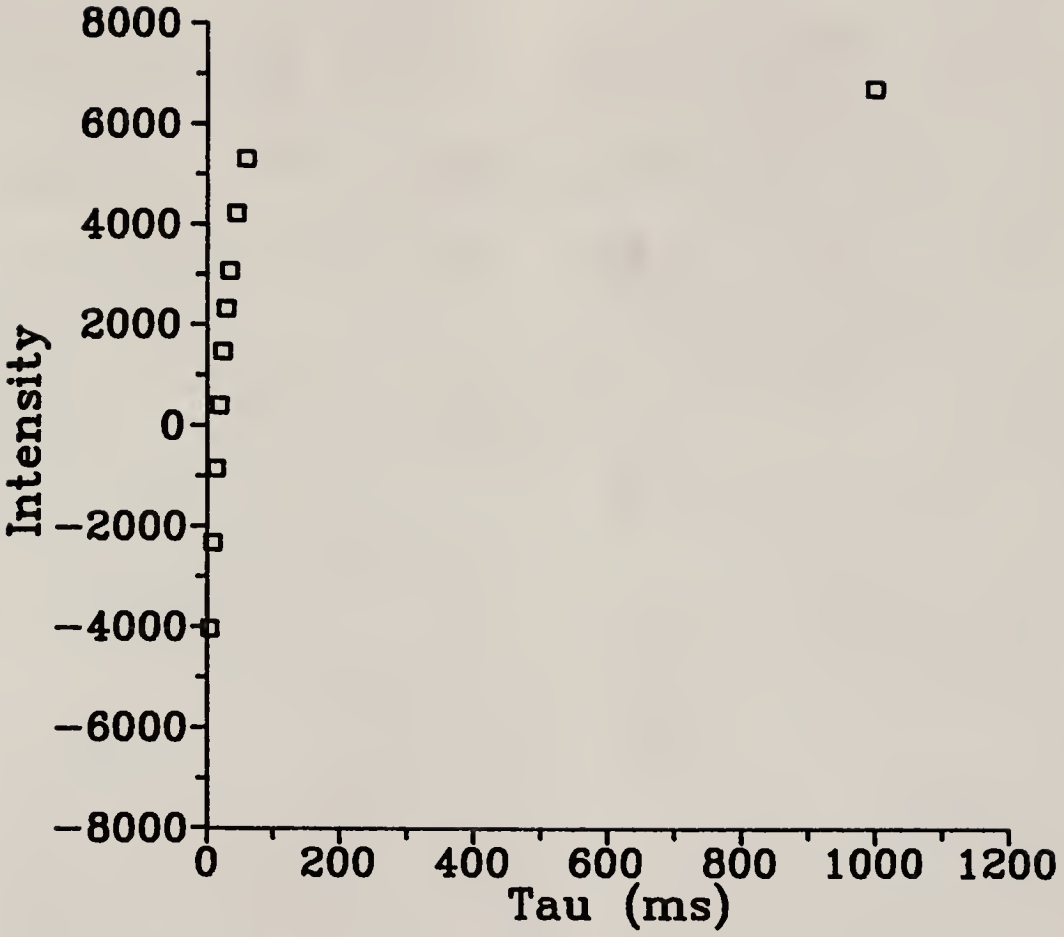

Figure 3.7. Plot of signal intensity versus τ for a solution containing GdDTPA-dextran 9400, pH = 7.4 phosphate buffer of 0.15 M ionic strength, 100 MHz, 25^{o}C.

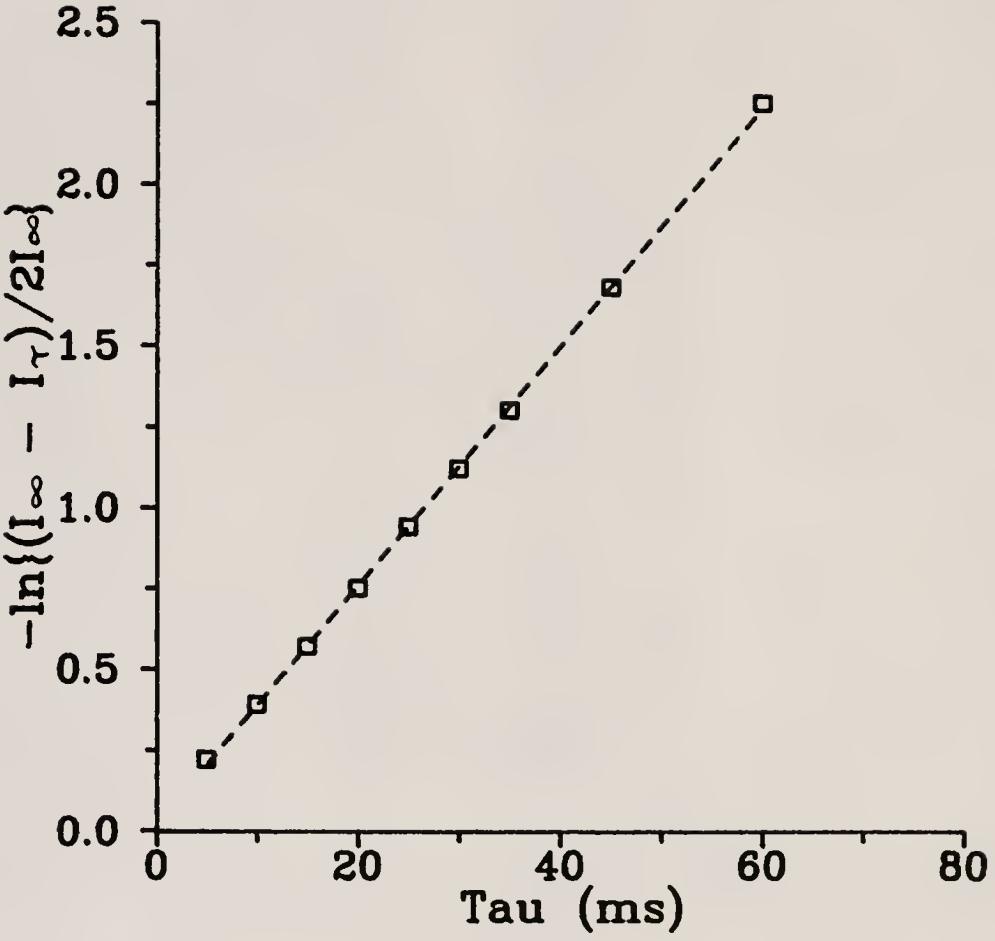

Figure 3.8. Natural log plot of signal intensity versus τ for a solution containing GdDTPA-dextran 9400, pH = 7.4 phosphate buffer of 0.15 M ionic strength, 100 MHz, 25^{o}C.

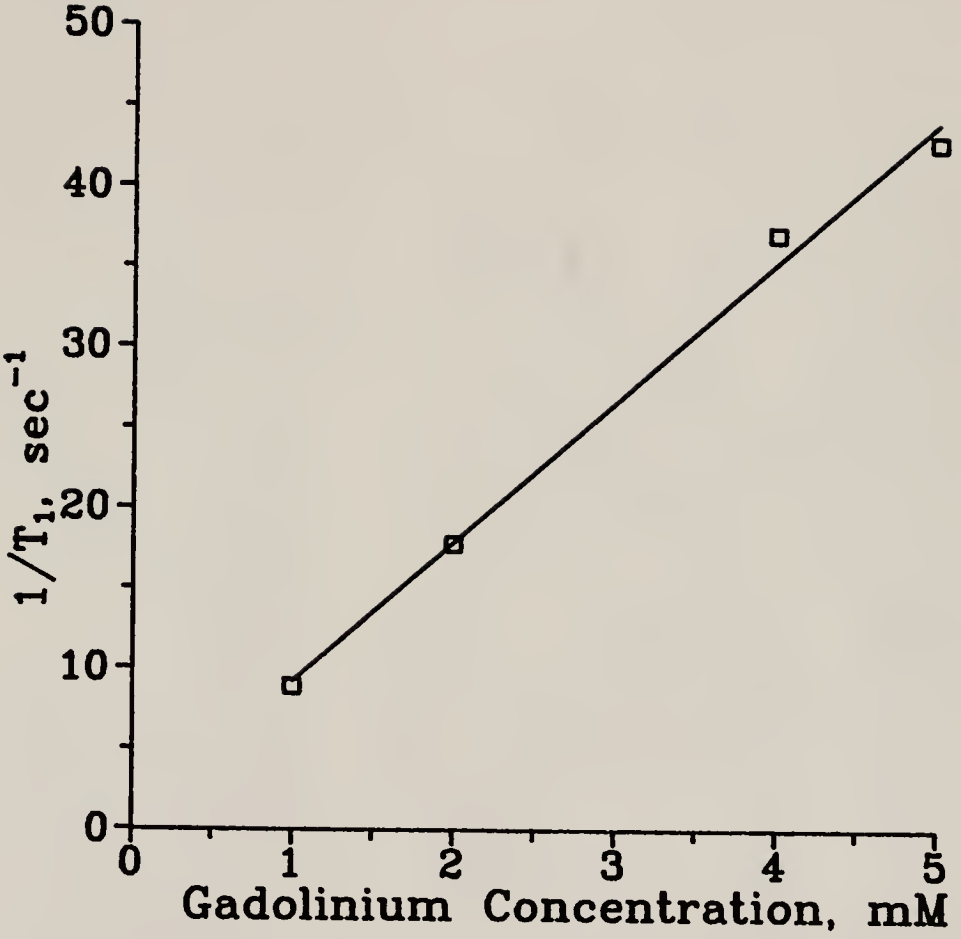

Figure 3.9. Relaxivity plot ($1/T_1$ versus gadolinium concentration) for GdDTPA-dextran 9400, pH = 7.4 phosphate buffer of 0.15 M ionic strength, 100 MHz, 25°C.

Table 3.5. T_1 Relaxivities at 100 MHz, 1 to 5 mM Gd^{3+}

Compound	Relaxivity[a] $(mM\ Gd\ sec)^{-1}$	Correlation Coefficient[b]
GdDTPA	3.8 ± 0.1	0.9993
GdDTPA-inulin	8.3 ± 1.0	0.9206
GdDTPA-dextran 9400	8.7 ± 0.6	0.9970
GdDTPA-dextran 40200	8.1 ± 0.3	0.9991
GdDTPA-dextran 70800	7.1 ± 0.7	0.9907
GdDTPA-dextran 487000	5.8 ± 0.5	0.9969

[a]Precision is expressed as population standard deviation and is equal to $[\Sigma(y_i-y_{avg})^2/n]^{1/2}$, where $y = 1/T_1$ for the solution evaluated and n = number of sample solutions tested.

[b]Correlation coefficient is equal to $[n(\Sigma xy)-(\Sigma x)(\Sigma y)]/[4(\Sigma x^2)-(\Sigma x)^2]^{1/2}[4(\Sigma y^2)-(\Sigma y)^2]^{1/2}$, where $y = 1/T_1$, x = gadolinium concentration of solution, and n = number of samples tested.

The observed increased relaxivities, R_1 (Table 3.5) of the new conjugates, relative to GdDTPA, may be due to several factors. The paramagnetically induced solvent T_1 relaxation contains inner-sphere and outer-sphere relaxation components.[82] The factors affecting the outer-sphere component are not well defined and an adequate model is not presently available. Factors that affect the rate of diffusion of water molecules in and through the outer sphere, such as hydrogen bonding, are included in the outer-

sphere component. Although hydrogen bonding may, for some species, contribute greatly to solvent relaxation, the outer-sphere component is generally considerably smaller than the inner-sphere term for paramagnetic species with at least one inner-sphere coordinated water molecule. The following equations summarize the theoretical treatment of inner-sphere relaxation parameters.[82]

$$R_1[Gd^{3+}] = 1/T_1 \text{ observed}$$

$$1/T_1 \text{ observed} = 1/T_1 \text{ paramag} + 1/T_1 \text{ diamag}$$

$$1/T_1 \text{ paramag} = 1/T_1 \text{ inner} + 1/T_1 \text{ outer}$$

$$1/T_1 \text{ inner} = Pq/T_{1m} + \tau_m$$

P = mole fraction of metal ion
q = # of water molecules bound to metal
T_{1m} = bound water proton relaxation time
τ_m = residence life of bound water

$$T_{1m} \alpha 1/T_{1e} + 1/\tau_m + 1/\tau_R$$

T_{1e} = longitudinal relaxation time of metal electrons in the complex
τ_R = metal-chelate-water rotational tumbling time

$$R_1 \alpha q(T_{1e} + \tau_R)/\tau_m \quad \text{(for } Gd^{3+} \text{ systems, 10 to 100 Mhz)}$$

Based on the above relationships, the higher relaxivities observed for the conjugates relative to GdDTPA may be due to one or a combination of the following: (i) an increase in rotational correlation time (possibly due to microviscosity)[48] by virtue of the rigid attachment of the metal chelate to the polysaccharide; (ii) an increase in the number of inner sphere coordinated water molecules

and/or their rate of exchange with bulk water molecules[82] by reduction of the denticity of the chelate upon esterification; (iii) an increase in the number of outer sphere coordinated water molecules and/or their rate of exchange[83] via entrapment by the polysaccharide, or a combination of all these effects. Additionally, the mechanism of inner sphere water ligand exchange with bulk water molecules may be significantly altered relative to GdDTPA by the presence of hydrogen bonding between the coordinated water molecules and the macromolecular carrier.[84] The somewhat lower relaxivities of these polysaccharide conjugates as compared to protein conjugates is likely due to the lack of globular tertiary structure in the polysaccharide complexes that results in lower rotational correlation times.

Indicated in Figure 3.10, an apparent trend in the observed relaxivities suggests a decrease in relaxivity with increasing dextran carrier molecular weight. It was observed that the polysaccharide alone made no significant contribution to the solvent relaxation over the concentration range (less than 200 mM glucopyranose) used in the T_1 studies (Figure 3.11) and increased solvent relaxation significantly only at high concentrations. At glucopyranose concentrations comparable with that in the GdDTPA-polysaccharide solutions, the solvent relaxation was observed to be within experimental error of the pure solvent

relaxation. It was therefore concluded that overall solution viscosity did not contribute to this apparent trend nor could the observed increased relaxivities relative to GdDTPA be attributed to solution viscosity effects.

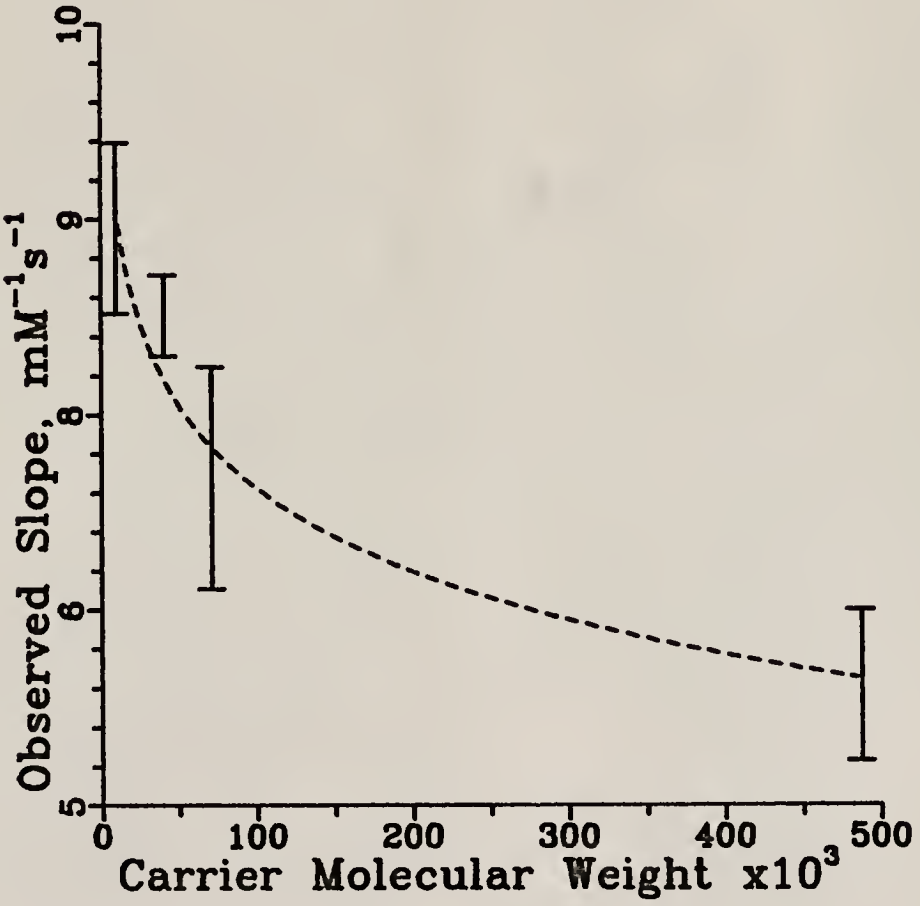

Figure 3.10. Plot of observed relaxivities for dextran conjugates of GdDTPA versus dextran carrier average molecular weight, pH = 7.4 phosphate buffer of 0.15 M ionic strength, 100 MHz, 25°C.

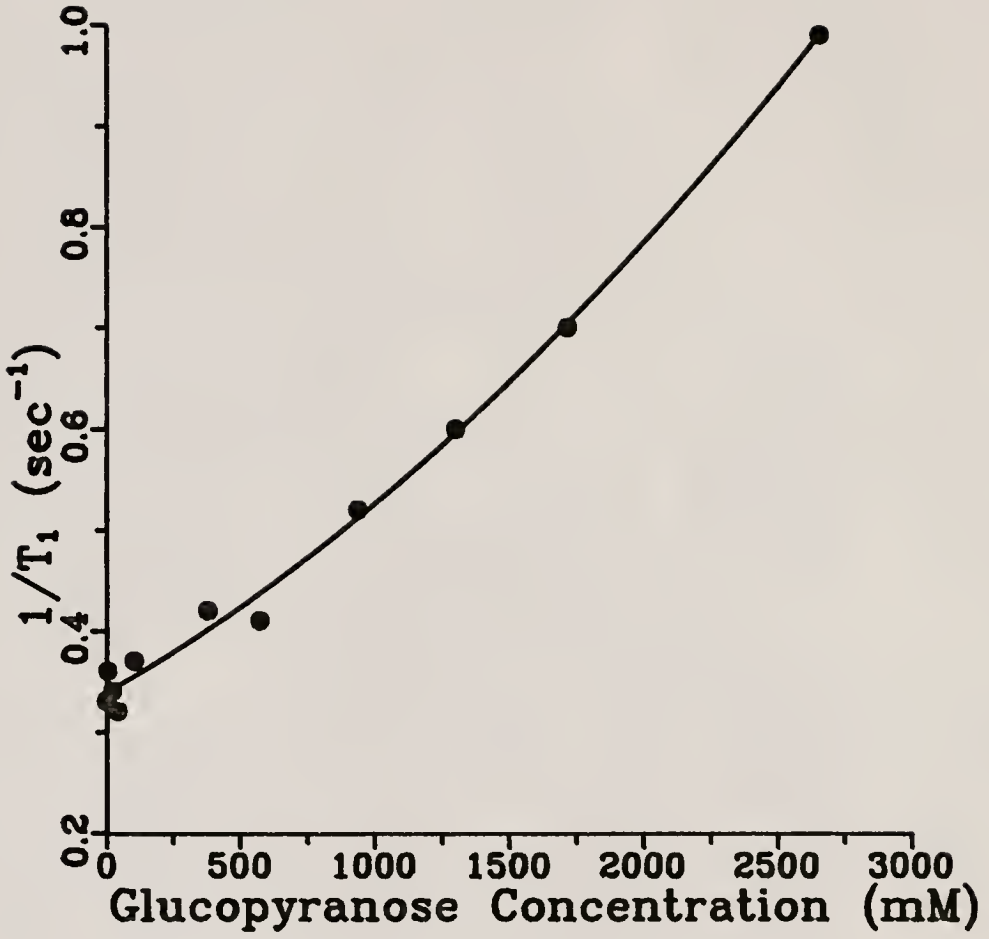

Figure 3.11. Plot of observed solution T_1 versus glucopyranose concentration for a series of solutions containing pH = 7.4 buffer and dextran 9400 only, 100 MHz, 25°C.

In the solutions studied, the level of loading was 0.38 ± 0.01 mole GdDTPA per mole repeating glucopyranose unit in the GdDTPA-dextran 9400, 40200, and 70800 complexes and the GdDTPA-Dextran 487000 complex contained 0.10 mole GdDTPA per mole glucopyranose. It was speculated that the observed lower relaxivity of GdDTPA-dextran 487000 may have been due to the presence of a substantially greater proportion of unmodified glucopyranose units relative to modified units as compared with the lower molecular weight conjugates. Experiments which involved the evaluation of the GdDTPA-dextran complexes, GdDTPA, and GdEDTA with and without the presence of unmodified glucopyranose were conducted in an attempt to address this possibility.

A significant increase in relaxivity for GdDTPA occurred only in the presence of greater than 20 fold excess of free dextran in solution (relative to dextran concentrations in the GdDTPA-dextran solutions) and is indicated in Figure 3.12. Although this result suggests that the relaxivity of the GdDTPA moiety in the dextran conjugates is not affected by possible interactions with the carrier, the possibility of microviscosity effects cannot be ruled out as the micro-environment of the covalently linked metal chelates may be significantly different than that of the noncovalently attached metal chelates.[48,83]

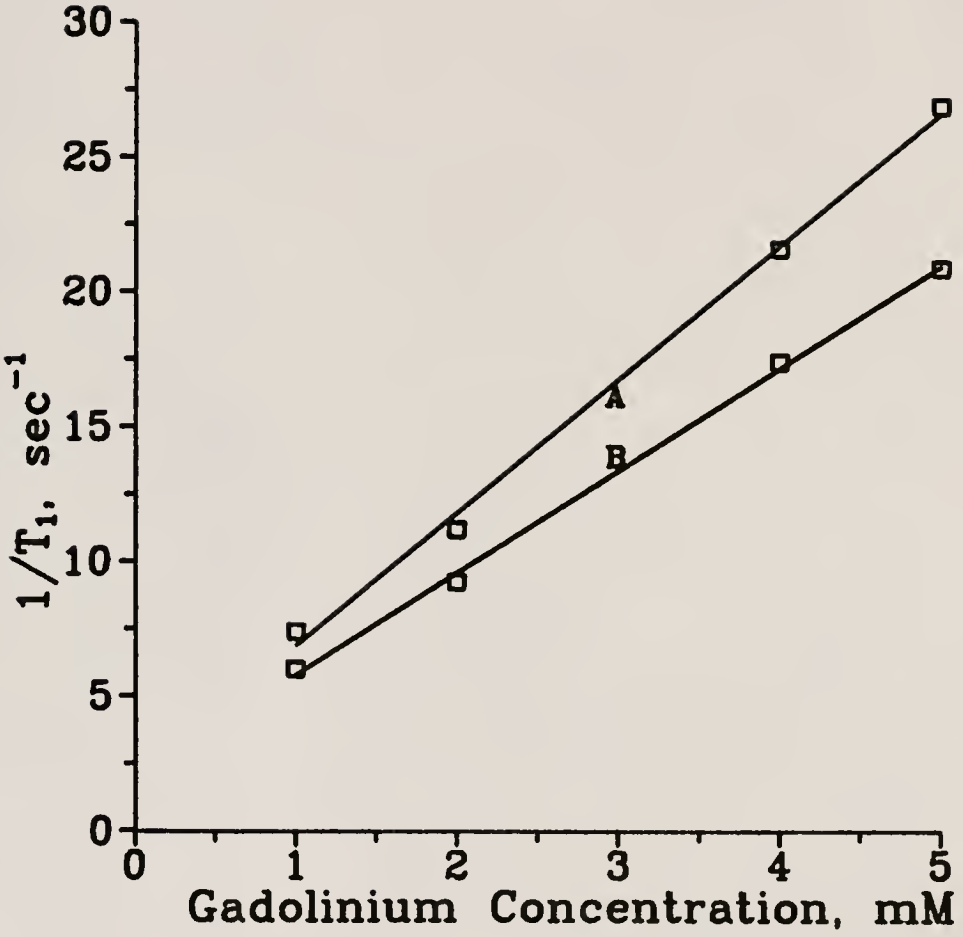

Figure 3.12. Plot of $1/T_1$ versus gadolinium concentration for (B) GdDTPA in the presence of 300 mM glucopyranose and (A) GdDTPA with no glucopyranose present in pH = 7.4 phosphate buffer of 0.15 M ionic strength, 100 MHz, 25°C.

The GdDTPA-dextran complexes exhibited significant relaxivity reduction when in the presence of equimolar concentrations of unmodified dextran, as shown in Table 3.6. This relaxivity reduction was not observed for GdDTPA but was observed for GdEDTA solutions in the presence of free dextran at concentrations equal to bound dextran concentrations in the GdDTPA-dextran solutions used in the T_1 evaluations, also shown in Table 3.6.

Table 3.6. Effect of free polysaccharide on T_1 relaxivities at 100 MHz of Gd^{3+} chelates.

Compound	T_1 Relaxivity[a] $(mM\ sec)^{-1}$
GdDTPA-dextran 40200	8.1 ± 0.3
GdDTPA-dextran 40200 with free dextran	5.2 ± 0.1
GdDTPA	3.8 ± 0.1
GdDTPA with free dextran	4.4 ± 0.5
GdEDTA	4.6 ± 0.1
GdEDTA with free dextran	3.3 ± 0.1
GdEDTA with free dextran and isopropanol	4.8 ± 0.7

[a]Reported precision is expressed as population standard deviation.

The results shown in Table 3.6 suggest that the GdDTPA-dextran complexes may be better emulated by GdEDTA, which has 2 inner sphere coordinated water molecules[65] in the crystal structure. The GdEDTA complex readily exchanges the coordinated water molecules for other available ligands[42] and it is possible that the observed effect free dextran has on GdEDTA solutions, as well as on GdDTPA-dextran solutions, may be due to coordinative displacement of water molecules by one or more alcohol groups of the polysaccharide. This observation can, however, also be explained in terms of hydrogen bonding between the coordinated water molecule(s) and the polysaccharide. The rate of exchange between ligand and bulk water molecules can be significantly reduced by hydrogen bonding interaction of this nature.[84] The observation that the reduction of relaxivity in the GdEDTA solutions in the presence of free dextran was negated by the presence of isopropanol supports either contention.

Chapter Summary

The synthetic method developed in this work for the production of polysaccharide conjugates of GdDTPA results in products in which reproducibly higher levels of loading by ester linkage of the paramagnetic chelate on to the carrier is obtained relative to other reported products.[52,53,71] The method resulted in an average of one GdDTPA moiety conjugated for every 2 to 3 repeating glucopyranose or

fructofuranose units of the polysaccharide. The mole ratio of Gd^{3+} to ester bonded DTPA was 1:1 in all preparations. No degradation of the polysaccharides upon esterification by the new method was observed and no evidence was found for significant chelate induced polysaccharide crosslinking. The conjugates were easily water solubilized, exhibited carbonyl stretching frequencies supportive of gadolinium (III) chelation, and, along with their respective nonmetallated chelates, exhibited potentiometric behavior consistent with products in which only one of the carboxyl functions of DTPA had been functionalized.

The thermodynamic stability of the new complexes is lower than that of GdDTPA but is greater than that of GdEDTA. Although high thermodynamic stabilities may suggest low *in vivo* toxicities of metal chelates, there is little correlation between thermodynamic stability and toxicity.[85] An important aspect of the potential toxicities these new compounds may exhibit *in vivo* could be addressed by evaluating the ion selectivity of the DTPA-polysaccharides under physiological conditions. The relative conditional stabilities of the zinc, calcium, iron, and copper complexes as compared with the gadolinium complex may be sufficiently high so that the endogenous metal ions compete effectively for the ligand. Since these new complexes were designed to persist *in vivo* for considerably longer periods of time than GdDTPA, there is greater probability for endogenous metal

displacement (the rate of renal clearance may approximate the rates of transmetallation). This would result in the release of the highly toxic[86] gadolinium ion from the complex. To address this possibility, the stabilities of the Zn^{2+}, Ca^{2+}. Cu^{2+}, Fe^{3+}, and Gd^{3+} complexes of the DTPA-polysaccharides should be determined in biological media at pH = 7.4.

One of the GdDTPA-dextran complexes undergoes ester hydrolysis considerably faster than the nonmetallated chelate. The feature of metal promoted hydrolysis of the ester linkage between the GdDTPA moiety and the polysaccharide carrier molecule may be important in understanding the biodistribution of the complexes. Additionally, the role of the rate of ester hydrolysis and its relationship to the level of toxicity these compounds may exhibit when used *in vivo* may be extremely important in the development of this type of new contrast agent. The *in vitro* T_1 relaxivities of the polysaccharide complexes are significantly greater than that of GdDTPA at 100 MHz and appear to be inversely dependent on the average molecular weight of the dextran carrier polysaccharides. The high relaxivities and degree of loading these new conjugates possess are particularly appealing in terms of circumventing potential problems associated with plasma expansion following clinical administration of the agents.[87] The solvent T_1 relaxation effects by these new compounds are

better emulated by GdEDTA rather than GdDTPA in comparative studies. The possibility of multiple coordination sites occupied by water molecules with hydrogen bonding between the carrier and inner sphere coordinated water molecules in these new compounds is suggested by the results of the *in vitro* T_1 relaxivity studies thus far. It is strongly recommended that the compounds be submitted for temperature dependent nuclear magnetic resonance dispersion (NMRD) profiles (plots of relaxivity versus magnetic field strength) so that more conclusive evidence regarding the number of inner-sphere coordinated water molecules can be obtained.[88] The observation that the GdEDTA relaxivity was significantly effected by the presence of free dextran in solution, possibly due to hydrogen bonding and/or coordination with the macromolecule, has implications concerning the use of EDTA in ligand competition based evaluations. This observation is of particular importance to investigators[47] who have used solution T_1 determinations from systems in which GdL-protein complexes were allowed to equilibrate with EDTA in solution in order to obtain conditional stability constants for the complexes. Values so obtained may be in gross error as a result of the interaction between GdEDTA and -OH containing macromolecules.

In addition to the probability of low thermodynamic stabilities in the chelate crosslinked gadolinium complexes

prepared in the work of Gibby et al.[52] relative to the noncrosslinked yet highly loaded compounds presented in this work, the antigenic or immunogenic properties of these agents have not been assessed. The crosslinked products reportedly ranged in average molecular weight from 17,000 to 2,000,000. Dextrans of greater than 90,000 average molecular weight elicit antibody production and in the weight range between 90,000 and 51,000 antibody production is not predictable.[89] The determination of the antigenic properties of the noncrosslinked products presented in this work is strongly advised and represents an area of study which has been neglected completely in all previous investigations concerning macromolecule-conjugated contrast agents.

CHAPTER 4

MAGNETIC RESONANCE IMAGING STUDIES USING GADOLINIUM CONJUGATES AS CONTRAST AGENTS

Chapter Overview

The method of MRI uses the proton relaxation properties and abundance of water associated with all physiological tissue types. When the most commonly applied pulse sequence in MRI is used, the soft tissue signal intensity is directly related to proton density and T_2 while inversely related to T_1[10] as shown in the following equation.

$$I = Hf(v)\ (1-e^{-TR/T1})e^{-TE/T2}$$

I = signal intensity

H = local proton concentration

f(v) = proton dispersion function

T_R = T_2 parameter, pulse interval

T_E = T_1 parameter, echo delay

Early in the development of MRI, it was found that slight differences in proton density, T_1, and T_2 existed for water protons associated with abnormal tissue relative to the surrounding normal tissue.[10,29,90] By varying the

instrumental parameters of T_R and T_E, images showing the area of abnormality could be obtained. These images, called T_1 weighted ($T_E << T_2$) and T_2 weighted ($T_R >> T_1$) images, were useful in the detection of large abnormalities but often did not clearly differentiate between abnormal and surrounding normal tissue.[91]

The development of contrast agents for MRI has ensued rapidly since 1983. Mallinckrodt and Schering simultaneously developed a prototype MRI contrast agent, GdDTPA. When the agent is used in MRI, the renal medulla and renal cortex are very sensitive to the compound (both regions of the kidney "light-up" in T_1 weighted images obtained shortly after intravenous administration of the contrast agent) and no other normal tissue images are enhanced by the agent.[35,36,92] At lesions (the interface between normal and abnormal tissue), however, GdDTPA freely crosses into the abnormal tissue and, with sufficient GdDTPA concentration, the small differences in T_1 of the abnormal versus normal tissues are amplified by the agent and image enhancement of the abnormal tissue results.

As mentioned in Chapter 3, GdDTPA is the only intravenously administered MRI contrast agent currently approved for human use. Since the compound is extracellular and rapidly undergoes renal excretion,[40] it is unsuitable for use in situations where a lengthy blood-pool persistence of the agent is required for specific organ or lesion uptake

to occur and unsuitable in evaluations requiring blood flow assessment.

Having been extensively characterized and clinically evaluated, GdDTPA has been compared with newly developed contrast agents.[93] Since the new conjugates developed in this work were designed to be blood-pool persistent, the imaging enhancement properties and compound distribution are expected to differ from those of GdDTPA and may enhance organ tissues other than, or in addition to, the renal medulla and cortex.

In evaluating these conjugates as contrast agents in MRI, two studies were undertaken. Phantom studies were conducted to provide a comparison between GdDTPA and the conjugates in terms of the *in vitro* concentration dependence as a function of signal intensity for different pulse sequences. From this type of study, it is possible to determine a range of dosages of the conjugates that would be suitable for *in vivo* studies and determine the most suitable pulse sequence for *in vivo* studies. Additionally, the results can be qualitatively compared with the carrier molecular weight trend observed in the *in vitro* NMR T_1 values obtained in Chapter 3. The second study involved the *in vivo* imaging of normal healthy rabbits of sufficient size to obtain discernable organ images.

Materials and Methods

Phantom Studies

Phantom solutions were prepared in deionized water and concentrations were based on 60 mL/kg blood volume of 2 kg rabbits at twice the normal recommended dosage of Magnevist (Berlex Imaging, Schering, 0.1 mmole/kg). Solution concentrations of GdDTPA-polysaccharides and GdDTPA (Magnevist, Berlex Imaging) ranged from 0.33 to 33.3 mM. The range of concentrations represented a 10-fold span dilution and concentration relative to twice the recommended dosage of Magnevist. All phantom tubes were 0.5 cm inner diameter and were fabricated from Kimax disposable glass pipettes such that the bulk of the solution to be evaluated was elevated approximately 2 cm above the plane of the tube container and approximately 5 cm above the plane of the MR imager table. The total volume of each solution was 250 microliters. A tube containing deionized water was used as a standard in the study.

A General Electric 1.5 Tesla (63.91 MHz Proton Larmor Frequency) clinical magnetic resonance imager with a standard knee coil was used. The image gray scale was attenuated manually (manual pre-scan) to maximize signal intensity at 70 to 75% ({signal intensity/baseline intensity} * 100). Signal intensity values using various pulse sequence settings could therefore provide only for

rough comparison. The pulse sequences evaluated were T_1 and T_2 weighted spin echo (T_R/T_E = 300/20 and 2500/80, respectively.) The raw data, ROI intensities and their standard deviations were normalized by the calculation of relative intensity for each sample. The relative intensity was obtained by dividing the ROI of the sample by the ROI of the standard water phantom.

Animal Imaging Studies

New Zealand White male rabbits ranging in weight from 2.0 to 3.5 kg were used in the study. All animal use was approved by the University of Florida Animal Care and Use Committee and governed by the principles of the "Guide for the Care and Use of Laboratory Animals" (NIH Publication No. 86-23, revised 1985). The rabbits were premedicated with intramuscular injections of ketamine (35 mg/kg, Ketaset, Bristol Laboratories, Syracuse, NY), xylazine (4 mg/kg, Rompun, Haven Lockhart Laboratories, Shawnee, OK), and glycopyrrolate (11 μg/kg, Robinul, A.H. Robins, Richmond, VA). Anesthetization was maintained by face mask administration of 0.5 - 1.5% isoflurane (Forane, Anaquest, Madison, WI). The animals were positioned laying on their side with the head elevated 1 cm. A butterfly infusion set (25 g X 3/4, Abbott Hospital, Chicago, IL) inserted into the superficial marginal ear vein was used to administer the test contrast agent and saline solution. All contrast

agents were injected at a dosage of 0.1 mmole Gd^{3+}/kg. Following administration of the contrast agent at a rate of 2 mL/min, one mL of saline solution was used to wash through the catheter.

A five inch surface coil was positioned under the abdominal area of the animal and three inch surface coil under the head. A General Electric 1.5 Tesla clinical magnetic resonance imager was used. Pre-contrast images of the brain, liver, kidney, intestines, and abdominal vascularity were obtained using the T_1 weighted spin echo pulse sequence with T_R/T_E = 300/20. Abdominal transverse images of 5 mm thickness were obtained with a 20 cm field of view. Head coronal images of 4.0 mm thickness were obtained with a 12 cm field of view. All images were obtained using automatic attenuation of gray scale signal intensity and no E.C.G. gating was used. Following pre-contrast images, images were obtained at regular intervals over a 90 minute period after injection of the contrast material.

The raw data, ROI intensities and their standard deviations, were normalized by the calculation of relative signal intensity for predefined areas of each tissue type evaluated. The relative intensity was obtained by dividing the tissue sample ROI by the ROI of the background (an area of constant number of pixels in the image in which signal intensity did not change significantly over time).

Results and Discussion

Phantom Results

The phantom studies were undertaken to provide a rough comparison with the T_1 relaxivity measurements (see Chapter 3) and to ascertain the concentration dependence of signal intensity for the new complexes as compared with GdDTPA (Magnevist, Berlex Imaging) using various pulse sequences. Although not directly apparent from the images obtained in each pulse sequence, as shown in Figure 4.1, the signal intensities in the region of interest (ROI) of each of the different concentration solutions of each compound were unique. In the T_1 weighted image, the GdDTPA-dextran complexes all exhibited suppression in relative signal intensity (sample signal intensity / solvent signal intensity) at concentrations greater than 3.33 mM relative to Magnevist. This effect, as shown in Figure 4.2, has been attributed[94] to the counteracting effects by macromolecular complexes on solvent T_2. In spin echo experiments there is a direct proportionality between signal intensity and T_1 and an inverse proportionality between signal intensity and T_2.[95] The results indicate that, at concentrations sufficiently greater than 3.33 mM, the contribution to signal intensity by paramagnetic effect on the solvent T_2 outweighs the T_1 contribution. At these concentrations, the relative signal intensity may be less than one and suggests

their potential application in ascertaining localized tissue concentration build up of the complexes when used *in vivo*.

Among the factors that do not allow for direct comparison of relaxivities determined in these phantom studies and those determined in the NMR experiments (see Chapter 3) are the differences in proton Larmor frequencies used (63 MHz versus 100 MHz, respectively), and the interdependence of pulse sequence and both T_1 and T_2 with signal intensity in the phantom studies. A trend, however, was calculated (Appendix) from the relative signal intensities (sample signal intensity / solvent signal intensity) for each of the T_1 weighted phantoms at concentrations up to 3.33 mM. As shown in Table 4.1, at concentrations less than or equal to 3.33 mM the T_1 weighted phantoms exhibited the same trend in T_1 relaxivity with carrier molecular weight as observed in the 100 MHz T_1 relaxivity studies.

As shown in Figure 4.3, the T_2 weighted phantom study resulted in increased relative signal intensity up to concentrations of 3.33 mM for the GdDTPA-dextran compounds and Magnevist. This trend was followed by a sharp decrease in signal intensity for the complexes relative to Magnevist with increasing concentration. Using T_1 values approximated from the T_1 weighted images, the calculated solvent T_2 decreased less rapidly with increasing concentration of the higher molecular weight dextran conjugated gadolinium

complexes than the lower molecular weight complexes, shown in Figure 4.4. The limited number of data points, however, does not allow for any conclusions in this regard.

Compound	Concentrations				
GdDTPA-dex 9400	33.3	16.7	3.33	0.67	0.33
GdDTPA-dex 70800	33.3	16.7	3.33	0.67	0.33
GdDTPA-inulin	33.3	16.7	3.33	0.67	0.33
GdDTPA-dex 40200	3.33	0.67	0.33	-	28.0
GdDTPA-dex 487000	3.33	0.67	0.33	-	19.0
GdDTPA	33.3	16.7	3.33	0.67	0.33
	H_2O				

a.

Figure 4.1. Phantom studies of the new conjugates, GdDTPA, and water as standard. Template of compounds and concentrations used in phantom solutions (a), images obtained for phantom solutions using (b) T_1 weighted pulse sequence (SE 300/20) and (c) T_2 weighted pulse sequence (SE 2500/80)

b.

Figure 4.1 --Continued.

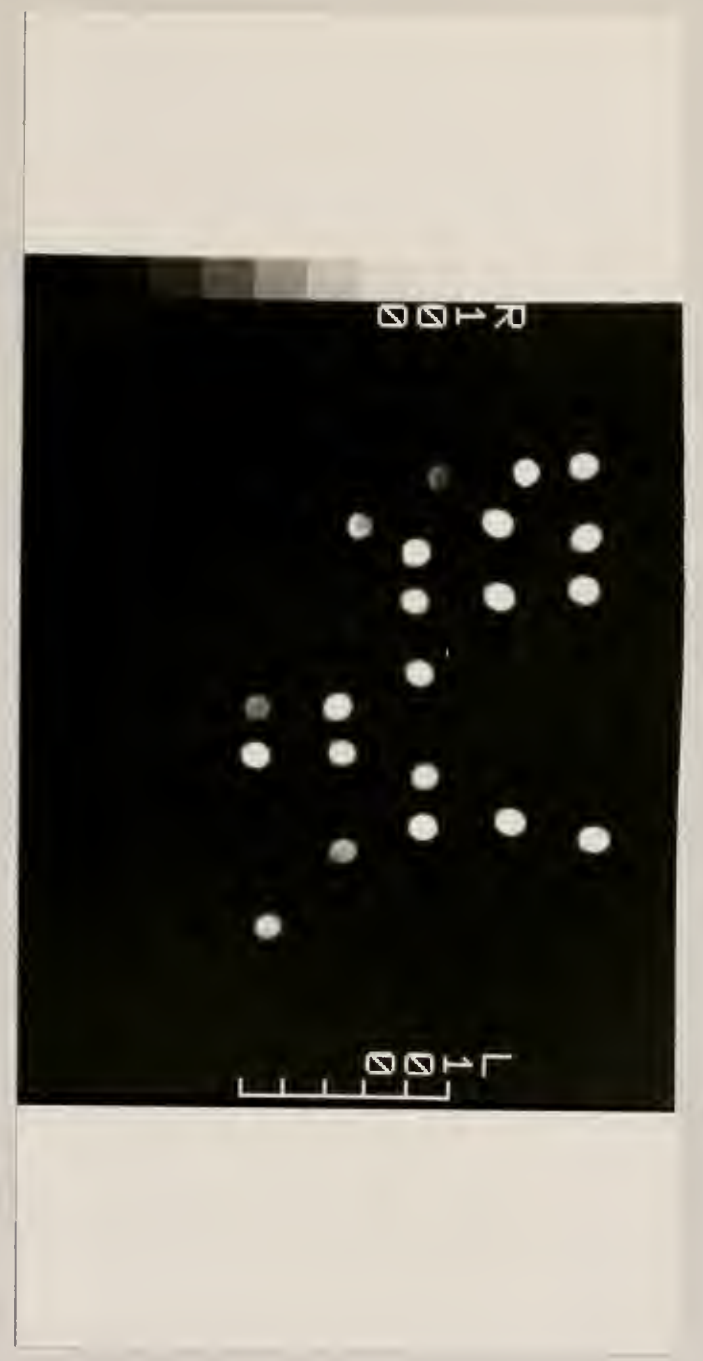

c.

Figure 4.1 --Continued.

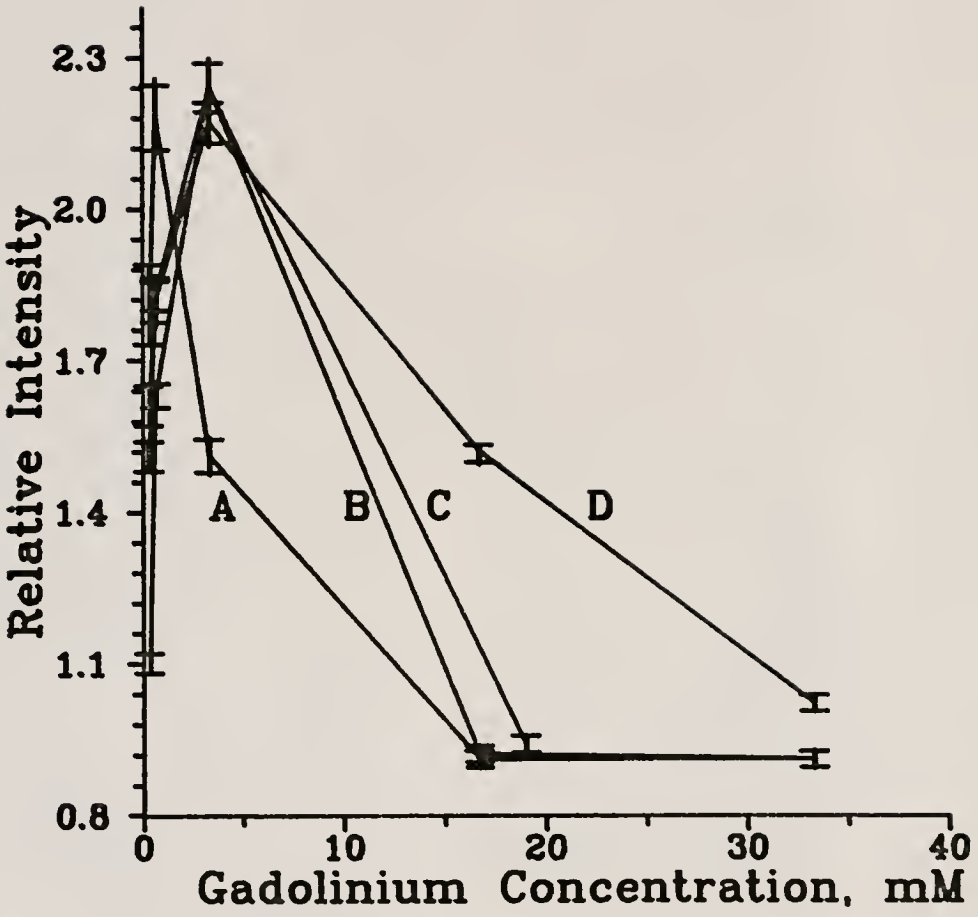

Figure 4.2. Plot of relative signal intensity versus gadolinium concentration for phantom solutions of GdDTPA-dextran 9400 (A), GdDTPA-dextran 70800 (B), GdDTPA-dextran 487000 (C), and GdDTPA (D) using T_1 weighted (SE 300/20) pulse sequence. Error bars represent standard error of the mean.

Table 4.1. Calculated T_1 relaxivities for prepared GdDTPA-polysaccharides at 63 MHz from phantom studies.

Compound	Relaxivity $(mM\ sec)^{-1}$
GdDTPA-inulin	0.84 ± .09
GdDTPA-dextran 9400	1.06 ± .14
GdDTPA-dextran 40200	0.78 ± .04
GdDTPA-dextran 70800	0.71 ± .10
GdDTPA-dextran 487000	0.54 ± .04

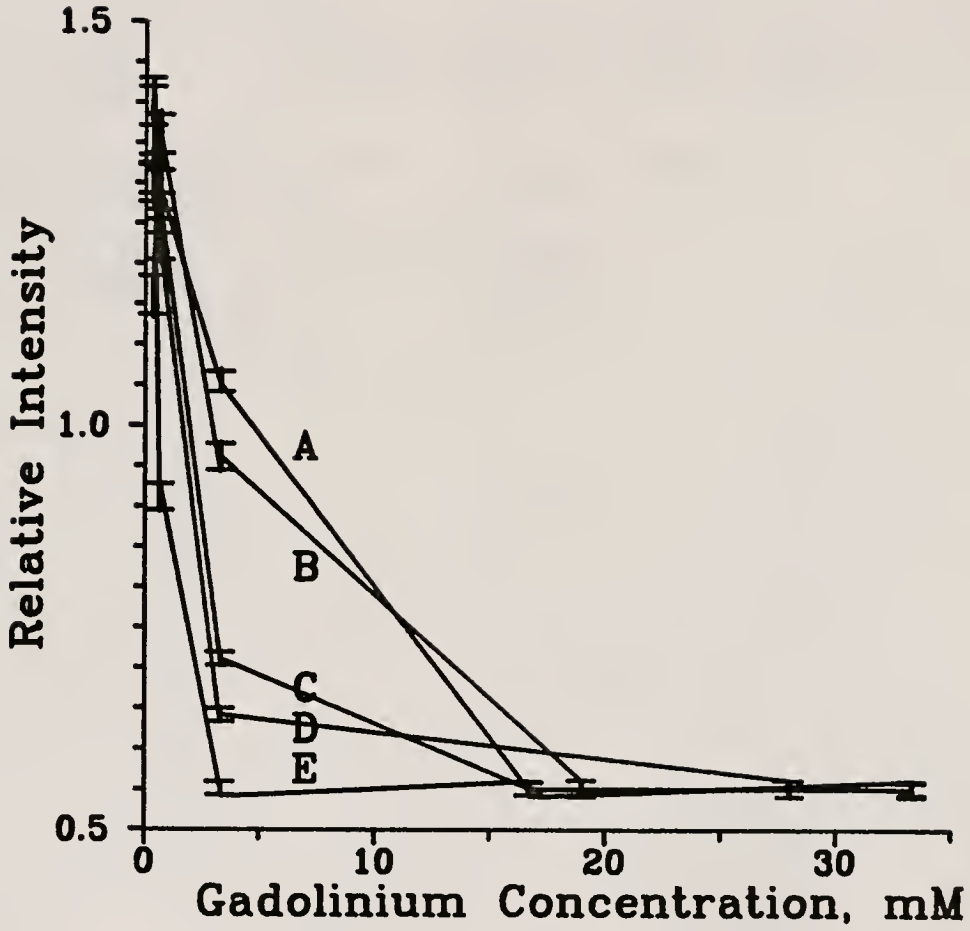

Figure 4.3. Plot of relative signal intensity versus gadolinium concentration for phantom solutions containing GdDTPA (A), GdDTPA-dextran 487000 (B), GdDTPA-dextran 70800 (C), GdDTPA-dextran 40200 (D), and GdDTPA-dextran 9400 (E) obtained when T_2 weighted (SE 2500/80) pulse sequence was used. Error bars represent standard error of the mean.

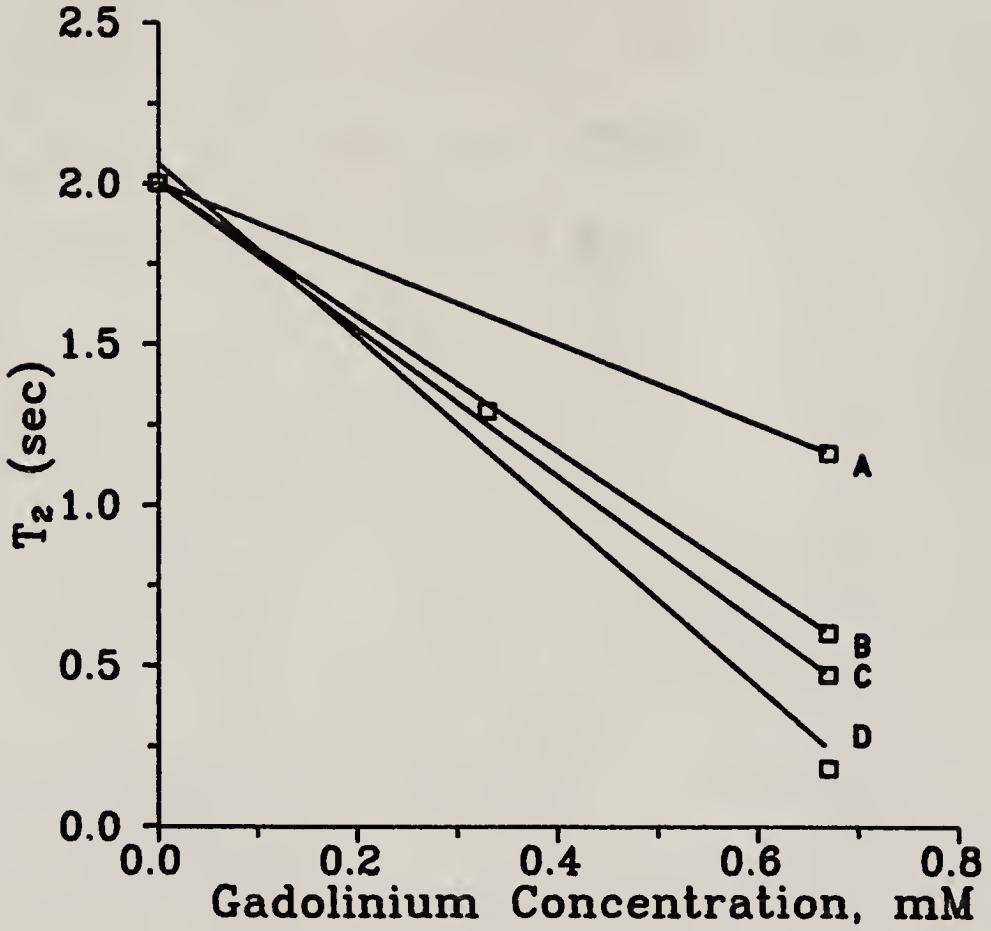

Figure 4.4. Plot of T_2 relaxivity versus dextran carrier average molecular weight for the GdDTPA-dextran complexes, A = GdDTPA-dextran 487000, B = GdDTPA-dextran 70800, C = GdDTPA-dextran 40200, D = GdDTPA-dextran 9400, obtained from T_2 weighted phantom solutions.

The GdDTPA-dextran complexes exhibited a greater effect on solvent T_1 relaxation than GdDTPA but at higher concentrations T_2 effects became more pronounced. The apparent inverse relationship between dextran carrier average molecular weight and T_1 relaxivity by the complexes, an observation made in this *in vitro* experiment and the relaxivity by NMR experiments conducted in Chapter 3, was not observed for the crosslinked products reported by Gibby et al.[52] Since there is generally increased branching of the polysaccharide as the molecular weight increases,[96] it is speculated that the observed trend of decreased T_1 relaxivity with increased dextran molecular weight may be a function of the number of bonded GdDTPA moieties and the number of unmodified glucopyranose units of the polysaccharide side branches. Highly crosslinked products may sterically prevent the metal chelate - carrier types of interactions from occurring.

The results of the T_1 and T_2 weighted phantom studies suggest that either pulse sequence is suitable when the new compounds at concentrations *in vivo* between 0.33 and 3.33 mM are used. These concentrations represent a range of 0.02 to 0.20 mmole Gd^{3+}/kg dosage. Since the recommended dosage for Magnevist (0.1 mmole Gd^{3+}/kg, Berlex Imaging TM) falls in the effective range for the dextran complexes, this recommended dosage was used for the subsequent *in vivo* studies. The T_1 weighted pulse sequence, which requires

significantly less time for data acquisition than the T_2 weighted pulse sequence, was also used for the subsequent *in vivo* imaging studies.

Animal Imaging Results

The preliminary *in vivo* imaging results, shown as qualitative images in Figures 4.5 and 4.6, indicate that GdDTPA-dextran 70800 strongly enhanced the kidney, vascularity of the liver, and liver parenchyma in excess of 60 minutes. As shown in Figure 4.5 a, the pre-contrast image of the kidney was of relatively low intensity (dark). Following injection of the contrast agent (Figure 4.5 b), the signal intensity of the kidney tissue was observed to increase rapidly and remained at high intensity relative to the surrounding tissue for in excess of 60 minutes. Shown in Figure 4.6 a-c, the pre-contrast image of the liver was of low intensity and three unexplainable areas (shown as dark spots) were observed. Shortly after administration of the GdDTPA-dextran 70800, the signal intensity of the liver tissue increased rapidly and remained of relatively high intensity for in excess of 60 minutes.

The torcula, a region of slow flowing blood in the brain, showed significant enhancement (Figure 4.7) for in excess of 80 minutes when the GdDTPA-dextran 70800 complex was used. Images of the brain, also shown in Figure 4.7, did not appear to be enhanced by the contrast agent.

Images obtained after administration of GdDTPA-dextran 9400 are shown in Figures 4.8 and 4.9. Shown in Figure 4.8, the pre-contrast kidney appeared dark in the interior (renal medulla) and somewhat lighter outside this area (renal cortex) in the image. Following administration of the contrast agent, both areas of the kidney were strongly enhanced within 10 minutes. The signal intensity of the renal cortex was considerably less than the renal medulla at 40 and 90 minutes post-contrast. After 100 minutes, the medulla and cortex regions were of similar intensity. Shown in Figure 4.9, the signal intensity of the liver increased rapidly after contrast agent administration and, at 90 minutes post-contrast, showed some evidence of retention in the hepatic parenchyma or microvascular regions of the liver. Additionally, a "black out" of signal intensity in some regions of the liver (to the left and right of arrow in the image obtained 90 minutes following contrast agent administration) was observed and suggests that the localized tissue concentration of the agent was greater than 0.2 mM Gd^{3+}.

Plots of relative signal intensity versus time for the tissues studied, shown in Figures 4.10 - 4.13, indicate that both of the evaluated complexes significantly enhanced the torcula, liver, renal medulla, and renal cortex for in excess of 60 minutes as relative signal intensities were

greater than one. The plots suggest that the rates of biodistribution for the two complexes differ.

a.

Figure 4.5. Transverse image of kidney (a) prior to administration of contrast agent, (b) 60 minutes after administration of GdDTPA-dextran 70800.

b.

Figure 4.5 --continued.

a.

Figure 4.6. Transverse images of the liver obtained (a) prior to administration of contrast agent, (b) 8 minutes following administration of GdDTPA-dextran 70800, and (c) 80 minutes following injection of GdDTPA-dextran 70800.

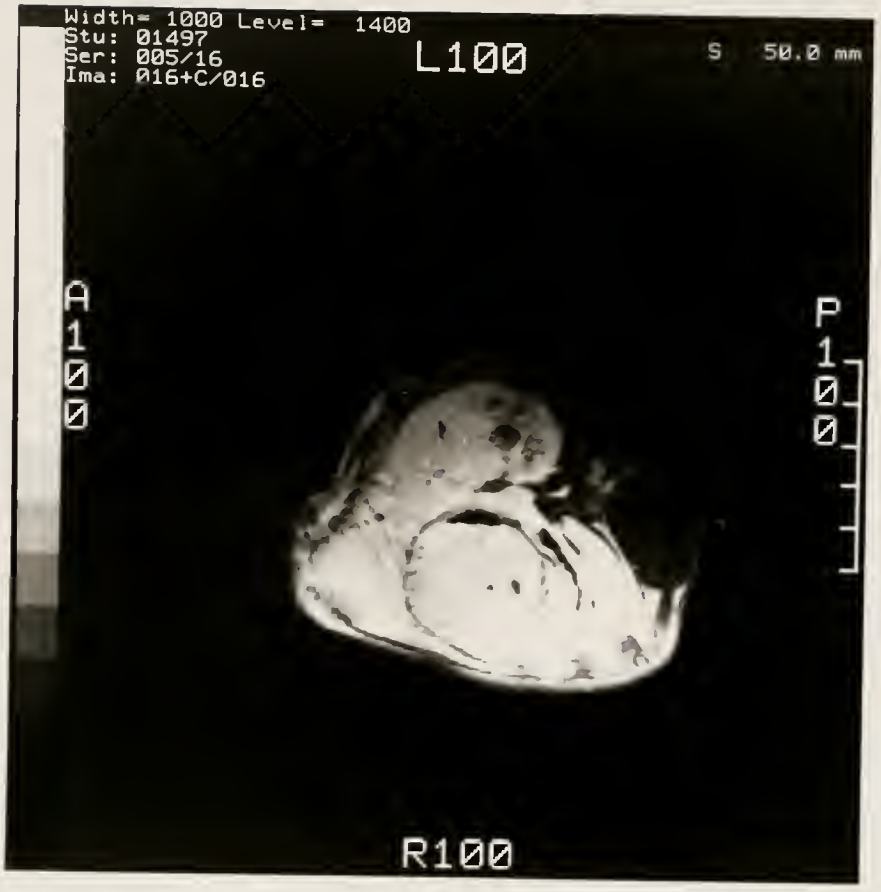

b.

Figure 4.6 --continued.

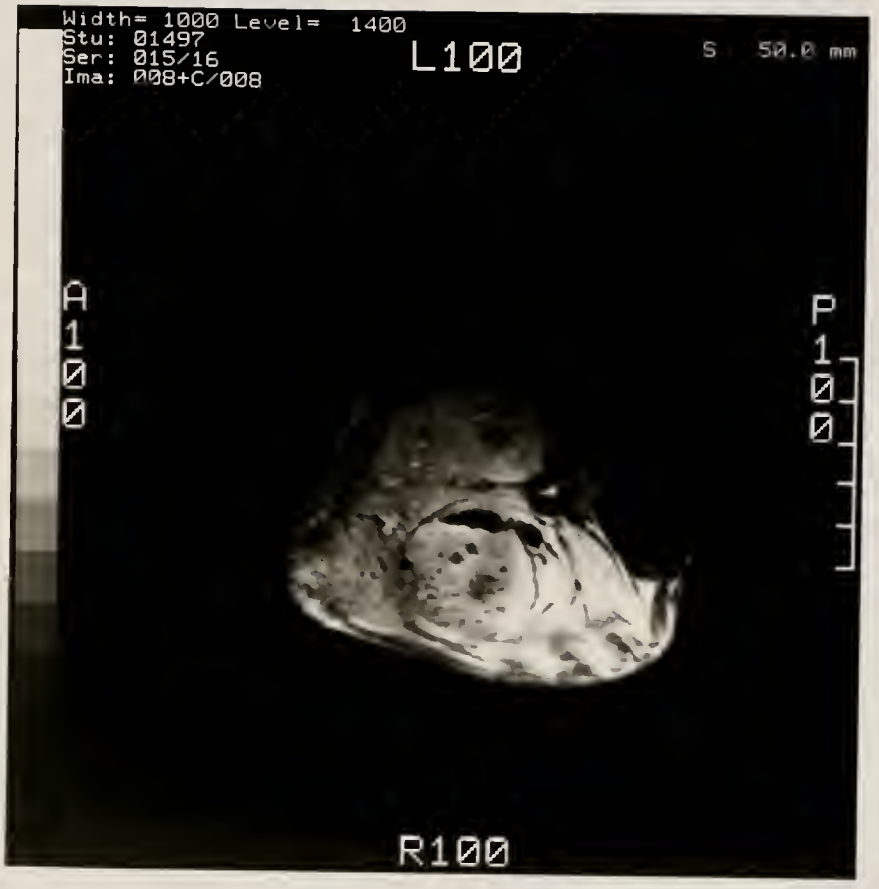

c.

Figure 4.6 --continued.

a.

Figure 4.7. Sagital images of the torcula obtained (a) prior to administration of contrast agent, (b) 10 minutes following injection of GdDTPA-dextran 70800, (c) 40 minutes following contrast agent injection, and (d) 80 minutes following contrast agent injection.

b.

Figure 4.7 --continued.

c.

Figure 4.7 --continued.

d.

Figure 4.7 --continued.

a.

Figure 4.8. Abdominal transverse images showing kidney obtained (a) prior to administration of GdDTPA-dextran 9400, (b) 40 minutes post-injection of contrast agent, (c) 70 minutes post-injection of contrast agent, and (d) 90 minutes.

b.

Figure 4.8 --continued.

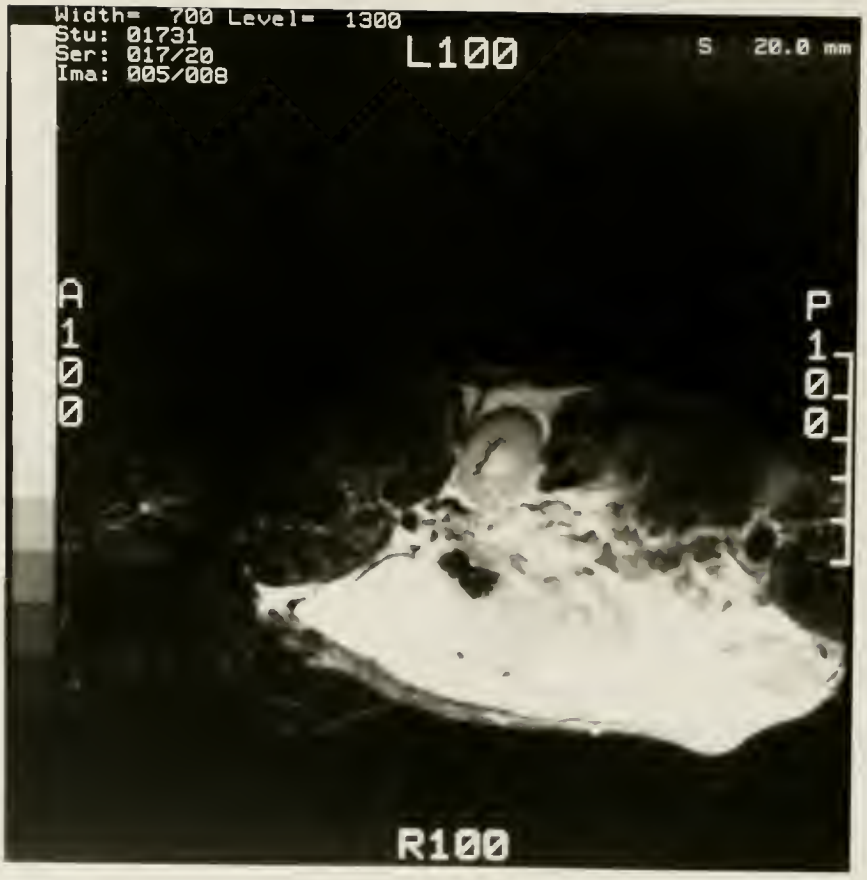

c.

Figure 4.8 --continued.

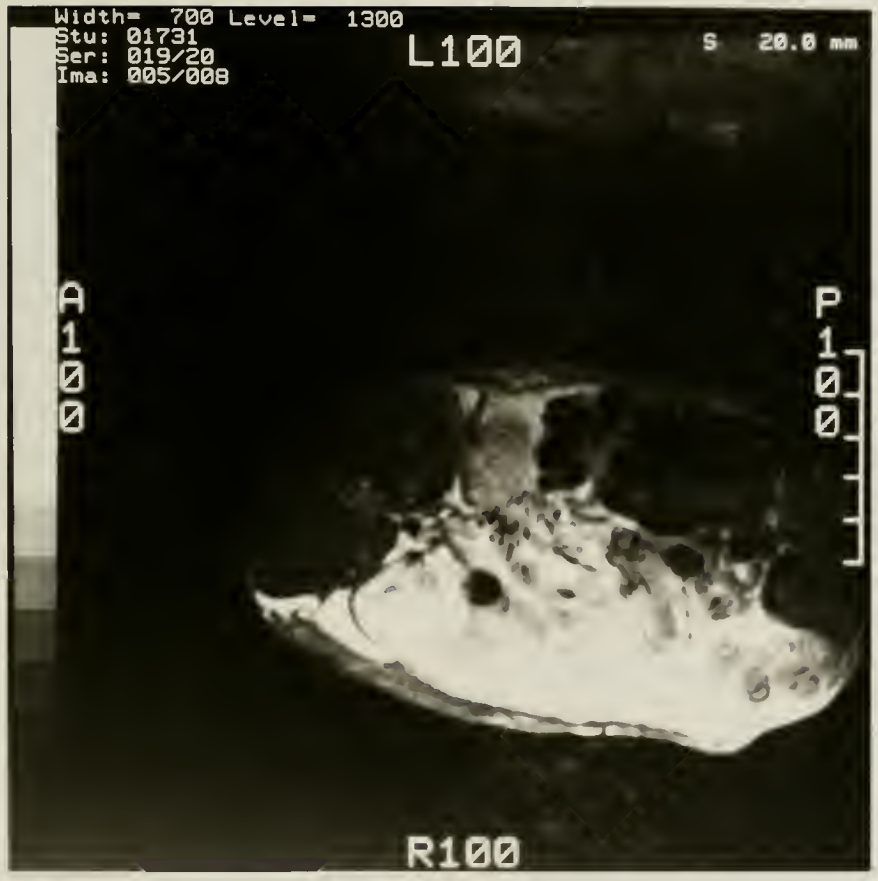

d.

Figure 4.8 --continued.

a.

Figure 4.9. Transverse images of the liver obtained (a) prior to administration of contrast agent, (b) 40 minutes following injection of GdDTPA-dextran 9400, and (c) 90 minutes after injection of GdDTPA-dextran 9400.

b.

Figure 4.9 --continued.

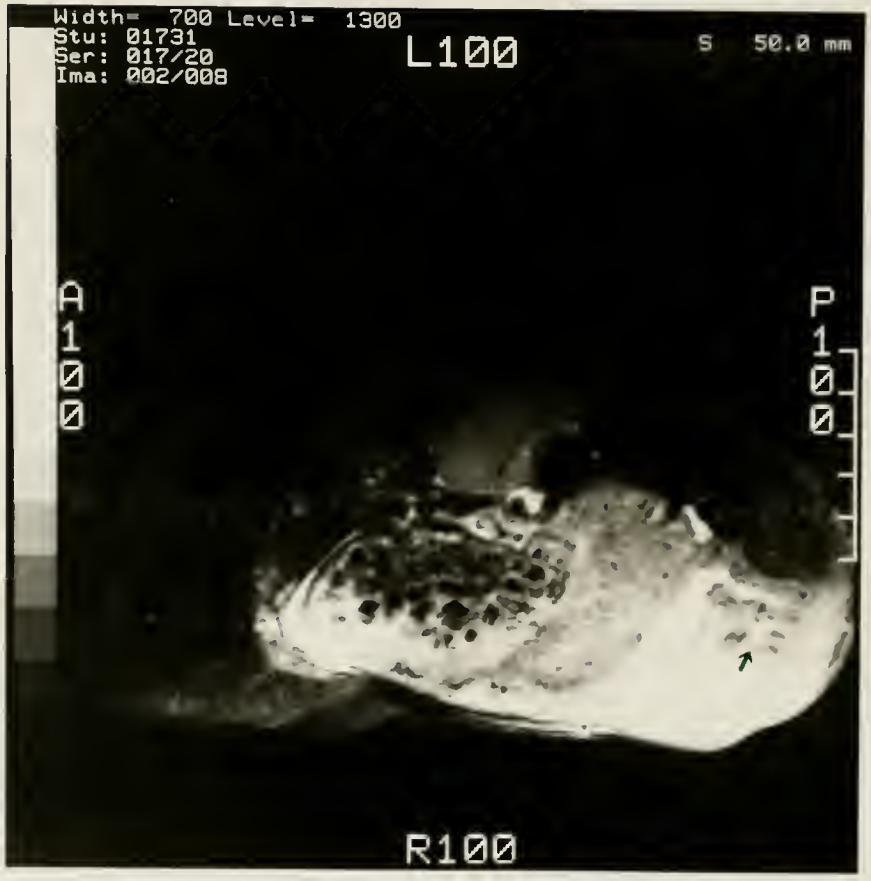

c.

Figure 4.9 --continued.

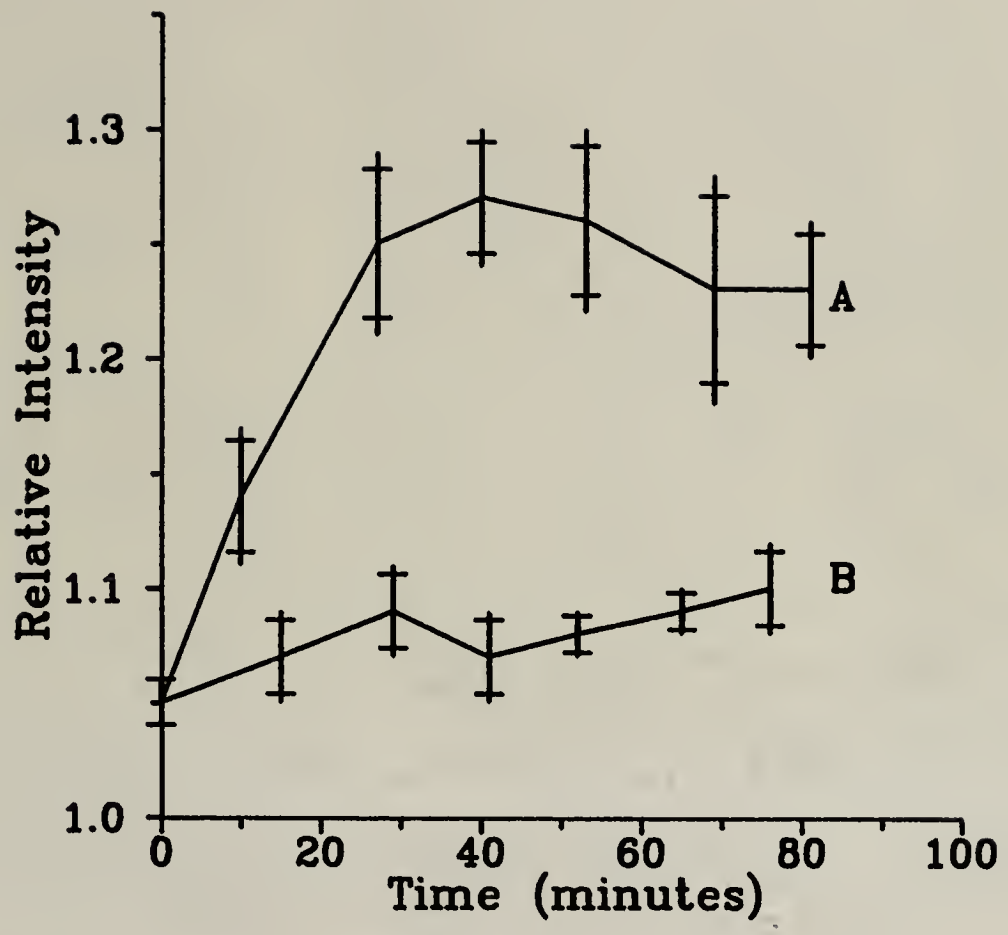

Figure 4.10. Plot of relative signal intensity of the torcula versus time after injection of (A) GdDTPA-dextran 70800 and (B) GdDTPA-dextran 9400. Error bars represent standard error of the mean.

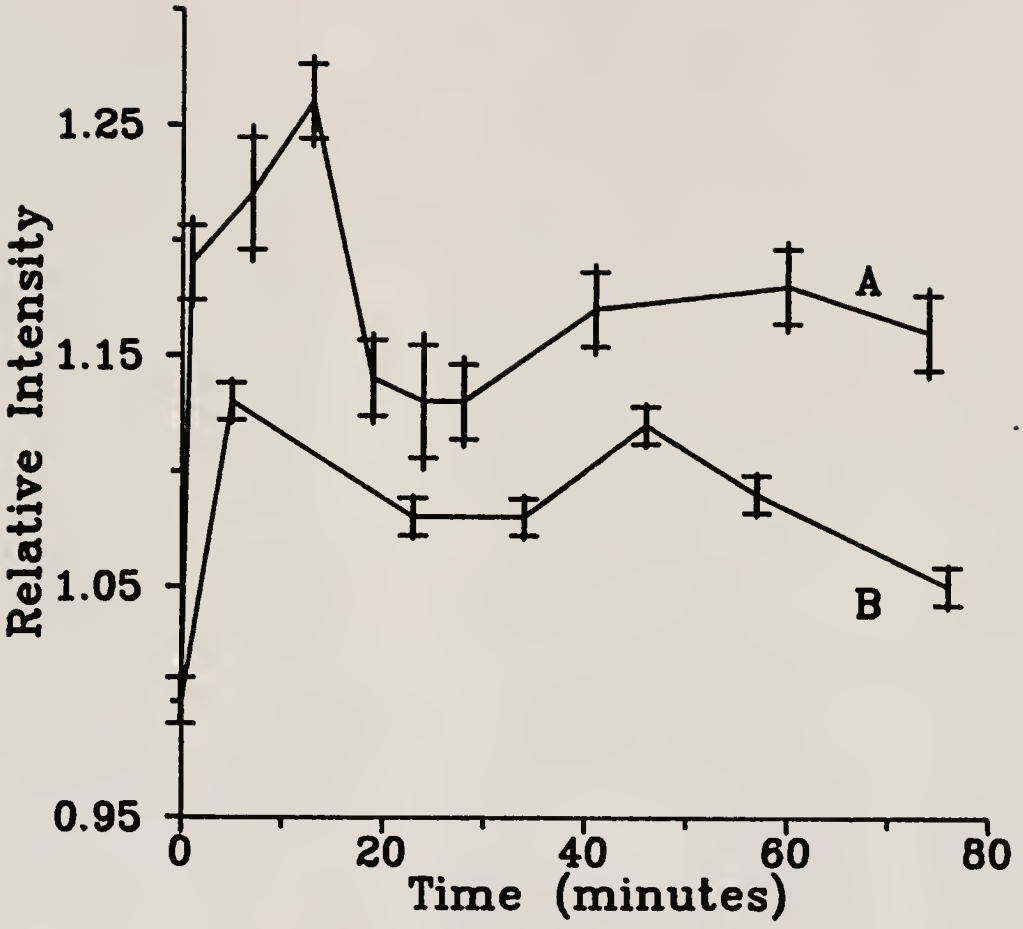

Figure 4.11. Plot of relative signal intensity of a region of the liver versus time following injection of (A) GdDTPA-dextran 70800 and (B) GdDTPA-dextran 9400. Error bars represent standard error of the mean.

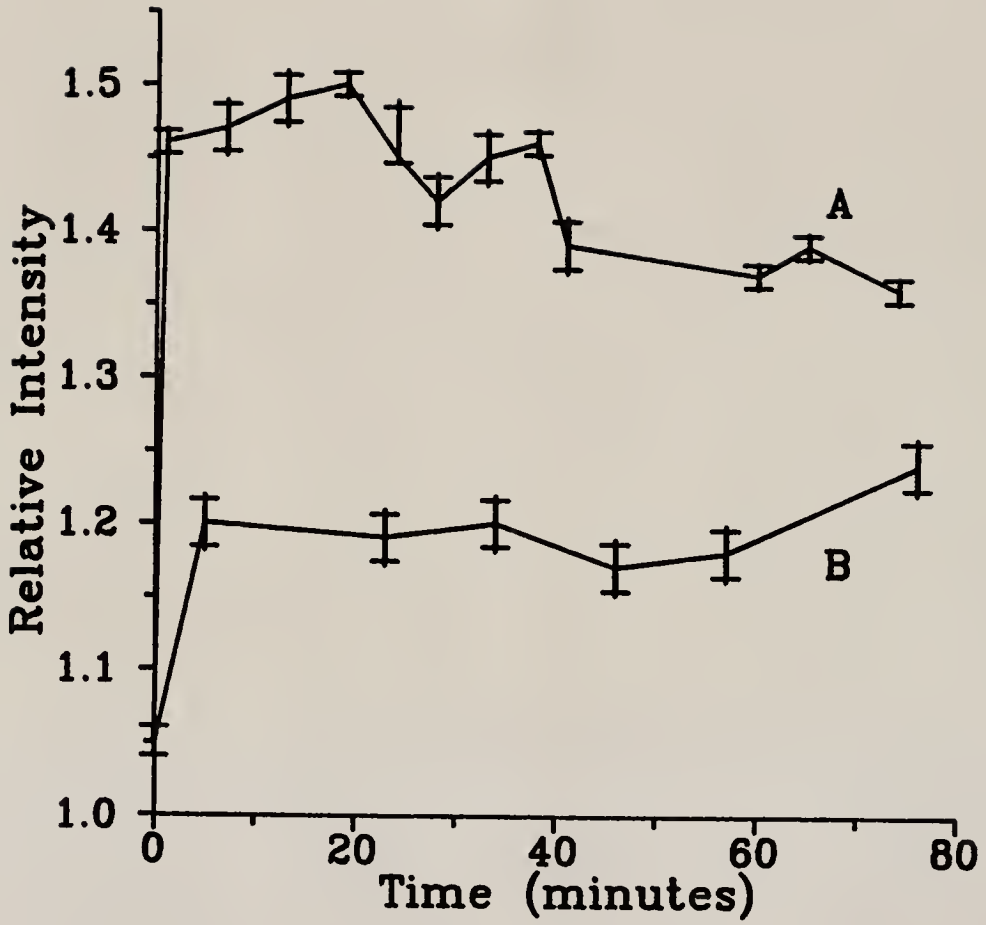

Figure 4.12. Plot of relative signal intensity of the renal medulla versus time following injection of (A) GdDTPA-dextran 70800 and (B) GdDTPA-dextran 9400. Error bars represent standard error of the mean.

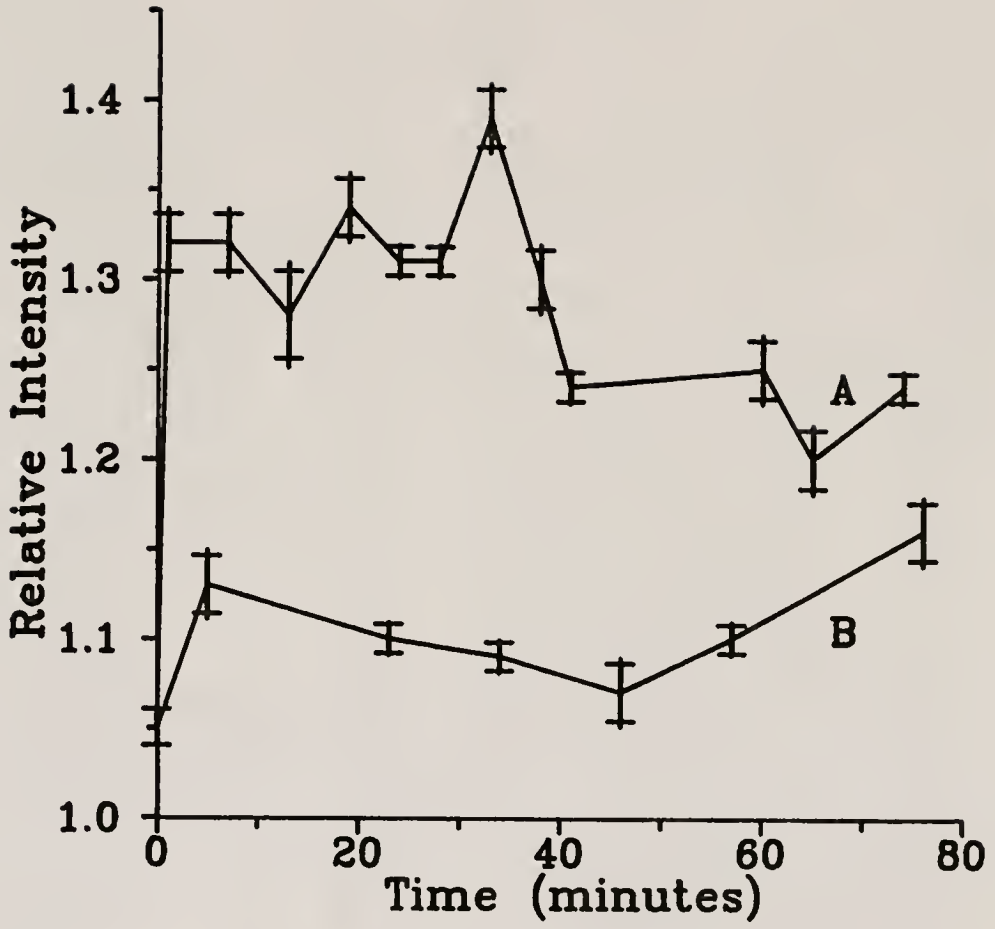

Figure 4.13. Plot of relative signal intensity of the renal cortex versus time following injection of (A) GdDTPA-dextran 70800 and (B) GdDTPA-dextran 9400. Error bars represent standard error of the mean.

The *in vivo* evaluations thus far support blood pool persistence in excess of 60 minutes for the GdDTPA-dextran complexes. A statistical number of studies using GdDTPA-dextran 70800 has been conducted and the results were very consistent for 5 of the 6 studies. The significant enhancement of liver and kidney tissue for in excess of 80 minutes may be partially accounted for by the presence of dextran metabolizing enzymes (dextranases) in these organs.[97] The *in vivo* imaging studies are continuing so that more statistically relevant data can be reported regarding differences in the biodistributive properties of the complexes as a function of dextran carrier average molecular weight.

In a recent presentation,[71] a 75,000 average molecular weight dextran was used to prepare a product which contained only 15 GdDTPA molecules per polysaccharide molecule and, when the compound was used in MRI, a 50% increase in bone marrow enhancement was reported. Bone marrow enhancement was also reported for the bovine serum albumin conjugate of GdDTPA[93] and the enhancement of this tissue suggests that Gd^{3+} was either displaced from the chelate or was present in nonchelated form at the onset. This can be deduced based upon the *in vivo* mode of toxic metal mobilization to areas of least potential damage.[98] The conjugates that we evaluated did not increase image enhancement of bone marrow based on the qualitative images of skull and jaw bone

obtained. Results thus far suggest that the biodistributional path of the new conjugates does not include transport to bone marrow and that the conjugates may not be releasing free gadolinium ion from the chelate when *in vivo*. Quantitative evaluations should, however, be conducted in future *in vivo* imaging studies and these studies should include imaging of larger marrow containing bones.

None of the animals used in evaluating these polysaccharide conjugates as contrast agents exhibited any observable adverse reaction to the compounds. Further work involving toxicity studies and serum stability half-lives of the complexes is needed.

The preliminary *in vivo* evaluation of two of the new compounds in normal rabbit tissue indicates that the blood pool persistence (greater than 60 minutes) of the compounds is considerably greater than that of GdDTPA,[40] which is an extravascular contrast agent. Enhancement of the liver, kidney, and abdominal vascularity is also evident for greater than one hour when either of the two compounds are used as contrast agents at dosages equal to that recommended for GdDTPA. Future work to characterize the image enhancing properties of the compounds when used in MRI of model tumors and their potential application to imaging enhancement of micro-perfusions is anticipated.

Chapter Summary

The results of the phantom studies support that the new conjugates exhibit different imaging properties than GdDTPA. The maximum signal intensities using the new conjugates were, however, obtained for solutions of concentrations comparable with that of the recommended dosage of GdDTPA. A trend of decreased T_1 relaxivity with increased dextran carrier average molecular weight was obtained from the phantom studies and reinforces the observed trend obtained in the NMR determined T_1 relaxivities study (Chapter 3).

The lower field strength of the imager (relative to the NMR that was used to determine T_1 relaxivity in Chapter 3) may account for what appeared to be less difference between the T_1 relaxivity of the conjugates and GdDTPA in the phantom studies than that observed in the NMR T_1 relaxivity study in Chapter 3. Macromolecular contrast agents generally exhibit nuclear magnetic resonance dispersion profiles of low relaxivity at low magnetic field strength followed by a sharp rise in relaxivity to a constant, relatively high, relaxivity at higher field strengths.[48,99] It is possible that the imager field strength is in, or lower than, the transitional range of field strength for the conjugates. To establish the relationship between magnetic field strength and T_1 relaxivity, it would be useful to

obtain nuclear magnetic resonance dispersion profiles for the conjugates.

When the new conjugates were used as contrast agents, the *in vivo* imaging results indicate that the compounds may be very suitable for applications where blood-pool persistence is required. The two compounds evaluated thus far also appear to significantly enhance images of the liver. These two aspects of the new conjugates (blood-pool persistence and liver tissue enhancement) are markedly different from the *in vivo* image enhancing properties of GdDTPA and suggest that these GdDTPA-polysaccharide conjugates may be a viable alternative to GdDTPA in certain diagnostic situations. Certainly, more *in vivo* imaging studies are necessary to assess the potential suitability of the agents when used in MRI. Imaging of lung and heart tissues when the new agents are used should be included in future studies of normal tissue enhancement. Additionally, the lesion permeability of the new compounds should be evaluated by using the compounds in imaging studies of animals which have tumor implants.

CHAPTER 5

SUMMARY

The primary emphasis of this work was to explore the chemistry of biomedically and biochemically useful metal chelates. The results obtained from the studies thus far provide considerable information about the properties of these metal chelates and provide a reference for the subsequent application of the complexes as biological probes. The studies additionally addressed a number of synthetic considerations so that a basis for the successful synthesis of the macromolecular conjugates was established.

The results in Chapter 2 indicate that a wide range of reduction potentials for Ru^{III}(Hedta)L can be obtained by varying the identity of the ligand, L. These complexes were synthesized by direct displacement of the water ligand from Ru^{III}(Hedta)H_2O. Although the L = H_2O complex can be synthesized by a number of methods, as indicated in the chapter, one method was developed in this work which results in the high yield production of the complex. This method, however, is not well suited for use when a protein modified EDTA is used as the ligand because the reaction conditions would likely denature the protein. For protein conjugates,

the better method for ruthenium chelation is by the production of $Ru(H_2O)_6^{3+}$ and its subsequent reaction with the chelate.

These complexes have potential usefulness following conjugation to redox active metalloproteins, M-protein, wherein the ruthenium chelate reduction potential can be tuned by ligand substitution, as shown in equation 5.1.

$$\text{M-protein-(Hedta)}Ru^{III}H_2O + L \longrightarrow \text{M-protein-(Hedta)}Ru^{III}L + H_2O \qquad (5.1)$$

By increasing the π acidity of the ligand, L, such that the ruthenium center is spontaneously reduced by the metal center of the protein, the reduction potential of the protein metal center can be approximated following the facile substitution of water by the ligand, L. By varying the position of the attached Ru(Hedta)L moiety on the protein, the distance dependence of the oxidation or reduction of the protein metal center by electron transfer may be investigated. These studies represent the most likely future applications of the ruthenium complexes evaluated in this work.

An additional application of potential usefulness involves the production of monoclonal antibodies (MAbs)

which have binding site(s) specific to the Ru(Hedta)L complex. The injection into mice of a protein or high molecular weight dextran conjugate of Ru(Hedta)H_2O could result in the production of antibodies. Following isolation and cloning of the desired Ru(Hedta)L specific MAbs, the binding strength of the MAb to the metal chelate could be assessed as a function of the redox potential of the tunable ruthenium center, again by varying the identity of the ligand, L.

In Chapter 3, the method of synthesis for the production of GdDTPA esterified polysaccharides resulted in reproducible and high levels of loading. No polysaccharide degradation and no evidence for significant levels of chelate induced crosslinking of the polysaccharides was observed. Higher levels of loading of GdDTPA on to the polysaccharide were obtained by the developed new method than any prior art method for the covalent attachment of GdDTPA on to macromolecular carriers. The compounds prepared in this work exhibited a higher thermodynamic stability than GdEDTA and greater *in vitro* T_1 relaxivities than GdDTPA.

The GdDTPA-dextran conjugates exhibited an unusual trend of decreased T_1 relaxivity with increased dextran carrier average molecular weight. This trend has been partially ascribed to intramolecular hydrogen bonding and/or coordinative displacement of inner-sphere coordinated water

molecule(s) by functional groups of the carrier molecule. This observation has potential implications regarding the development of future members of this type of macromolecule-gadolinium chelate contrast agent in that the degree of loading may significantly effect the T_1 relaxivities of the conjugates. An "induced" tertiary structure may result from the high loading of gadolinium chelates on to macromolecular carriers such as polysaccharides which typically have no globular tertiary structure when no metal chelate is linked to the carrier. This induced structure may arise as a result of intramolecular interactions between the charged GdDTPA moiety and the polysaccharide functional groups. The effect of tertiary structure to increase T_1 relaxivity is quite large as the rotational correlation time of the metal chelate is slowed considerably.[48] A study involving the determination of T_1 relaxivities for polysaccharide linked gadolinium chelates which have different degrees of loading is suggested.

The polymer nature of the prepared esterified polysaccharides needs to be addressed. An assessment of the molecular weight dispersity of the products and unmodified polysaccharides is necessary in order to properly characterize the new compounds and should be done prior to any quantitative biodistribution studies of the gadolinium conjugates.

The observed improved T_1 relaxivities of the conjugates as compared with GdDTPA, their high thermodynamic stability, and the possible importance of Gd^{3+} promoted ester hydrolysis in assuring the complete excretion of the metal ion in the form of GdDTPA, make this type of compound appealing as contrast agents for use in magnetic resonance imaging. The *in vivo* imaging studies support that the conjugates exhibit imaging properties which overcome the limitations of the commercially available contrast agent and suggest that the biodistributive properties of the conjugates may be dependent on the carrier molecular weight.

The future work required in the polysaccharide based gadolinium chelates as contrast agents project includes an evaluation of the toxicity of the prepared compounds and the development of a chemical basis for the observed toxicity levels. This would involve the assessment of rates of gadolinium promoted hydrolysis, rates of enzymatic polysaccharide hydrolysis, rates of *in vivo* excretion, and thermodynamic stability and kinetic lability of the conjugates toward gadolinium ion and endogenous metal ions. The development of a chemical basis for toxicity for this type of contrast agent as a function of the chelating agent would provide a foundation on which to design new conjugates as potential contrast agents for use in noninvasive diagnostic medicine.

APPENDIX

Mathematical determination of T_1 and T_2 relaxivities from phantom studies.

Part a. (Applicable to the determination of both T_1 and T_2 for phantom solutions.)

For spin echo pulse sequence:

$$I = hf(v)\ (1-e^{-TR/T1})e^{-TE/T2}$$

$$\text{Relative } I = RI = I_{soln}/I_{solv}$$

Assumption 1: $hf(v)_{soln} = hf(v)_{solv}$

let $C = (1-e^{-TR/T1})e^{-TE/T2}$ solvent

Therefore, $RI = (1-e^{TR/T1})e^{-TE/T2}{}_{soln}/C$

where $T_{1\ solv} = T_{2\ solv} = 2$ sec.

Part b. Solving for solution T_1:

$$T_{1\ soln} = -T_R/\ln\{1-(CRI/e^{-TE/T2})\}$$

Assumption 2: $T_{2\ soln} = T_{2\ solv}$ = 2 sec at low concentrations of paramagnetic species.

Known parameters from T_1 weighted spin echo pulse sequence: T_E = 20 msec and T_R = 300 msec.

Part c. Solving for solution T_2:

$$T_{2\ soln} = -T_E/\ln\{CRI/(1-e^{-TR/T1})\}$$

Assumption 3: $T_{1\ soln}$ = values obtained from T_1 weighted phantom solutions (part b).

Assumption 4: Accuracy of $T_{2\ soln}$ equation is greatest at high concentrations of paramagnetic species.

Known parameters from T_2 weighted spin echo pulse sequence: T_E = 80 ms and T_R = 2500 ms.

REFERENCES

(1) Chaberek, S.; Frost, A.E.; Doran, M.A.; Bicknell, N.J. *J. Inorg. Nucl. Chem.* **1959**, *11*, 184.

(2) Harris, W.R.; Martell, A.E. *Inorg. Chem.* **1976**, *15*, 713.

(3) Moeller, T.; Thompson, L.C. *J. Inorg. Nucl. Chem.* **1962**, *24*, 499.

(4) Bohigian Jr., T.A.; Martell, A.E. *Inorg. Chem.* **1965**, *4*, 1264.

(5) Bulman, R.A. *Structure and Bonding* **1987**, *67*, 91.

(6) Meares, C.F.; Wenzel, T.G. *Acc. Chem. Research* **1984**, *17*, 202.

(7) Alazraki, N.P.; Taylor Jr., A.T. *Invest. Radiol.* **1988**, *23*, 414.

(8) Gray, H.B.; *Chem. Soc. Rev.* **1986**, *15*, 17.

(9) Mauk, A.G.; Bordignon, E.; Gray, H.B. *J. Am. Chem. Soc.* **1982**, *104*, 7654.

(10) Brasch, R.C. *Radiology* **1983**, *147*, 781.

(11) Pykett, J.L. *Scientific American* **1982**, *246*, 78.

(12) Taube, H. *Pure & Appl. Chem.* **1979**, *51*, 901.

(13) Matsubara, T.; Creutz, C. *J. Am. Chem. Soc.* **1978**, *100*, 6255.

(14) Sulfab, Y.; Taylor, R.S.; Sykes, A.G. *Inorg. Chem.* **1976**, *15*, 2388.

(15) Oyama, N.; Anson, F.C. *J. Am. Chem. Soc.* **1979**, *101*, 1634.

(16) Oyama, N.; Anson, F.C. *J. Electroanal. Chem.* **1978**, *88*, 289.

(17) Matsubara, T.; Creutz, C. *Inorg. Chem.* **1979**, *18*, 1956.

(18) Meares, C.F.; Goodwin, D. *J. Protein Chem.* **1984**, *3*, 215.

(19) Scherzer, J.; Clapp, L.B. *J. Inorg. Nucl. Chem.* **1968**, *30*, 1107.

(20) Mercer, E.E.; Buckley, R.R. *Inorg. Chem.* **1965**, *4*, 1692.

(21) Makaida, M.; Okuno, M.; Ishimari, T. *Nippon Kagaka Zasshi* **1965**, *86*, 589. Procedure translated by Q.R. Billi, Georgetown University.

(22) Cady, H.H.; Connick, R.E. *J. Am. Chem. Soc.* **1958**, *80*, 2646.

(23) Kallen, T.W.; Earley, J.E. *Inorg. Chem.* **1971**, *10*, 1149.

(24) Connick, R.E.; Fine, D.A. *J. Am. Chem. Soc.* **1960**, *82*, 4187.

(25) Shepherd, R.E.; Taube, H. *Inorg. Chem.* **1973**, *12*, 1391.

(26) Ni, C-L.; Anson, F.C.; Osteryoung, J.G. *J. Electroanal. Chem.* **1986**, *202*, 101.

(27) Oyama, N.; Anson, F.C. *J. Am. Chem. Soc.* **1979**, *101*, 3480.

(28) Diamantis, A.A.; Dubrawski, J.V. *Inorg. Chem.* **1981**, *20*, 1142.

(29) Damadian, R. *Science* **1971**, *171*, 1151.

(30) Zawadzki, M.B.; Norman, D.; Newton, T.H.; Kelly, W.M.; Kjos, B.; Mills, C.M.; Dillon, W.; Sobel, D.; Crooks, L.E. *Radiology* **1984**, *152*, 71.

(31) Partain, C.L.; James, A.E.; Rollo, F.D., Price, R.R. *Nuclear Magnetic Resonance (NMR) Imaging*; Saunders: Philadelphia, 1983.

(32) Gadian, D.G.; Payne, J.A.; Bryant, D.J.; Young,I..; Carr, D.H.; Bydder, G.M. *J. Comput. Assist. Tomogr.* **1985**, *9*, 242.

(33) Graif, M.; Steiner, R.E. *Brit. J. Radiol.* **1986**, *59*, 865.

(34) Runge, V.M.; Schoerner, W.; Niendorf, H.P.; Lanaido, M.; Koehler, D.; Claussen, C.; Felix, R.; James, A.E. *Magn. Reson. Imaging* **1985**, *3*, 27.

(35) Brasch, R.C.; Weinmann, H.J.; Wesbey, G.E. *Am. J. Roentgenol. (AJR)* **1984**, *142*, 625.

(36) Carr, D.H.; Brown, J.; Bydder, G.M.; Steiner, R.E.; Weinmann, H-J.; Speck, U.; Hall, A.S.; Young, I.R. *Am. J. Roentgenol. (AJR)* **1984**, *143*, 215.

(37) Runge, V.M.; Clanton, J.A.; Herzer, W.A.; Gibbs, S.J.; Price, A.C.; Pertain, C.L.; James, A.E. *Radiology* **1984**, *153*, 171.

(38) Carr, D.H.; Brown, J.; Leung, A.W-L.; Pennock, J.M. *J. Comput. Assist. Tomogr.* **1984**, *8*, 385.

(39) Widder, D.J.; Greif, W.L.; Widder, K.L.; Edelman, R.E.; Brady, T.J. *Am. J. Roentgenol. (AJR)* **1987**, *148*, 399.

(40) Weinmann, H-J.; Brasch, R.C.; Press, W.R.; Wesbey, G.E. *Am. J. Roentgenol. (AJR)* **1984**, *142*, 619.

(41) Meyer, D.; Schafer, M.; Bonnemain, B. *Invest. Radiol.* **1988**, *23(suppl. 1)*, S232.

(42) Tweedle, M.F.; Gaughan, G.T.; Hagan, J.; Wedeking, P.W.; Sibley, P.; Wilson, L.J.; Lee, D.W. *Nucl. Med. Biol.* **1988**, *15*, 31.

(43) Gillis, P.; Koenig, S.H. *Magn. Reson. Med.* **1987**, *5*, 323.

(44) Bino, A.; Johnston, D.C.; Goshorn, D.P.; Halbert, T.R.; Stiefel, E.I. *Science* **1988**, *241*, 1479.

(45) Strich, G.; Hagan, P.L.; Gerber, K.H.; Slutsky, R.A. *Radiology* **1985**, *154*, 723.

(46) Carr, D.H.; Brown, J.; Bydder, G.M.; Weinmann, H.J.; Speck, U.; Thomas, D.J.; Young, I.R. *Lancet* **1984**, *1*, 484.

(47) Lauffer, R.B.; Brady, T.J. Brown, R.D.; Baglin, C.; Koenig, S.H. *Magn. Reson. Med.* **1986**, *3*, 541.

(48) Koenig, S.H.; Brown, R.D.in *Magnetic Resonance Annual* H.Y. Kressel, Ed.; Raven Press: New York, 1987; p263.

(49) Poznansky, M.J.; Cleland, L.G. In *Drug Delivery Systems*, R.L. Juliano Ed. Oxford Univ.: New York, 1980; pp 253-375.

(50) Ogan, M.; Grodd, W.; Paajanen, H.; Huberty, J.; Revel, D.; Eriksson, U.; Tozer, T.; Sosnovsky, G.; White, D.; Engelstad, B.; Brasch, R.C. *Radiology* **1985**, *157(P)*, 100.

(51) Schmiedl, U.; Ogan, M.D.; Moseley, M.E.; Brasch, R.C. *Am. J. Roentgenol. (AJR)* **1986**, *147*, 1263.

(52) Gibby, W.A.; Bogdan, A.; Ovitt, T.W. *Invest. Radiol.* **1989**, *24*, 302.

(53) Ranney, D.F.; Weinreb, J.C.; Cohen, J.M.; Srikanthan, S.; K-Breeding, L.; Kulkarni, P.; Antich, P. In *Contrast Agents in Magnetic Resonance Imaging proceedings of an International Workshop January 1986*; Runge, V.M., Clausson, C., Felix, R., James, Jr., A.E., Eds.; Exerpta Medica: San Diego, 1986; pp 81-87.

(54) Sherwood, R.F.; Baird, J.K.; Atkinson, T.; Wublin, C.N.; Rutter, D.A.; Ellwod, D.C. *Biochem. J.* **1977**, *164*, 461.

(55) Leach, B.E.; Angelici, R.J.; *J. Am. Chem. Soc.* **1968**, *90*, 2504.

(56) Krejcarek, G.E.; Tucker, K.L. *Biochem. Biophys. Res. Com.* **1977**, *77*, 581.

(57) Eckelman, W.C.; Karesh, S.M.; Reba, R.C. *J. Pharmaceut. Sci.* **1975**, *64*, 704.

(58) Halpern, S.; Stern, P,; Hagan, P.; Chen, A.; Frinke, J.; Bartholomew, R.; David, G.; Adams, T. In *Radioimmunoimaging and Radioimmunotherapy*; Burchiel, S.W., Rhodes, B.A., Eds.; Elsevier Science Pub: New York, 1983; pp 197-205.

(59) Bombardieri, G.; Rotilio, G.; Crifo, C.; DeMarco, C. *Arch. Biochem. Biophys.* **1968**, *127*, 766.

(60) Dubois, M.; Gilles, K.A.; Hamilton, J.K.; Rebers, P.A.; Smith, F. *Anal. Chem.* **1956**, *28*, 351.

(61) Wenzel, T.J.; Ashley, M.E.; Sievers, R.E. *Anal. Chem.* **1982**, *54*, 615.

(62) Martell, A.E.; Motekaitis, R.J. *Determination and Use of Stability Constants*; VCH: New York, 1988.

(63) Brown, M.A.; Johnson, G.A. *Med. Phys.* **1984**, *11*, 67.

(64) Skoog, D.A.; West, D.M. *Fundamentals of Analytical Chemistry, 4th Ed.*; Saunders: New York, 1982; p 198.

(65) Weinmann, H-J. in *Contrast Agents in Magnetic Resonance Imaging, Proceedings of an International Workshop January 1986*; Runge, V.M., Clausson, C., Felix, R., James Jr., A.E., Eds.; Exerpta Medica: San Diego, 1987; pp 19-23.

(66) Shallenberger, R.S.; Birch, G.G. *Sugar Chemistry*; AVI Pub.: Westport CT, 1975; pp 81-82.

(67) Goodall, D.M.; Norton, I.T. *Acc. Chem. Rev.* **1987**, *20*, 59.

(68) Fordyce, C.R. *Adv. Carbohyd. Chem.* **1945**, *1*, 309.

(69) Hnatowich, D.J.; Friedman, B.; Clancey, B.; Novak, M. *J. Nucl. Med.* **1981**, *22*, 810.

(70) Blanc, H.G. *Comptes Rendus* **1907**, *144*, 1356.

(71) Wikstrom, M.; Wang, S.C.; White, D.L.; Moseley, M.E.; Rongved, P.; Klaveness, J.; Brasch, R.C. in *Book of Abstracts. Presented at the Society of Magnetic Resonance in Medicine, Seventh Annual Meeting, San Francisco August 20-26*, 1988, 533.

(72) Harder, R.; Chaberek, S. *J. Inorg. Nucl. Chem.* **1959**, *11*, 197.

(73) Rendleman, J.A. *Adv. Carbohyd. Res.* **1966**, *21*, 209.

(74) Cox, J.S.G.; King, R.E.; Reynolds, G.F. *Nature* **1965**, *207*, 1202.

(75) Sherry, A.D.; Cacheris, W.P.; Kuan, K.T. *Magn. Reson. Med.* **1988**, *8*, 180.

(76) Hnatowich, D.J.; Layne, W.W.; Childs, R.L. *J. Appl. Radiat. Isot.* **1982**, *33*, 327.

(77) Kroll, H. *J. Am. Chem. Soc.* **1952**, *74*, 2036.

(78) Geraldes, C.F.G.C.; Sherry, A.D.; Cacheris, W.P.; Kuan, K.T.; Brown, R.D.; Koenig, S.H.; Spiller, M. *Magn. Reson. Med.* **1988**, *8*, 191.

(79) Lauffer, R.B.; Brady, T.J. *Magn. Reson. Imaging* **1985**, *3*, 11.

(80) Paajanen, H.; Reisto, T.; Hemmila, I; Komu, M; Niemi, P.; Kormano, M. *Magn. Reson. Med.* **1990**, *13*, 38.

(81) Kabalka, G.W.; Buonocore, E.; Hubner, K.; Davis, M.; Huang, L. *Magn. Reson. Med.* **1988**, *8*, 89.

(82) Lauffer, R.B. *Chem. Rev.* **1987**, *87*, 901.

(83) Koenig, S.H.; Baglin, C.; Brown, R.D. *Magn. Reson. Med.* **1984**, *1*, 496.

(84) Koenig, S.H.; Brown, R.D. *Magn. Reson. Med.* **1984**, *1*, 478.

(85) Cole, W.C.; DeNardo, S.J.; Meares, C.F.; McCall, M.F.; DeNardo, G.L.; Epstein, A.L.; O'Brien, H.A.; Moi, M.K. *J. Nucl. Med.* **1987**, *28*, 83.

(86) Weinmann, H.J.; Brasch, R.C.; Press, W.R.; Wesby, G.E. *Am. J. Roentgenol. (AJR)* **1984**, *142*, 619.

(87) Melton, R.G.; Wiblin, C.N.; Baskerville, A.; Foster, R.C.; Sherwood, R.F. *Biochem. Pharmacol.* **1987**, *36*, 113.

(88) Villafranca, J.J. *Methods in Enzymology* **1989**, *177*, 403.

(89) Kabat, E.A.; Bezer, A.E. *Arch. Biochem. Biophys.* **1958**, *78*, 306.

(90) Carr, D.H.; Gadian, D.G. *Clin. Radiol.* **1985**, *36*, 561.

(91) Wolf. G.L.; Burnett, K.R.; Goldstein, E.J.; Joseph, P.M. in *Magn. Reson. Annual 1985*, H.Y. Kressel, Ed.; Raven Press:New York, 1985; p231.

(92) Runge, V.M. *Nucl. Med. Biol.* **1988**, *15*, 37.

(93) Schmiedl, U.; Ogan, M.D.; Moseley, M.E.; Brasch, R.C. *Am. J. Roentgenol. (AJR)* **1986**, *147*, 1263.

(94) Koenig, S.H.; Gillis, P. *Invest. Radiol.* **1988**, *123 (suppl 1)*, S224.

(95) Pykett, I.C.; Newhouse, J.H.; Buonanno, F.S.; Brady, T.J.; Goldman, M.R.; Kistler, J.P.; Pohost, G.M. *Radiology* **1982**, *143*, 157.

(96) Sandford, P.A. *Adv. Carbohyd. Chem. Biochem.* **1979**, *36*, 265.

(97) Walker, G.J. *Biochem. Carbohyd. II* **1978**, *16*, 75.

(98) Jones, M.M.; Pratt, T.H. *J. Chem. Ed.* **1976**, *53*, 342.

(99) Muller, R.N.; Vander-Elst, L.; Rinck, P.A.; Vallet, P.; Maton, F.; Fischer, H.; Roch, A.; Van Haverbeke, Y. *Invest. Radiol.* **1988**, *23 (Suppl 1)*, S229.

BIOGRAPHICAL SKETCH

Frances Elizabeth Armitage was born in San Francisco, raised on a farm in Ithaca, New York, and finished her public schooling at Charlotte High School in Punta Gorda, Florida. She obtained her first job at age 15 as a veterinary assistant and supplemented the income by working at a restaurant. Frances was on her own at 17 and discovered that she, among other things, was not "ready" to begin a college career. She worked full time at a bookkeeping job while continuing weekend duties at the animal hospital and taking courses at a branch of Manatee Jr. College.

She moved to Gainesville, Florida, in 1979 and began taking classes at Santa Fe Community College, while working full time at the college. She was granted a scholarship from the Business and Professional Woman's Club, received her A.A. degree in 1983 and was selected "Outstanding Woman Student" by the Commission on the Status of Women at the college.

She received the DuPont Scholarship from the Department of Chemistry at the University of West Florida in Pensacola. Although she worked two jobs, she obtained her B.S. degree

in 1985, was nominated to the National Dean's List and received the Merck award for teaching services rendered to the department.

Frances was accepted to graduate school with the Department of Chemistry at the University of Florida in Gainesville and began work under the advisement of David E. Richardson in August 1985. She was awarded the Chemistry Department Teaching Award in 1987 and defended for the doctorate degree in May of 1990. Her post-graduation plans include a low-stress country life and gainful employment to support her musical and gardening hobbies.

I certify that I have read this study and that in my opinion it conforms to acceptable standards of scholarly presentation and is fully adequate, in scope and quality, as a dissertation for the degree of Doctor of Philosophy.

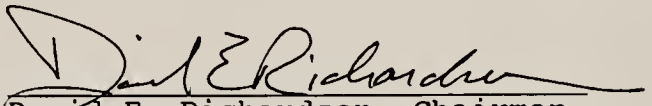

David E. Richardson, Chairman
Associate Professor of Chemistry

I certify that I have read this study and that in my opinion it conforms to acceptable standards of scholarly presentation and is fully adequate, in scope and quality, as a dissertation for the degree of Doctor of Philosophy.

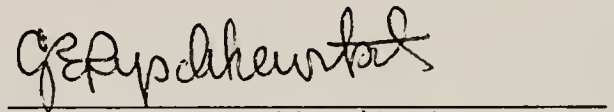

George E. Ryschkewitsch
Professor of Chemistry

I certify that I have read this study and that in my opinion it conforms to acceptable standards of scholarly presentation and is fully adequate, in scope and quality, as a dissertation for the degree of Doctor of Philosophy.

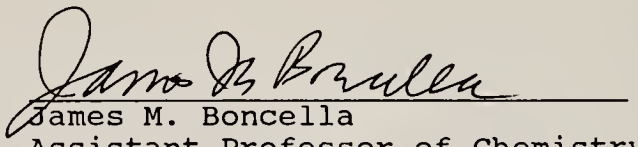

James M. Boncella
Assistant Professor of Chemistry

I certify that I have read this study and that in my opinion it conforms to acceptable standards of scholarly presentation and is fully adequate, in scope and quality, as a dissertation for the degree of Doctor of Philosophy.

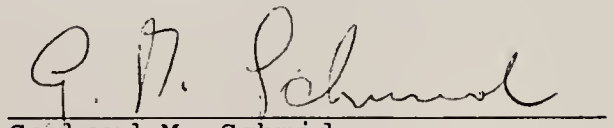

Gerhard M. Schmid
Associate Professor of Chemistry

I certify that I have read this study and that in my opinion it conforms to acceptable standards of scholarly presentation and is fully adequate, in scope and quality, as a dissertation for the degree of Doctor of Philosophy.

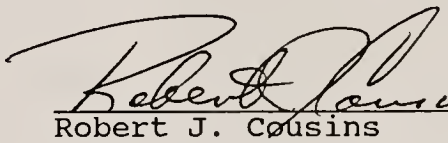

Robert J. Cousins
Boston Family Professor of
Human Nutrition

This dissertation was submitted to the Graduate Faculty of the Department of Chemistry in the College of Liberal Arts and Sciences and to the Graduate School and was accepted as partial fulfillment of the requirements for the degree of Doctor of Philosophy.

August 1990

Dean, Graduate School

UNIVERSITY OF FLORIDA
3 1262 08553 8089